AUS DEM
MAX-PLANCK-INSTITUT FÜR HERZ- UND LUNGENFORSCHUNG, BAD NAUHEIM
AM FACHBEREICH BIOLOGIE UND CHEMIE
DER JUSTUS-LIEBIG-UNIVERSITÄT GIEßEN

Identification and Characterization of Bronchioalveolar Stem Cells and Oct4 Positive Cells in Adult Mouse Lung

Inaugural-Dissertation
zur Erlangung des Grades Doktor der Naturwissenschaften
-Dr. rer. nat.-
der naturwissenschaftlichen Fachbereiche (Fachbereich 08 Biologie und Chemie)
der Justus-Liebig-Universität Gießen

vorgelegt von
M.Sc. Cell.Biol. Célimène Galiger (geb. Koumba)
aus Libreville, Gabun

Gießen 2013

Dekan :	Prof. Dr.Holger Zorn Heinrich-Buff-Ring 58, 35392 Gießen
Erstgutachter:	Prof. Dr. Adriaan Dorresteijn Allgemeine Zoologie und Entwicklungsbiologie Stephanstr. 24, 35390 Gießen
Zweitgutachter:	Prof. Dr. med. Werner Seeger Medizinische Klinik und Poliklinik II Exzellenzcluster Kardiopulmonales System (ECCPS) Lungenzentrum der Universität Gießen (UGMLC)

Die vorliegende Arbeit wurde im Rahmen des Graduiertenkollegs *International Max Planck Research School for Heart and Lung Research (IMPRS-HLR) am* Max-Planck-Institut für Herz- und Lungenforschung in Bad Nauheim in der Zeit von September 2010 bis December 2013 unter der Leitung von Prof. Dr. Adriaan Dorresteijn angefertigt. Das Thema und das Labor wurden von Prof. Dr. med. Werner Seeger bereitgestellt, unter dessen Betreuung diese Arbeit entstand.

TABLE OF CONTENTS

SECTION 1: INTRODUCTION

SECTION 2: MATERIALS AND METHODS

SECTION 3: RESULTS

SECTION 4: DISCUSSION

SECTION 5: CONCLUSIONS-PERSPECTIVES

ABBREVIATIONS AND SYMBOLS

ANOVA: Analyse of variance

α-MEM: Alpha-minimun essential medium eagle

α-SMA: Alpha-smooth muscle actin

BADJ: Bronchioalveaolar duct junction

BSA: Bovine serum albumin

BASCs: Bronchioalveolar stem cells

CCSP: Clara cell secretory protein

CD (CD34, 45): Cluster of differentiation

cDNA: Complementary DNA

° C: Degree Celsius

DAB: 3, 3'-Diaminobenzidine

DAPI: 4', 6-Diamidino-2-phenylindole

DMEM: Dulbecco´s modified eagle medium

Δ (Ct): Delta (threshold cycle)

EDTA: Ethylenediaminetetraacetic acid

EM: Electron microscopy

EpCAM: Epithelial cell adhesion molecule

ESCs: Embryonic stem cells

ESPCs: Epithelial stem/progenitor cells

E.14.5: Embryonic day 14.5

FACS: Fluorescence-activated cell sorting

GFP: Green fluorescent protein

GAPDH: Glyceraldehyde 3-phosphate dehydrogenase

H_2O_2: Hydrogen peroxide

HEPES: 2-[4-(2-Hydroxyethyl) piperazin-1-yl] ethanesulfonic acid

ICC: Interstitial Cajal cells

ICLC: Interstitial Cajal-like cells

ICM: Inner cell mass

KCl: Potassium chloride

KD: Knockdown

KH_2CO_3: Potassium bicarbonate

KH_2PO_4: Potassium dihydrogen phosphate

LCM: Laser capture microdissection

MSCs: Mesenchymal stem cells

ml: Milliliter

mM: Millimolar

mm: Millimeter

min: Minute

mRNA: Messenger RNA

MUC5AC: Mucin-5AC

NaCl: Sodium chloride

Na_2HPO_4: Sodium phosphate dibasic

NGS: Normal goat serum

ng: Nanogramme

NH_4Cl: Ammonium chloride

Oct4: Octamer-4

PBS: Phosphate buffered saline

PCNA: Proliferating-cell-nuclear-antigen

PDGFR-a: Platelet-derived growth factor receptor-alpha

PDGFR-b: Platelet-derived growth factor receptor-beta

PEI: Polyethylenimine

PFA: Paraformaldehyde

PNX: Pneumonectomy

qPCR: Quantitative polymerase chain reaction

rpm: Revolutions per minute

RT: Room temperature

RT-PCR: Reverse transcription polymerase chain reaction

SDS-PAGE: Sodium dodecyl sulfate- Polyacrylamide gel electrophoresis

SEM: Standard error of mean

SPC: Surfactant protein C

TBS/T: Tris Buffered Saline with Tween 20

TEMED: N, N, N´, N´-tetramethylethylenediamine

VEGF: Vascular endothelial growth factor

v/v: Volume to volume

w/v: Mass/volume

YFP: Yellow fluorescent protein

µl: Microliter

SECTION 1: INTRODUCTION

1.1. Background and context of the study

Organ regeneration in mammals is hypothesized to require a functional pool of stem or progenitor cells which have the capacity to replace damage cells or tissues [1, 2]. But, the role of these cells in lung regeneration is still unclear [3, 4]. A better understanding of the contribution of lung stem cells in repair and regeneration is imperative to provide an insight to lung diseases. Chronic diseases like cancer, Chronic Obstructive Pulmonary Disease (COPD) and Bronchopulmonary Dysplasia (BPD) remain an important cause of morbidity and mortality [5, 6]. These diseases imply changes of the cells in the lungs. Research on lung stem cells could enlighten the causes of such diseases, and may provide approaches for clinical therapies. Lung stem cells may serve as a treatment in future to tackle life-threatening respiratory diseases and improve the quality of life/patients prognosis. Lung stem cells have mostly been identified and characterized in genetically modified mice [7, 8]. In the adult lung, it is well established that there are many sources of stem/ progenitor cells. But, it is still unclear which is the most effective in terms of lung repair and remodelling [9-12]. The long-term goal for studying stem cells in the adult lung will be the development of new therapeutic strategies for causal treatment of destructive lung diseases. One way to achieve this goal is to develop new technical approaches for the identification of stem cells by identifying markers, and to understand their role in normal lung physiology and lung diseases. Indeed, adult stem cells have already been utilized for therapies for several years and novel treatments are constantly developed. Hematopoietic stem cells and mesenchymal stem cells for example are currently evaluated for clinical tests [13, 14].

1.2. Generalities and characteristics of stem cells

The vast majority of cells that compose the body are differentiated. They are specialized for different functions and thus, they are not capable of generating other cell types [3]. Neurons, blood cells, muscles and skin are all made up of mature cells [4]. However, there are cells which are undifferentiated, able to divide and have the ability to give rise to other cell types. These cells are called stem cells. Stem cells display two main characteristics. They are able to create unlimited copies of themselves maintaining the same features by cell division; a property known as self-renewal, and to give rise to

specialized cell types such as skin cells, muscle cells or neural cells. Living organisms rely on this continual mechanism of self-renewal to grow; it is indispensable for the replenishment of the body cells after loss or tissue damage during life process [13] [15] [16]. During early development, stem cells undergo symmetric cell division. Each stem cell give rise to identical daughter cells maintaining the same characteristics including the ability to proliferate, to self-renew and to produce daughter cells. Later in the development, asymmetric cell division takes place. Stem cells divide to give rise to identical daughter cells and to committed progenitor cells that undergo differentiation, thereby, providing self-renewal and sustaining tissue homeostasis [17, 18]. Progenitor cells also called transient amplifying (TA) cells or precursor cells, undergo asymmetrical cell division and produce specialized cells [19]. For instance, epithelial stem cells of mouse small intestine produce TA cells that differentiate into various cell types of the villi crypts [20]. Stem cells self-renewal and differentiation are regulated by the cell cycle to enable the cell fate. In fact, stem cell maintenance is important for homeostasis, thereby, cell cycle is necessary for controlling the cell number in organisms [21] [22]. Cell cycle is composed of four distinct phases. The gap before DNA synthesis (G_1), the S phase , the gap after the S phase (G_2) and the M phase called mitosis [23]. These four phases are devoted to the replication of the chromosomal DNA and to the transmission of the genetic material to daughter cells. The G_1 phase also called "start" is the first checkpoint of the cell cycle. The cells are committed to full cell division cycle [21]. During this phase, the cells become bigger and expand. They synthesize molecules such as mRNA and proteins which are necessary for DNA synthesis. The cells which undergo proliferation and regeneration stay in G_1 phase [24]. The G_1 phase ends when the cells enter the S phase. During the S phase, the cells synthesize DNA and replicate. During embryogenesis, most of the cells are in S phase. Loss of pluripotency causes changes in the cells and they enter the G_1 phase [25]. The G_2 phase is the second checkpoint of the cell cycle for any problem which have might occurred during the S phase. The cells synthesize proteins and prepare for the cell division. Finally, during mitosis, the cells divide and give rise to identical daughter cells that enter the G1 phase. The cells that have stopped to divide such as nerve cells and skeletal muscle cells enter the G_0 phase [21] (Fig. 1).

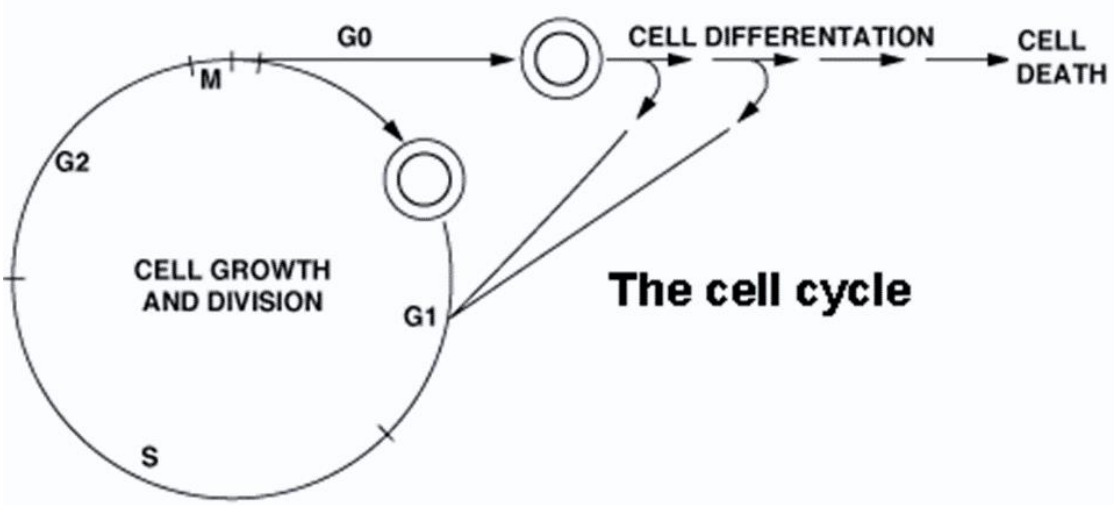

Fig. 1 The cell cycle stages of a stem cell

The cell cycle begins in G_1. In G_1, the stem cells grow and prepare to enter the S phase. In S phase, the cells duplicate their DNA. At this stage, a high proportion of the cells are pluripotent with a very short G_1 phase. In G_2, the cells prepare to inter the M phase (mitosis). During the M phase, the stem cells divide and each cell produces two identical daughter cells. One daughter cell enters the G_1 phase and the other cell enters the G_0 phase. In G_0, cells are differentiated. At this stage, they can undergo cell death or reenter the G_1 phase. Adapted from department biology: Lund University, Sweden. Source:http://www4.lu.se/cell-proliferation-group/research/the-role-of-the-polyamines-in-cell-cycle-control-and-program.

1.3. Origin of stem cells

Once a sperm fertilizes an oocyte, the fertilized egg undergoes several rounds of cell division; the cells start to differentiate. At a very early stage of the development, any cell can develop into a new individual [26]. These cells are known as totipotent stem cells [27]. They have the ability to give rise to specialized tissues or organs such as liver, pancreas, blood, brain, skin and cardiac muscle [28, 29]. This ability to give rise to all cell types is a common property of the fertilized oocyte and early embryonic cells known as developmental plasticity [27, 30, 31]. Sorted in two groups, totipotent stem cells will contribute either to the placenta or to embryo formation. Actually, the primary four-celled embryo undergoes cell division and becomes a hollow ball called blastocyst [32]. The outer cell layer of the blastocyst is only composed of cdx2-expressing cells which build the trophoblast. The inner cell mass (ICM) is composed of Oct3/4-expressing cells which compose the embryo and have the ability to differentiate [33]. In the ICM, these cells are known as pluripotent embryonic stem cells (ESCs) [27] [34]. Pluripotent ESCs are similar to totipotent stem cells in that they can differentiate into all the tissue types of the organism; however, they cannot produce a new individual because they cannot form extra-embryonic tissues or placenta. These ESCs generate the body plan. During

development, many cells die and need to be replaced. This is carried out by multipotent stem cells. They reside in developed tissues, leading their growth and maintenance through life processes. For example, hematopoietic stem cells are able to produce progenitors to all blood cells types which need to be replaced regularly [35]. Unipotent stem cells which originate from multipotent stem cells produce specific stem cells. Skin cells, which are in the epithelium, are one of the most abundant source of unipotent stem cells including bulge stem cells or interfollicular epidermis [36, 37] (Fig. 2).

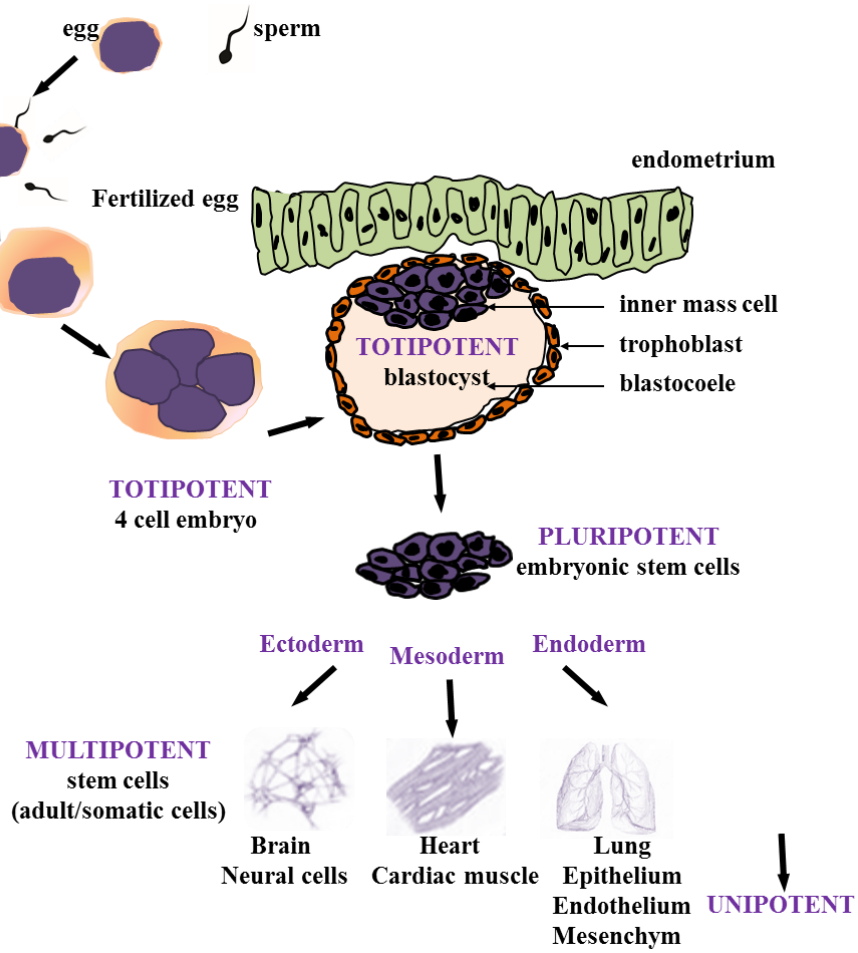

Fig. 2 Origin of stem cells.
A fertilized egg divides and develops into a blastocyst (totipotent stem cells). The inner cell mass of the blastocyst forms the embryo (pluripotent stem cells). The embryo give rise to the three primary germs layers: ectoderm, mesoderm, and endoderm (multipotent stem cells) that give rise to all the cell types of the body. Source: wikipedia. Modified from Blastocyst.png 2007.

1.4. Different types of stem cells

Generally, there are two main types of stem cells. Embryonic stem cells (ESCs) which are the cells found in embryo and adult stem cells also called somatic stem cells of which the origin is still unclear [27, 36].

1.4.1. Embryonic stem cells

ESCs originate from the inner cell mass of the blastocyst and they are mostly characterized by their ability to regenerate indefinitely in culture and keeping their undifferentiated state [27, 38, 39]. Their capacity to remain undifferentiated has been studied *in vitro* through avian ESCs where it has been shown that they were able to be maintained for long-term in culture [40]. Many human ESCs lines have also been reported to proliferate indefinitely *in vitro* [41]. ESCs can differentiate into the three primitive germ layers; ectoderm, mesoderm and endoderm which develop into specialized tissues and organs (Fig. 2). The ectoderm develops into the skin (epidermis), brain and neural cells [42]. The mesoderm develops into the skeleton, the muscles, the circulatory system, skin (dermis). The mesoderm which covers the surface of the lungs develops into the visceral pleura and the somatic mesoderm which covers the body wall from the inside, develops into the parietal pleura. The endoderm develops into the respiratory system and the gastrointestinal system [43] [44].

1.4.2. Adult stem cells

While ESCs are defined by their origin as the cells found in embryo, the origin of adult stem cells is still unclear [27]. The term "adult stem cell" refers to the fact that those cells are found in postnatal tissues. They are present in infants, children and as well as in adults. Investigators use also the term "somatic stem cell" as it means cell of the body, to describe an adult stem cell. Adult stem cells are found in many tissues and organs including brain [45], skin [46], pancreas [47], bone marrow [48], liver [49], lung [3] and skeletal muscles [50] [51]. For instance, (i)-the stem cells in brain can generate different types of neural tissues including astrocytes and neurons. (ii)- Hematopoietic stems cells which reside in the bone marrow have the ability to generate all the blood cells types. (iii)- Following injury, hepatocytes which are normal liver cells, can reenter the cell cycle division to repair the tissues [27, 52].

1.5. Adult lung stem cells

Adult lung stem cells include mesenchymal and epithelial stem cells. Mesenchymal stem cells (MSCs) are multipotent stem cells and they can give rise to different cell types such as chondroblasts, osteoblasts, endothelial, perivascular cells and adipocytes [53, 54] [55] [56]. They were isolated for the first time in 1970 from the bone marrow and spleen suspensions [57]. They have been since then identified in many organs including lungs. They are able to proliferate and differentiate into fibroblasts, myofibroblasts and probably into lipofibroblats [56] [58]. The real function of MSCs is not well understood yet in different organs except the fact that they represent a microenvironment for the hematopoietic stem cells niche [59]. Moreover, in the lungs they have been shown to stimulate for instance, the growth of bronchioalveolar stem cells (BASCs) when they were seeded in co-culture growth conditions/experiments [60]. In addition, they have also been shown to contribute to lung repair after injury in mouse model of Bronchopulmonary Dysplasia [61] and *in vitro* in wound healing assay in alveolar type 2 cells [62]. Epithelial cells, which cover the entire surface of the airways also contain different types of cells which have been involved in lung repair and regeneration. From the upper to the lower airway regions, the epithelium harbors various stem cell niches whose cells are able to self-renew, proliferate and regenerate the tissue during the normal turnover or after tissue damages [63] . Basal cells, Clara cells or BASCs for instance have been proved to participate to these mechanisms by using animal models for lineage tracing and injuries [11, 12, 64-66].

1.6. Lung epithelial stem cells niches and their contribution in adult lung

The lung consists of two main regions (Fig. 3). The upper part composed of the trachea, the two main bronchi and the bronchioles represents the conducting airway part. The second part composed of alveoli give rise to the site of the gas exchange surface. In the upper airways, the epithelium is pseudostratified and columnar and is mostly made up of goblet cells, basal cells and submucosal glandular epithelium. In the lower airways, meaning the bronchioles where the epithelium is cuboidal, Clara cells are predominantly expressed compared to the ciliated cells and neuroendocrine cells. In distal alveolar space, the epithelium is squamous and contains alveolar type 1 and type 2 cells. Alveolar type 1 cells are indeed less abundant than type 2 cells but they line 95 % of the alveolar surface by forming a thin flat squamous cell layer [67] . This complex anatomy of the lung is indeed reflected by various stem cell niches present at different anatomical levels [68]

(Fig.3). The study of lineage tracing and models of injury in the mouse lung have suggested that epithelial repair and regeneration is sustained by different stem/progenitor cells which dwell in particular microenvironments through the upper-lower airway regions [67]. Basal cells in trachea show stem/progenitor cell characteristics. For instance, it has been shown that after injury, keratin-14-expressing basal cells were able to replenish the trachea [65]. Clara cells are thought to be the progenitors of other Clara and ciliated cells. Rawlins et al [11] showed by lineage tracing that Sgb1a1-expressing Clara cells generate both ciliated cells and Clara cells in the trachea. Furthermore, they could contribute to tracheal repair with low potential of self-renewal, but not to the alveolar epithelium repair. Alveolar type 2 cells as well show stem cell capacity; they renew themselves and alveolar type 1 cells as reported in recent studies [69] . BASCs called also variant Clara cells of the bronchiolar–alveolar duct junction (BADJ) appear to regenerate both the bronchioles and the proximal alveolar region [12]. More recently, $CD45^{neg}CD31^{neg}EpCAM^{high}CD24^{low}$ cell population exhibiting stem cell properties has been described as epithelial stem/progenitor cells (ESPCs) in adult mouse lung [70].

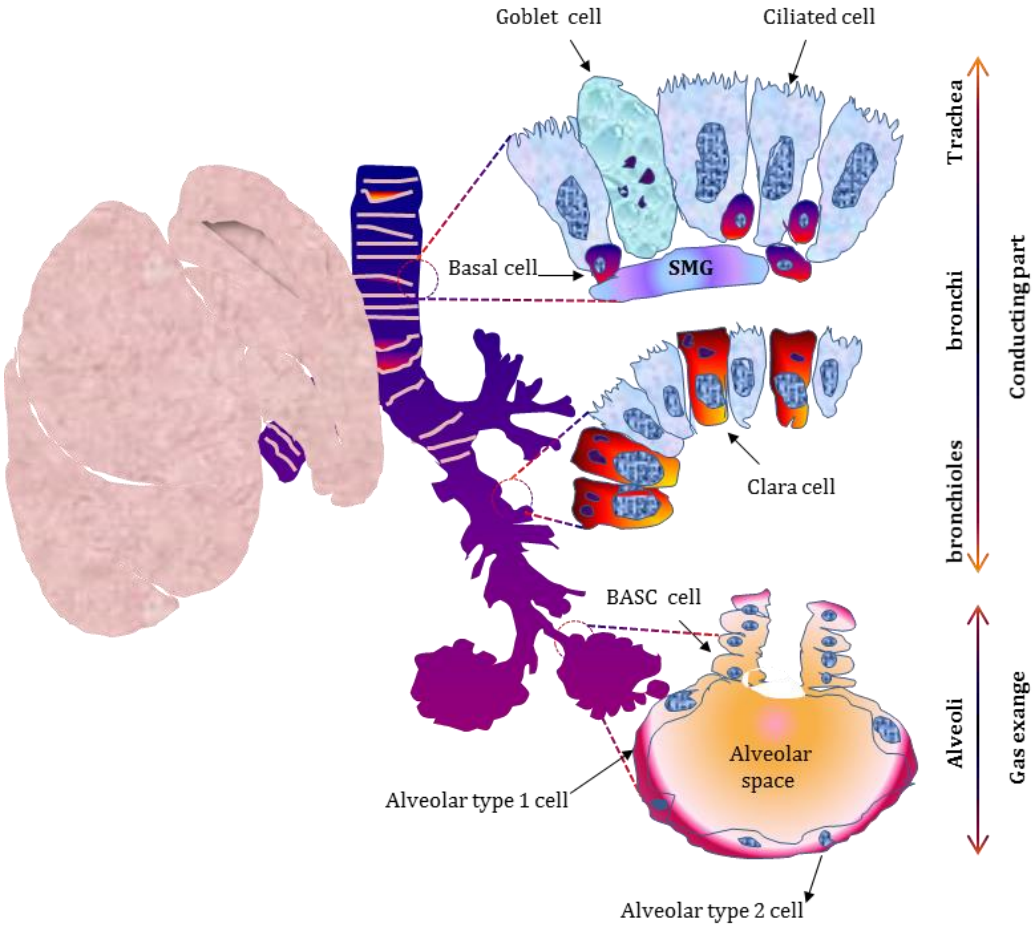

Fig. 3 Architecture of the lung and epithelial stem cells niches.

The circled areas represent the different stem cell niches described in adult mouse lung and the discontinuous lines represent the cells which reside in these microenvironments. Modified from Expert Rev Resp Med. 2008;2(3):365-380.

1.7. Bronchioalveolar stem cells and their contribution in adult lung

BASCs, which are present at the duct junction between the terminal bronchioles and the alveolar space have the potential to contribute substantially to the lung repair and regeneration [71]. They were described in mice to have many of the properties expected of stem cells that they could contribute to the regeneration of terminal bronchioles and their associated alveoli. They are co-stained for CCSP (Clara cell secretory protein) and SPC (surfactant protein C), markers of Clara cells found in the bronchioles and alveolar type 2 cells respectively [12]. Based on the Sca-1^{pos}CD34^{pos} cell fraction, BASCs were cloned and passaged on feeder cells and shown to differentiate to Clara-like cells and alveolar type 2-like cells *in vitro*. However, others studies performed in adult mouse lung

indicate that the Sca-1^{pos} cell fraction is predominantly representative of mesenchymal cell lineages [70]. This highlights that Sca-1 is not a selectable marker for epithelial stem cells in the adult murine lung. Several questions remain to generalize BASCs as stem cells for distal components of the airways and the lung parenchyma [72]. First, they have only been tested in the bleomycin, a model of lung damage, which is more a model of fibrosis than true damage and regeneration. They proved resistance to naphthalene that damage bronchiolar epithelium [10]. Not only BASCs survive to these treatments. In summary, the evidence that BASCs serve as a real stem cells is highly challenged, therefore the alternative functional assays are clearly needed for the identification and characterization of BASCs.

1.8. New approaches for the characterization of BACS

Harold A. Chapman et al. [73] were able to demonstrate that embryonic lung cells transplanted under the kidney capsule of an immunodeficient mouse were able to grow into structures which resemble the lungs with branching and alveolar spaces. This model mimics the lung structure and was proven to be relevant for cell fate mapping and as well as to validate their regenerative ability. Therefore this model can be used as an alternative method to identify BASCs and to confirm their regenerative potential *in vivo. In vitro,* there are no novel studies which address BASCs as putative stem cells. Recent published studies described a small population of epithelial cells which is CD45^{neg}CD31^{neg}EpCAM^{high}CD24^{low} as epithelial stem/progenitor cells (ESPCs) whose descendants give rise to all the epithelial cell lineages in adult mouse lung. This population represents around 1 % of the total epithelial cell population and has the capacity to self-renew and generate different types of epithelial colonies *in vitro* including, MUC5AC-expressing colonies, CCSP-expressing colonies and alveolar type-2- expressing colonies which were observed in matrigel cultures [70]. However, they did not show any relation of EpCAM^{high}CD24^{low} to BASCs. This observation raised the hypothesis that BASCs as stem cells may then be included in the EpCAM^{high}CD24^{low} cell fraction. On this basis, our strategy was to demonstrate whether EpCAM^{high}CD24^{low} cell fraction contained BASCs and to test also whether BASCs could grow into colonies. For these experiments, wild type mice were used. In addition, double-fluorescent Cre reporter mice expressing YFP and mCherry under the control of SPC and CCSP promoters were used for follow-up studies to find out whether they will conform to initial clonogenic studies.

1.9. Oct4 positive cells: a novel subset of putative mesenchymal stem cells in adult lung

1.9.1. Generalities

The study of lung stem cells is mostly understood by using genetically engineered mice and lung disease models. This contributes indeed, to the identification of stem cell populations by mean of different stem cell markers [3] such as stem cell antigen 1 (Sca-1) , Clara cell secretory protein (CCSP), CD34 and Octamer-4 (Oct4) [74]. It has been reported that Oct4 is expressed in postnatal mouse pulmonary cells infected with SARS coronavirus [74]. In this context, Oct4 can also be used as a stem cell descriptor for lung adult stem cells. Actually, a role for maintaining pluripotency and self-renewal of ESCs is ascribed to Oct4 as a marker of pluripotency [75]. Specially expressed in ESCs, Oct4 can also be detected in adult stem cells such as bone marrow-derived mesenchymal stem cells. As a matter of fact, several studies suggest a role for Oct4 in sustaining self-renewal capacity of adult somatic stem cells [76]. However, there is also evidence that Oct4 gene ablation in somatic stem cells revealed no abnormalities in homeostasis or regenerative capacity. Data strongly argue that Oct4, even if expressed at low levels in somatic cells, is dispensable for the self-renewal of somatic stem cells, for tissue homeostasis, and for the regeneration of adult tissues [77]. This is the conclusive scan of Oct4 that it is not a key pluripotency regulator in adult stem cells. Moreover, Oct4 was found to be expressed in telocytes; in human skeletal muscle cell niche [78]. In mouse lungs, telocytes line the perivascular and peribronchial spaces and they extend to the alveolar compartment [79] (Fig.3).

1.9.2. Telocytes: a novel interstitial-stromal cell type of mesenchymal origin

Telocytes are a novel described interstitial (stromal) cell type in the stem cell field showing particular features, with long extensions up to 100 µm called telopodes [80]. These telopodes are self-organized in thin fragments called podomers and more enlarged fragments called podoms. The telocytes form a 3-dimensional network with intercellular junctions [79]. They were discovered in 2005 by Laurențiu M. Popescu's group from Bucarest, Romania. They described these cells in various organs including pleura, epicardium, myocardium, endocardium, intestine, uterus, pancreas, mammary gland and in several others organs [81] [82-86]. They were first named interstitial Cajal-like cells (ICLC) [87] [88-91]. For the short story, more than 100 years ago, Ramón y Cajal

described a particular cell type that was named interstitial neurons because they resembled nerve cells [92]. At the early 1970s, these cells were investigated by electron microscopy (EM) and it became obvious that they were not neurons and they were therefore renamed interstitial Cajal cells (ICC) [93] [94]. The studies of ICC for the ten past years revealed that those cells were similar to ICLC [88-91]. Moreover, the EM studies showed that ICLC had particular features which discriminate them from ICC or other interstitial cell types like fibrocytes or fibroblasts. They presented different ultrastructure and phenotype than ICC; very long extensions with a monoliform shape (a form resembling a string of beads). The definitive survey of ICLC was that there were not ICC and thus, they proposed to rename those cells *telocytes,* and *telopodes* for their prolongations [95]. They express different markers in different organs including CD34, αSMA, Sca-1, PDGFR-b, S-100, C-kit, vimentin and VEGF in human epicardium, human term placenta or skeletal muscle cell niche [78]. Telocytes are cells of mesenchymal origin based on their expression markers (c-kit, vimentin, PDGFR-b) and their similarities to ICC which were confirmed to be also from mesenchymal source [96]. A role of telocytes in inter-cellular signaling via paracrine secretion as well as by shed vesicles and exosomes has been suggested due to their distinguished architecture with thin and long telopodes [97]. Their presence in microenvironment of stem cell niches as well as the expression of stem cell markers suggests a role in regeneration of tissues [78, 98]. They have recently been identified in human and mouse terminal and respiratory bronchioles as well as in the alveolar ducts [79] (Fig. 4).

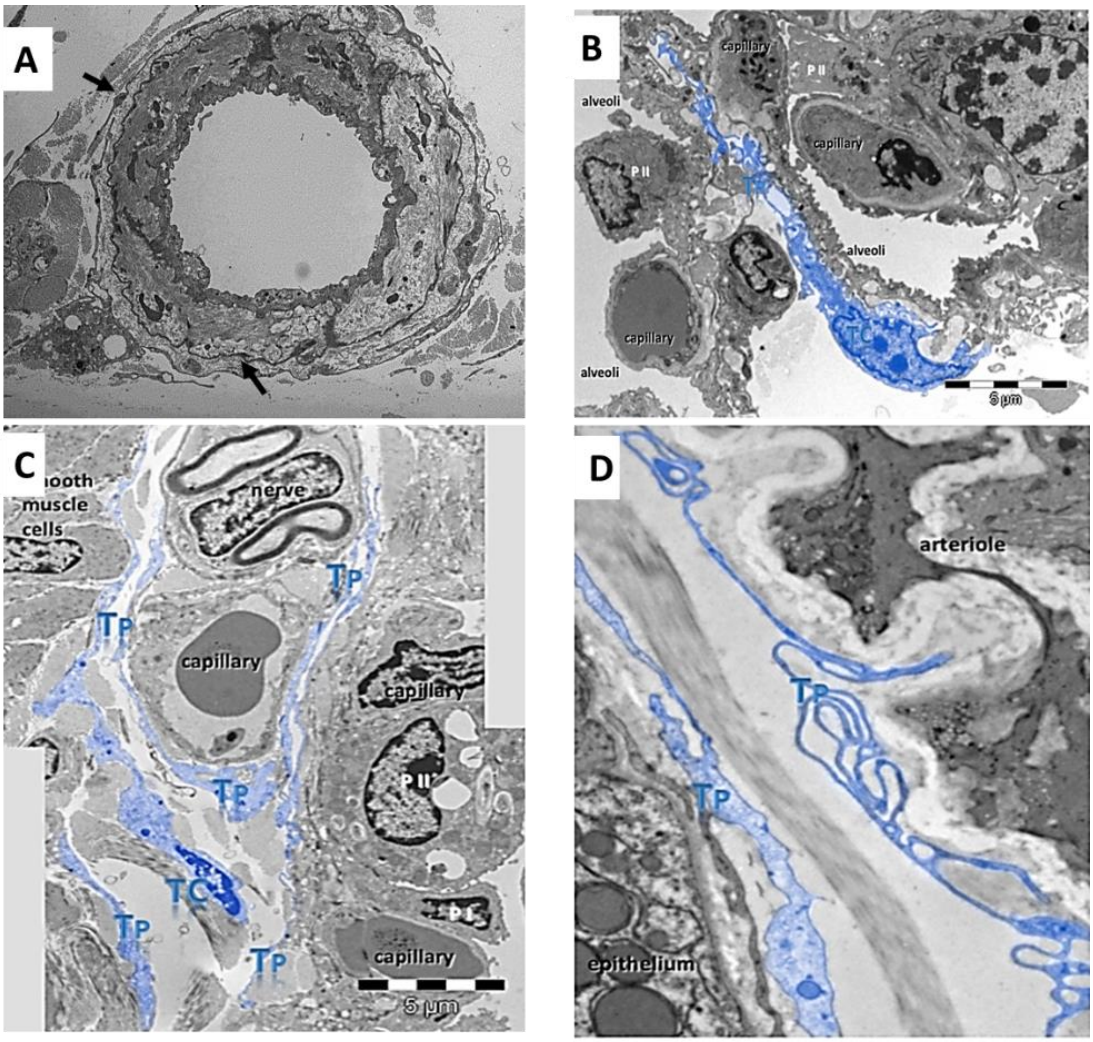

Fig. 4 Identification of telocytes in adult mouse lung tissues.

(A) Telocytes in the perivascular space (black arrows). (B) Telocytes in alveolar duct between the respiratory bronchioles and the adjacent alveoli. (C) Telocytes in the peribronchial space at the terminal bronchiole. (D) Telocyte in the peribronchial space at the respiratory bronchiole. TC: telocyte; Tp: telopode. Source: Max-Planck-Institut for Heart and Lung Research. The pictures were kindly provided by PD. Dr. Sawa Kostin.

1.10. Identification and characterization of Oct4 positive cells in adult mouse lung

Transgenic animals are nice tools to monitor the activity of a specific gene in cells or in tissues. Homozygous Oct4 transgenic mice expressing green fluorescent protein (GFP) are known to be especially useful for identifying and isolating mouse germ cells *in vivo* at different stages of the development [99]. The construct used for transgenesis was generated at the European Molecular Biology Laboratory (EMBL, Heidelberg, Germany) by the research group of Dr. Hans Schöler. Oct4-GFP transgenes have been generated

using different regions Oct4 gene promoter to drive expression of GFP, which enable the activity of the Oct4 promoter to be monitored in cells and tissues [100]. Therefore, GFP can be used as reporter to observe the expression of Oct4 and to target its localization in adult lung tissues. These mice can be also very important for the quantification (flow cytometry method) and isolation of Oct4 positive cells (cell sorting method) based on GFP endogenous fluorescence. Phenotypical features of Oct4 positive cells with telocytes can then be validated by microscopy after isolation. In addition, double immunofluorescence against Oct4 and different markers of telocytes can be especially useful to study the correlation of Oct4 positive cells to telocytes. Laser capture microdissection which consists to isolate specific cells of interest from tissue sections with a laser coupled to a microscope can be used to characterize Oct4 positive cells. In fact, this method is useful for extracting and purifying DNA or RNA from the cells of interest. Therefore, the RNA expression levels of Oct4 and different markers of telocytes can be analyzed in order to support immunohistohemical analyses.

1.11. Hypotheses and aims

Based on previous data which showed that BASCs are stem cells and they are involved in mouse lung repair and regeneration, we aimed to elucidate whether BASCs are stem cells of the distal mouse lung. This hypothesis was approached using three experimental steps (i), identification of BASCs in adult mouse lung tissues. (ii), analysis of their role in repair and regeneration using animal models of injury (naphthalene) and compensatory lung growth (pneumonectomy) and (iii), characterization of BASCs and $EpCAM^{high}CD24^{low}$ cell fraction *in vitro* and in *vivo* using transgenic approaches. Since Oct4 represents an important stem cell marker and has been demonstrated to be expressed in the lung, Oct4 expression and function should be analyzed in BASCs**.**

SECTION 2: MATERIALS AND METHODS

2.1. Materials

2.1.1. Animals

The mice used for experiments were adult (> 8 weeks) and from different mouse strains (table 1). The CCSP-mCherry/SPC-YFP mice were generated and kindly provided by Dr. Marten Szibor; Department of cardiac development MPI Bad Nauheim, director: Prof. Dr. Dr. Thomas Braun. They were bred and maintained in our animal facilities and housed according to the European Laboratory Animal Welfare Act and Regulations in animal housing facility at Max-Planck-Institute for Heart and Lung Research in Bad Nauheim, Germany (status of approval: assessment from ethics committee with the permission for animal laboratory experimentations; numbers B2/336 and B2/337 Regierungspräsidium Darmstadt). All animals were kept at room temperature in a barrier facility with purified air, supplied with food and water *ad libitum* and exposed to a 12:12-hours (h) light-dark cycle.

Mouse strains	Genotype	Source	Breeding & maintenance
C57BL/6-Ola	Wild-type (WT)	Max-Planck (MPI)	MPI
C57BL/6J	$Oct4^{GFP}$	Jackson Lab	MPI
BALB/C	NOD/SCID	Charles River	MPI
BALB/C	CCSP-mCherry/SPC-YFP	MPI	MPI

Table 1. Mouse strains used for the experimentations.

Oct4-GFP: transgenic mice expressing green fluorescent protein (GFP) under the control of Oct4 promoter. **NOD/SCID**: immunodeficient mice with deficient natural killer cells and impaired T and B lymphocytes development. **CCSP-mCherry/SPC-YFP** double transgenic mice are knock in mouse line generated from the crossing between single mouse line; Clara cell secretory protein (CCSP) and surfactant protein C (SP-C) promoter driven-expression of inactive Cre fragments. The generation of functional CCSP-SPC protein is only possible in these double transgenic mice upon co-expression of BASC-defining marker proteins. MPI: Max-Planck-Institute Bad Nauheim.

2.1.2. Antibodies

All antibodies which were used in the present study are shown in the tables 2 and 3.

Primary antibodies	Cat#number	Company	Source	Application & (targets)	Dilution (µl)
Polyclonal pro-SPC	AB3786	Millipore	Rabbit	IF, FC (alveolar epithelial type 2 cells)	1:400
Polyclonal CC 10 (T - 18)	sc-9772	Santa-Cruz	Goat	IF, FC (bronchiolar epithelial Clara cells)	1:200
Monclonal Oct3/4 (C-10)	sc-5279	Santa-Cruz	Mouse	IF,IHC,ICC, WB (mesenchymal cells-telocytes)	1:50-100 (IF) 1:1000 (WB)
monoclonal anti-vimentin	C 9080	Sigma	Mouse	IF (mesenchymal cells-telocytes)	1:500
monoclonal α-SMA- Cy3	C6198	Sigma	Mouse	IF (smooth muscle-blood vessels)	1:500
polyclonal PDGFR-β (958)	sc-432	Santa Cruz	Rabbit	IF (mesenchymal cells-telocytes)	1:100
Anti-Mouse Ly-6A/E /Sca-1	553333	BD Bioscences	Rat	IF (mesenchymal stem cells-telocytes)	1:100
Polyclonal C-kit(C-19)	sc-168	Santa Cruz	Rabbit	IF (stem cells-telocytes)	1:100
Polyclonal VEGF(A-20)	sc-152	Santa Cruz	Rabbit	IF (mesenchyme-telocytes)	1:100
Anti-PDGFR –α	ab90967	Abcam	Rabbit	IF (fibroblasts)	1:100
DAPI				Nuclear staining	1:1000
PCNA (F - 2)	sc-25280	Santa Cruz	Mouse	Proliferation	1:100
monoclonal anti-β-actin	A5316	Sigma	Mouse	WB	1:5000
Anti-mouse CD45-FITC	11-0451-82	eBioscience	Rat	FACS	1µl/ 5 million cells
Anti-mouse CD 31-FITC	11-0311-81	eBioscience	Rat	FACS	1µl/5 million cells
Anti-mouse CD45-APC	17-0451-82	eBioscience	Rat	FACS	1µl/5 million cells
Anti-mouse CD31-APC		eBioscience	Rat	FACS	1µl/ 5 million cells
Anti-mouse EpCAM (CD326)	25-5791-80	eBioscience	Rat	FACS	1µl/ 5 million cells
Anti-mouse CD24 -PE	12-0242	eBioscience	Rat	FACS	1µl/ 5 million cells
Anti-mouse CD-24-PerCP	45.0242-82	eBioscience	Rat	FACS	1µl/ 5 million cells

Table 2: List of the primary antibodies.

IF: Immunofluorescence: IHC: immunohistochemistry; ICC: immunocytochemistry; WB: western blot; FC: flow cytometry; PCNA: proliferating-cell-nuclear-antigen; FACS: fluorescence-activated cell sorting.

Secondary antibodies	Cat#number	Company	Source	Application	Dilution (µl)
Alexa fluor 488	A11055	Invitrogen	Donkey anti-goat	IF, FC	1:500-1000
Alexa fluor 488	A11001	Invitrogen	Goat anti-mouse	IF	1:500-1000
Alexa fluor 555	A21432	Invitrogen	Donkey anti-goat	IF, FC	1:500-1000
Alexa fluor 647	A21247	Invitrogen	Goat anti-rat	IF	1:500-1000
Alexa fluor 647	A21246	Invitrogen	Goat ant-rabbit	IF, FC	1:500-1000
IgG2a Isotyp Control-FITC	11-4321-80	eBioscience	Rat	FACS	1µl/ 5 million cells
IgG2b Isotype Control-PE	12-4031	eBioscience	Rat	FACS	1µl/ 5 million cells
IgG1 k PECy7	25-4301	eBioscience	Rat	FACS	1µl/ 5 million cells
IgG1 k Control PerCP-Cy5.5	45-4301	eBioscience	Rat	FACS	1µl/ 5 million cells
IgG2a K Isotype Control -APC	17-4321	eBioscience	Rat	FACS	1µl/ 5 million cells

Table 3: List of the secondary and IgG control antibodies.

IF: Immunofluorescence: IHC: immunohistochemistry; FC: flow cytometry; FACS: fluorescence-activated cell sorting.

2.1.3. Primers used for the real-time quantitative PCR

All the primers used for the real-time quantitative PCR are summarized in table 4

Primer names	Foward	Reverse	Company	Application
Oct4	5´-caagttggcgtggagactttgc-3´	5´-ccccaaggtgatcctcttctgc-3´	Eurofins MWG operon	LCM (laser capture microdissection)
Vimentin	5´-gagatcgccacctacaggaa-3´	5´-tccatctctggtctcaaccg-3´	Eurofins MWG operon	LCM
PDGFR-β	5´-aggggcgtgatgactagc-3´	5´-ttccaggagtgataccagctt-3´	Eurofins MWG operon	LCM
Sca-1	5´-gcctgcaaccttgtctgag-3´	5´-cagactccatcagggtaggg-3´	Eurofins MWG operon	LCM
VEGF	5´-ggagatccttcgaggagcactt-3´	5´-ggcgatttagcagcagatataagaa-3´	Eurofins MWG operon	LCM
C-kit	5´-tgtaaggcctccaacgatgt-3´	5´-cagagtgtgggcctggattt-3´	Eurofins MWG operon	LCM
CCSP	5´-gatcgccatcacaatcactg-3´	5´-cagagttccgaagaagctga-3´	Eurofins MWG operon	Lung homogenate
GAPDH	5′-tgaggccggtgctgagtatgtcg-3′	5′-ccacagtcttctgggtggcagtg-3′	Eurofins MWG operon	LCM

Table 4: List of the primer sequences used for the real-time quantitative PCR.

2.2. Methods

2.2.1. Lung isolation and tissue processing for paraffin embedding

Mice were anesthetized with lethal dose of isofluran (liquid for inhalation; Baxter). A large incision was made up to the neck of the mouse. 10 ml cold PBS (Phosphate Buffered Saline; Dulbecco) was perfused through the right ventricle until lungs cleared of blood. After pulling back the skin above the head of the mouse to expose the throat, the rest of the rib cage was removed carefully and other tissues around to expose the trachea. The forceps was placed under the trachea to separate the trachea from the oesophagus. 2-3 ml paraformaldehyde (PFA cat#0335.3; Roth) at 4 % dissolved in 1x PBS (4.3 mM Na_2HPO_4, 137 mM NaCl, 2.7 mM KCl, 1.4 mM KH_2PO_4) was injected into the trachea until the lungs inflate. Gently, lungs were dissected and dropped into 15 ml conical tube with a large volume of 4 % PFA and left at 4 °C overnight. After 24 h, lungs were washed and kept with PBS for a maximum of one week or in 50 % ethanol for a long-term period. For paraffin processing, the lungs were put into plastic cassettes and placed in tissue processor (ASP200 S: Leica Microsystems Nussloch GmbH, Germany) where they ran through increasing concentrations of alcohol which dehydrate the tissues, and in paraffin which infiltrate into the tissues; the next step, the tissues were embedded into paraffin blocks.

2.2.2. Tissue preparation and histology

2.2.2.1. Immunohistochemistry with DAB (3, 3'-diaminobenzidine) on paraffin-embedded tissues

10 µm paraffin-embedded sections were placed at 65 °C for 20 min (minutes) and serial steps of deparaffinization and hydration with decreasing concentration of alcohol were performed. The sections were incubated in 3 washes of rotihistol (cat#6640.4; Roth) for 10 min each, then in 2 washes of 99.9 % of ethanol for 5 min each, 1 time in 96 % of ethanol for 5 min and 1 time in ethanol 70 % for 5 min. To block endogenous peroxidase, the tissues were immersed in 2 % BSA (bovine serum albumin, cat# K45-00; PAA Laboratories, Austria) with 0.5 % NP40 and 3 % NGS (normal goat serum). Slices were stained overnight with mouse monoclonal Oct4 primary antibody diluted (1:50) in 2 % BSA with 0.5 % NP40. The tissues were rinsed 3 times for 5 min each in 1x PBS, and incubated 1h at RT (room temperature) with appropriate biotin-labeled antibody (M.O.M kit cat#PK-2000; Vector Laboratories, Burlingame, Canada) at 1:1000. After 3 washing

steps in 1x PBS for 5 min, the tissues were incubated for 1h at RT with the ABC substrate (M.O.M kit); 2 drops reagent A + 2 drops reagent B in PBT (1x PBS with 0.1% Tween 20 and rapidly vortexed). The slides were washed 3 times, incubated with 10 mg DAB tablet (cat#D4168; Sigma) in PBT solution with 30 % H_20_2 for 15-30 min at RT. The counterstaining with DAPI (1:1000) was for up to 10 min and the slices were mounted with mowiol (4-88 reagent cat#475904; Merck chemical Ltd).

2.2.2.2. Immunofluorescence on paraffin-embedded tissues

Deparaffinization and hydration steps were performed as described previously and the tissues were permeabilized with methanol 100 %. The sections where submerged in distillated water for 5 min and incubated for 10 min at 37 °C with trypsin working solution (Digest All cat#003008; Invitrogen) for antigen unmasking. After washing with 1x PBS, the tissues were blocked with 5 % BSA for 1h at RT and incubated with appropriate primary antibodies (1:50-500) diluted in histobuffer (3 % BSA , 0,2 % TritonX-100 in PBS) for 1h at RT or overnight at 4 °C. They were after that washed with 1x PBS and incubated with appropriate secondary antibodies (1:500-1000) for 1h at RT, washed with 1x PBS and counterstained with DAPI (1:1000) for 10 min. The slices were mounted with mowiol and scanned with Zeiss LSM 710 laser scanning confocal microscope.

2.2.2.3. Resorcin-fuchsin staining on paraffin-embedded tissues

After deparaffinization and hydration steps, the slices were immediately put in resorcin-fuchsin (cat#2E-030; Waldeck) working solution (173 g of 70 % ethanol, 7.2 ml of 25% HCl, and 10 ml weigert resorcin-fuchsin) and kept overnight. After one step of washing with distillated water, the slices were counterstained with Kernechtrot-Aluminium sulfate (cat#2E-012; Waldeck) and washed 2 times again with water, dehydrated with ethanol (1 time in 70 % for 1 min, 1 time in 96 % for 2 min and 2 times in 99.9 % for 2 min) ,washed 3 times with rotihistol (2 times for 10 min and 1 time for 5 min), then dehydrated in 2 washes of isopropanol for 5 min and transferred in xylene for 5 min. The slices were afterward mounted with pertex (cat# 1.07960.0500; Merck).

2.2.3. Immunocytochemistry of sorted cells: preparation of cytospin from single sorted cell suspension

Directly after sorting (2.2.4), the cells were washed in PBS and resuspended in 10 % FCS. The slides were mounted with filter pad paper in a metal holder; 100 µl of PBS per 5 x 10^4

cells were loaded onto the slides and spin down at 400 x g for 5 min. The cells were fixed with methanol 100 % for 10 min, washed with water, blocked with 5 % BSA for 1h and incubated with the appropriate primary and secondary antibodies for 20 min each and counterstained with DAPI up to 10 min. The slices were after that mounted with mowiol and scanned.

2.2.4. Flow cytometry and fluorescence-activated cell sorting (FACS)

Twelve- to twenty-weeks-old mice lungs were isolated and filled with 1-2 ml dispase (cat# 354235; BD Bioscience) by intra-tracheal instillation; dissected and minced with sterile scalpel and incubated with 2 µg/ml collagenase B (cat# 11088815001; life sciences) and 0,001% (w/v) DNAse (cat#18535; Serva Electrophoresis) in DMEM for 15 min at 37 °C. The resulting cell suspension was filtered through 100 µm (cat#352360) and 40 µm cell strainers (cat#352340; BD Falcon) and centrifuged at 400 x g, 5 min at 4 °C. Cells were resuspended in cell blood lysis buffer (0.15 M NH4Cl, 10 mM KHCO3, 0.1 mM EDTA) for 5 min, washed in PBS and resuspended in FACS-buffer (PBS, 2 mM EDTA, 25 mM HEPES) at 1 million cells/100 µl and incubated for 20 min on ice with a mixture of appropriate antibodies (1µl/5million cells) . Labeled cells were washed with PBS and resuspended in FACS-buffer for flow cytometry or FACS sorting. Cells were labelled with DAPI for cell viability. The flow cytometric analyses were performed with BD LSR II flow cytometer and the data were interpreted with flowJo7.6.4 software. The BD FACSAria III cell sorter was used for cell-sorting procedures.

2.2.5. Cell suspension cultures and clonogenic assays

Cells were sorted and directly collected in FACS-tubes filled with α-MEM medium (cat# 41061; Invitrogen) containing 10 % (v/v) FCS, 1× penicillin/streptomycin (100× stock solution), 1× insulin/transferrin/selenium (100× stock solution cat#51500-56; Invitrogen), 2 mM l-glutamine (cat#P04-80100; PAN Biotech) and 0.0002 % (w/v) heparin (cat#H3149; Sigma), and immediately centrifuged for 5 min at 400 x g at 4° C, washed , and resuspended in the α-MEM cocktail medium. Oct4 positive cells sorted based on GFP fluorescence were cultured in suspension in normoxic conditions (21 % O_2, 5 % CO_2, 37° C) for 5 days and the medium was exchanged every two days. Epithelial stem/progenitor cells (ESPCs) selected based on $CD45^{neg}CD31^{neg}EpCAM^{high}CD24^{low}$, were in contrast, when sorted for clonogenic assays, tested for differentiation on 3D matrigel cultures mixed with feeder cells.

The sorted cells were resuspended in the medium and mixed with the matrigel (1:1). Millicel inserts (Millicel® 0.4 µm, 12mm diameter, cat#PICM01250; Millipore) were placed in 12 well-plates and 90 µl of the cell suspension was put on the top of the insert. After, this plate was incubated in normoxic condition for 5 min and 400 µl of the cocktail medium was added into the plate. The cultures were grown in hypoxic conditions (1 % O_2, 5 % CO_2, 37 °C) for one week and the medium was exchanged every two days. The cultures were imaged with light microscope and then stained with appropriate antibodies for the immunofluorescence confocal microscopy analyses.

2.2.6. Western blot analysis

Proteins were isolated from lung tissue lysates. 20 -30 mg of tissues were transferred into bead tubes and homogenized using a precellys homogenizer (Precellys® 24/ PeqLab; 91-PCS24) at 6500 rpm for 1 min in RIPA lysis buffer (cat# 89901; Thermo Scientific) with protease and phosphatase inhibitor cocktail (cat#18161284; Thermo Scientific). After homogenization, the samples were centrifuged at 12 000 rpm at 4 °C for 30 min. The supernatant was collected in new tubes and a colorimetric protein assay kit (Bio-Rad protein assay kit: cat#210003399) was used to measure the concentration of the proteins. For the standard curve, a serial dilution of 0.1, 0.2, 0.4, 0.8 and 1.6 ng/µl of BSA was prepared. 5 µl of each dilution step and 5 µl of the protein samples were put in a 92 well-plate. 5 µl of distilled water were used for the blank sample. A mixture of 25 µl of S and A reagents (1:20), and 200 ml of B reagent from the protein kit were added into each well containing a sample. The plate was left 10 min at RT and the concentration of the proteins was determined with the monochromator Infinite® 200 NanoQuant microplate reader (Tecan Group Ltd. Männedorf, Switzerland). Before electrophoresis, the samples were mixed with Laemmli buffer [375mM, SDS 10 % (w/v), glycerol 50 % (v/v), β-mercaptoethanol 12.5 % (v/v), bromophenol blue 0.02 % (v/v)], centrifuged for 12 seconds at 12 000 rpm, heated at 95 °C for 5 min and then centrifuged for 12 seconds before loading. The samples were run on 10 % SDS-PAGE (375 mM Tris/Cl pH 8.9, 10 % acrylamide, 0.20 % SDS, 0.05 % APS and 0.10 % TEMED) for 1h 15 min with 80-100 V and transferred onto a nitrocellulose membrane (cat# S80209: Pall Corporation, Dreieich, Germany) for 1h 15 min with 100 V. The membrane was after that rinsed with TBS/T (tris buffered saline with 1 % Tween 20), blocked in 5 % milk (cat# M740: Sigma-Aldrich, St-Louis, USA) with TBS/T for 1h 30 min at RT on an orbital shaker plate. The membrane was then incubated with the appropriate primary antibodies 1:1000 (sc-5279) overnight

at 4° C on an orbital shaker plate, then washed 3 times for 5 min each in a large volume of TBS/T and incubated 1h with the secondary antibody 1:3000; then washed 3 times for 10 min each with TBS/T. The Super Signal® reagent (1:1) (Thermo Scientific: prod# 34096) was used for developing the membrane. The bands were detected with the luminescent image analyzer LAS-4000 mini (Fujifilm, Tokyo, Japan). After the exposure, the membrane was washed 4 times for 5 min each in TBS/T, submerged in 25 ml stripping buffer (cat#21059; Thermo Scientific) and incubated for 1h at RT with agitation on a shaker plate. After two steps of washing for 10 min each, the membrane was blocked in 5 % milk and the immunodetection protocol was repeated as described previously with mouse monoclonal anti-β-actin antibody 1:5000 (cat#A5316; Sigma) and the appropriate secondary antibody.

2.2.7. Reverse-transcription PCR

The reverse-transcription PCR (RT-PCR) was carried with high capacity cDNA reverse transcription kit (Applied Biosystems; USA). The master mix per 20 µl reaction contained 2 µl of 10x RT buffer, 0.8 of 25x dNTP mix (100 mM), 2 µl of 10x random primers, 4.2 µl nuclease-free water and 100 ng of total RNA per 10 µl reaction (table 5). The volume of the master mix was calculated according to the required number of reactions and all the steps were carried out on ice. The RT-PCR (2.2.8) was run with the thermal cycling program referred in table 6.

Components	Volume per reaction (µl)
25X dNTP Mix (100 mM)	2
10X RT Random Primers	0.8
Reverse Transcriptase	2
Nuclease-Free H_2O	4.2
RNA template (up to 1 µg)	10
Total per reaction	20

Table 5: Preparation of the master mix for the cDNA synthesis.

Parameters	Step 1	Step 2	Step 3	Step 4
Temperature (°C)	25	37	85	4
Time (minutes)	10	120	5	∞

Table 6: Thermal cycling program of the RT-PCR.

2.2.8. Real- time quantitative PCR

To ensure the efficiency of the PCR, primer efficiency test was carried out. The efficiency of the PCR was tested by performing ten-fold dilution series of the cDNA templates in triplicate (1:10; 1:100; 1:1000). By using the Ct slope method (see the calculation below), the baseline and threshold were set and the slope of the standard curve was translated into an efficiency value:

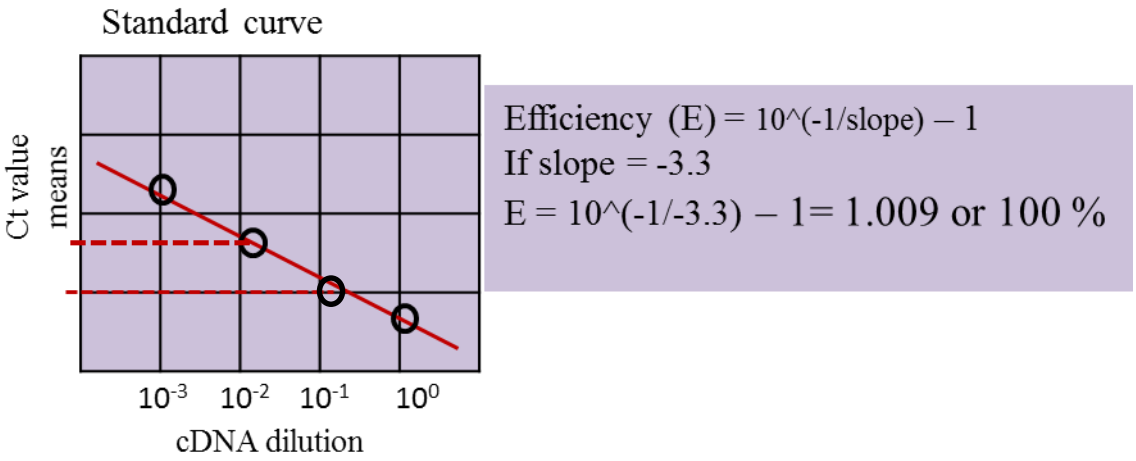

The PCR was efficient between 90–100 % (−3.6 ≥ slope ≥ −3.3). The efficiency was 100 %, when the Ct values of the 10 fold dilution were 3.3 cycles apart. The real time PCR reaction mixture and the thermal cycling program are summarized in tables 7 and 8. The real time PCR was run with ViiA™ 7 Real-Time PCR System (Applied Biosystems) using SYBR Green dye for the detection of the double-stranded DNA; the mRNA levels were expressed as ΔCt values compared to GAPDH housekeeping gene control.

Components	Voulume per reaction (µL)
SYBR Select Master Mix	10
Nuclease-Free H_2O	7
Foward primer	0.5
Reverse primer	0.5
cNDA template	2
Total per reaction	20

Table 7: Master mix for the real-time quantitative PCR reaction.

Parameters	Hold stage		PCR stage			Melt curve stage		
	Step 1	Step 2	Step1	Step 2	Step 3	Step 1	Step 2	Step 3
Temperature (°C)	50	95	95	59	72	95	60	95
Time (minutes)	2	10	15	15	20	5	1	15

Table 8: Thermal cycling program for the real-time quantitativePCR.

2.2.9. Laser capture microdissection

This method required frozen tissues which were labeled prior the microdissection. 10 µm tissues sections were placed in 70 % ethanol for 60 seconds and directly passaged in sterile distillated water for 10 seconds. The slides were then after stained with hematoxylin (cat#MHS16; Sigma) for 10 seconds, washed in sterile water and tap water for 10 seconds each. Rapid steps of dehydration with increasing concentrations of ethanol (15 seconds each; in 70 %, twice in 95 %, once in 100 % and 1 min in 100 % ethanol) were performed in order to maintain the integrity of the RNA. The microdissected samples were collected in tubed filled with 350 µl of RLT buffer (QIAGEN), vortexed for 30 seconds and RNA was isolated using the RNeasy Plus Micro Kit (QIAGEN® Kit cat#74034). The RT-PCR (see master mix reaction in table 9 and the thermal cycling in table 10) was performed with cDNA kit from Bio-Rad (iScript™ Select cDNA Synthesis Kit #170-8896) and the mRNA levels of different genes were measured by real-time quantitative PCR during 40 cycles of amplification (see master mix reaction in table 7 and the thermal cycling in the table 8). The primers used for this test identified Oct4, PDGFR-b, Sca-1, VEGF, vimentin, C-kit gene expression levels. Primer sequences are shown in table 4. The mRNA expression levels were shown as ΔCt values compared to GAPDH housekeeping gene control.

Components	Volume per reaction (µl)
5X iScript reaction mix	**4**
iScript reverse transcription	**1**
Nuclease-Free H2O	**5**
RNA template (100 fg to 1µg)	**10**
Total per reaction	**20**

Table 9: Master mix for the cDNA synthesis after LCM.

Parameters	Step1	Step 2	Step 3	Step 4
Temperature (°C)	25	37	85	4
Time (minutes)	5	30	5	∞

Table 10: Thermal cycling program for the RT-PCR after LCM samples.

2.2.10. Naphthalene injury model

Naphthalene was injected intraperitoneally at 250 mg/kg in 30 mg of powder (Sigma; cat#84679) per ml of corn oil (Sigma; cat#8001-30-7) in conscious adult mice (> 8 weeks old). The control group received the equivalent volume of corn oil per body weight. The treatment was given once and the lungs were harvested at different time points to perform the analyses.

2.2.11. Pneumonectomy (PNX) model

2.2.11.1. Preparation of the animal

Mice were first put in a chamber filled with 5 % isofluran until they reached deep anesthesia. Depth of anesthesia was monitored via lack of response to the hind toe pinch and subjective respiratory rate. The eyes were protected from drying by application of Dexpanthenol-ointment. The animal was directly placed on a warm platform under a microscope and intubated orally with a 21G cannula. Afterwards, the intubation tube was carefully introduced into the trachea and connected to a volume-controlled ventilator (100/min respiratory rate, puff volume 250 µl). The surgery was performed aseptically; the animal was maintained under isofluran dispenser at 2-2.5 % which was itself connected to a ventilator.

2.2.11.2. Surgery procedure

Under deep anesthesia, 8-10 mm cut was made between the 4^{th} and 5^{th} left rib. The chest cavity was opened and the left lung was lifted cautiously out of it. The left lung was after that, ligated and resected at the left hilus (site of incoming and outgoing vessels/bronchi). The thorax was then closed with one suture around the 4^{th} and 5^{th} rib. Skin was continuously sutured. Sterile glucose solution (1 ml 5%) was injected subcutaneously to serve as fluid support in order to maintain the animal's hydration. After PNX, the animal was placed under a heat lamp and monitored for 60 min. Post-surgery analgesia was applied through a

reinjection of buprenorphine (0.05 mg/kg) after 8 h. Carprofen (4 mg/kg) was administered *ad libitum* via drinking water for 5 days. The sham procedure was similar to the PNX but without left lung resection. The chest was left open for 5 min to mimic the procedure of PNX and then the rib cage was closed as previously described.

2.2.12. In vivo lung organoid assays and kidney capsule model

2.2.12.1. Preparation of lung organoid for the transplantation

Single cell suspension of embryonic lung cells dissociated from E14.5 mouse was prepared and centrifuged at 400 x g for 5 min. The compact pellet was mixed up and down; 5-6 µl were pipetted on the top of a 13 mm sterile polycarbonate filter with 8 microns pore size (Millipore; cat#TETP01300) floating on the top of DMEM + 10 % FCS. Afterwards, the organoids cultures were incubated at 37 °C for 24 h (Fig. 5).

2.2.12.2. Organoid transplantation: kidney capsule model

The organoids were implanted under the kidney capsule of immunodeficient NOD/SCID mice 24 h after the organoid´s preparation. The animal was first anesthetized as described for the PNX surgery. When the mouse was fully anesthetized, the animal was placed on warm towels on ventral position. The skin was cleaned with betadine; an incision of 2-3 cm was made with scissors from the base of the tail. The skin was separated from the dermis; the kidney was then visible. With the thumbs on the animal's abdomen, a gentle pressure was applied to expose the kidney out of the body. With the forceps, the organoid was inserted under the capsule and the kidney was immediately replaced into the body. The skin was then closed and sutured. After surgery the mouse was placed in a clean cage to recover. Ibuprofen 0.11 mg/ml (30 mg/kg/day) was administered *ad libitum* via drinking water for 5 days post-surgery.

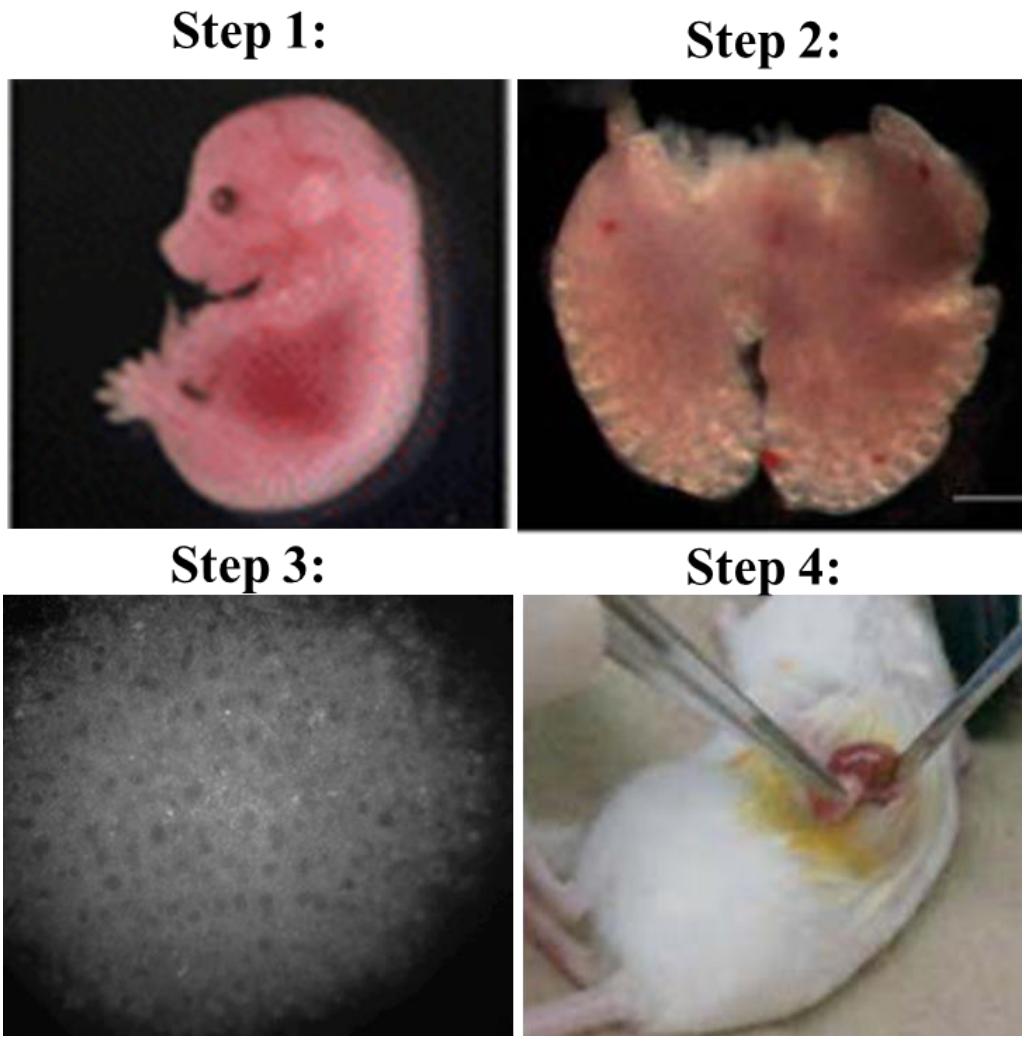

Fig. 5 Different steps of the kidney capsule model.

Step 1: isolation of E.14.5 mouse lung at day 1. **Step 2**: lung tissue digestion at day 1. **Step 3**: preparation of the pellet suspension which forms organoids after 24h in culture at 37 °C. **Step 4**: after 24h in culture, transplantation of the organoids under the kidney capsule of an immunodeficient mouse.

2.2.13. Statistical analyses

Data were assembled using GraphPad Prism software (GraphPad Software, USA) and One-way ANOVA (for comparing three or more groups) or Two-way ANOVA (for comparing different parameters in one or several groups). Data were expressed in mean ± SEM (standard error of the mean) and considered significant when the p value was less than 0.05 (*$p < 0.05$).

SECTION 3: RESULTS

3.1. Identification of BASCs in adult mouse lung tissues and in lung organoid transplants

BASC cells were identified based on the co-expression of CCSP, the bronchiolar epithelial Clara cell marker and SPC, the alveolar epithelial type 2 cell marker. BASCs were present at the bronchioalveolar duct junction (BADJ) between the terminal bronchiole and alveolar space (Fig. 6A). The higher magnification of the BADJ showed overlapping of CCSP and SPC markers in BASCs (Fig. 6B; merge). In addition, we obtained 3-dimensional images of BASCs using different focal planes within the tissue sections called z-stacks (Fig. 7A-D) which showed as well overlapping between CCSP and SPC markers in the cytoplasmic compartment. BACS were identified using and we *in vivo* lung organoid transplantation (2.2.12). Embryonic day 14.5 lung cells were cultured for 24 h in normoxic conditions and then transplanted under the kidney capsule of NOD/SCID immunodeficient mice. The organoids were grown for 6 (Fig. 8A) and 14 days (Fig. 8B), and the histological analyses of the organoid sections showed a structure which resembled to airway architecture (Fig. 8C; 8D). The immunofluorescence staining was carried out on day 14 organoid sections and showed the presence of cells which co-expressed CCSP and SPC (Fig. 9A; 9B).

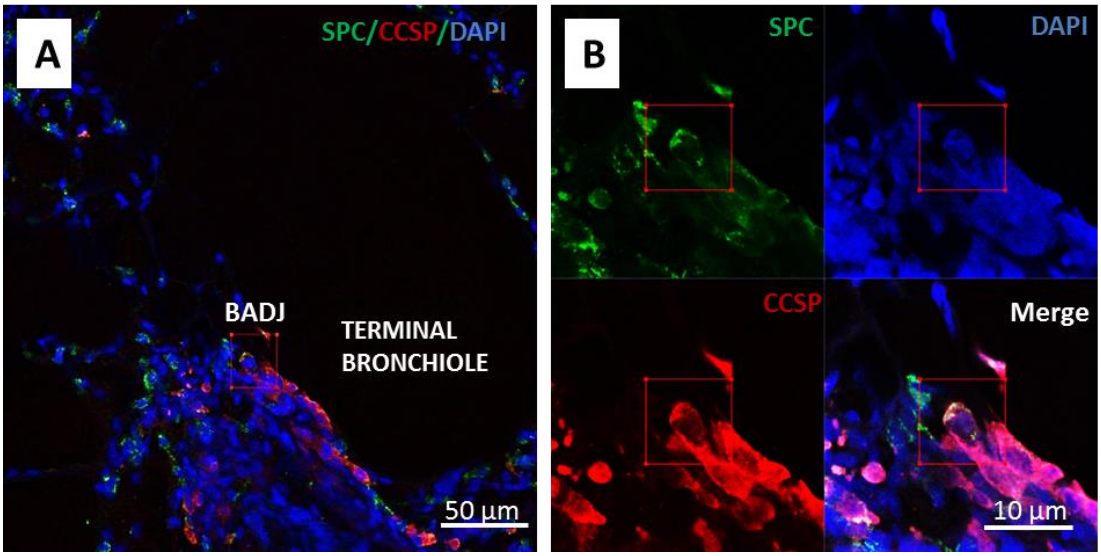

Fig. 6 Identification of BASC cells in lung tissues of adult wild type mouse.
Immunofluorescence for CCSP (red), SPC (green) and nuclear stain DAPI (blue) on mouse lung tissue. (A) Co-lacalization of CCSP and SPC at the bronchiolaveolar duct junction (BADJ) between

the terminal bronchiole and the alveolar space. (B) Higher magnification, CCSP and SPC in the cytoplasmic compartment.

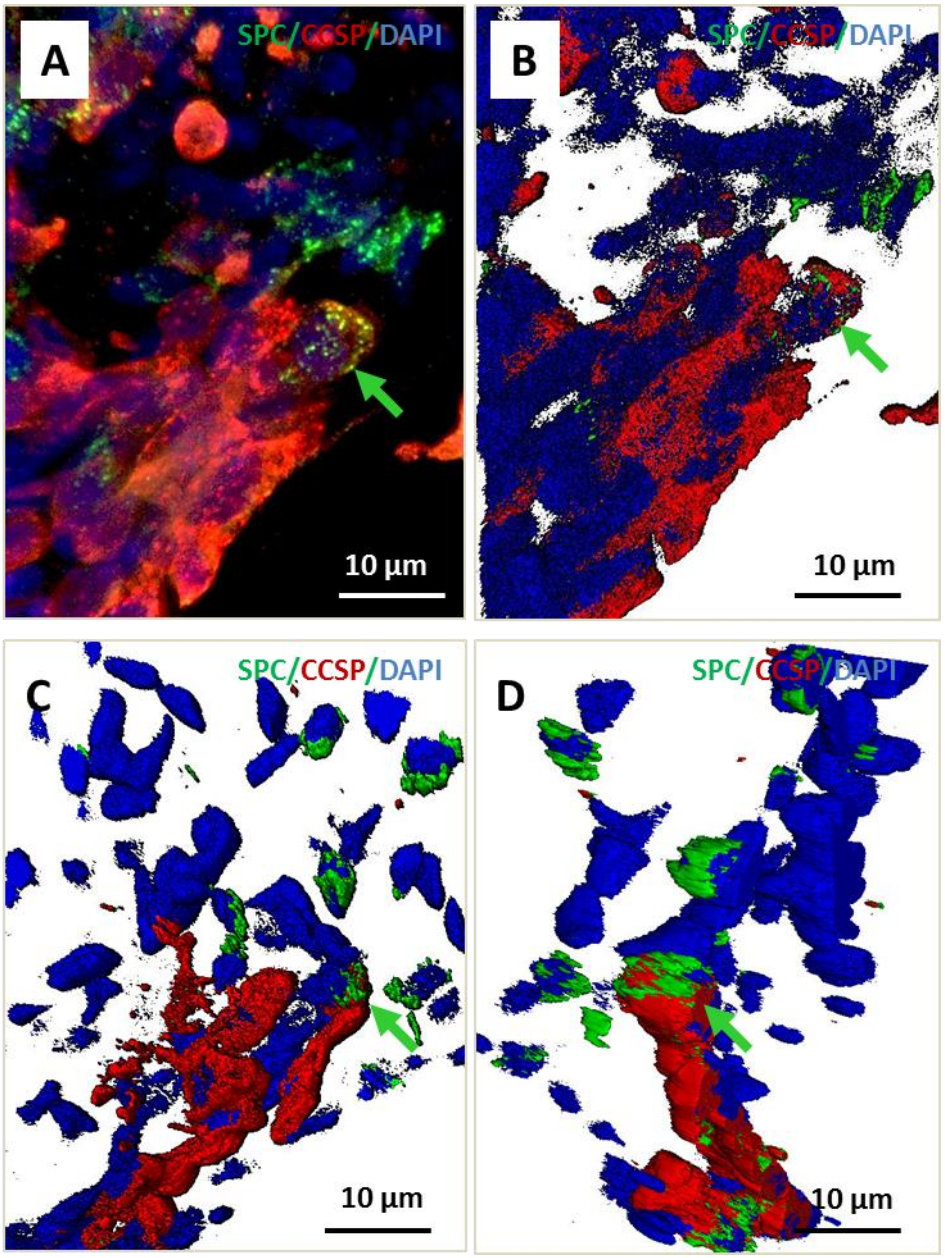

Fig. 7 3D co-localization analysis of a BASC cell.

(A), (B), (C) and (D) demonstrate a BASC cell (green arrows) in 3D images acquired using different focal planes (z-stacks) within 10 µm paraffin-embedded tissue sections of adult mouse lung. Including all focal planes, a co-localization between CCSP and SPC markers in the cytoplasmic compartment is shown.

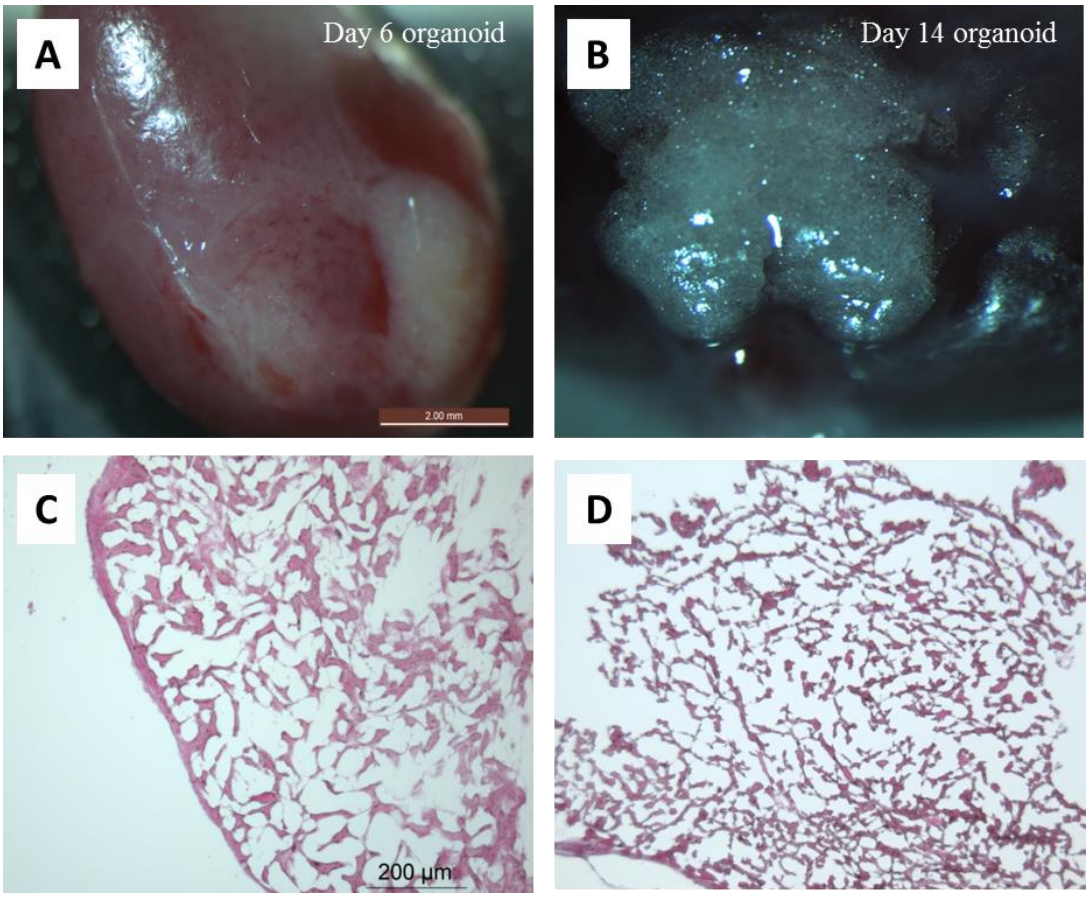

Fig. 8 Formation of organoids under the kidney capsule and staining of the organoid sections.
E.14.5 organoids under the kidney capsule of immunodeficient NOD/SCID mice. (A) Day 6 organoid under kidney capsule. (B) Day 14 organoid. (C, D) Resorcin-fuchsin staining of the organoid sections. (C) After 6 days, and (D) 14 days, organoids develop into an airway-like structure.

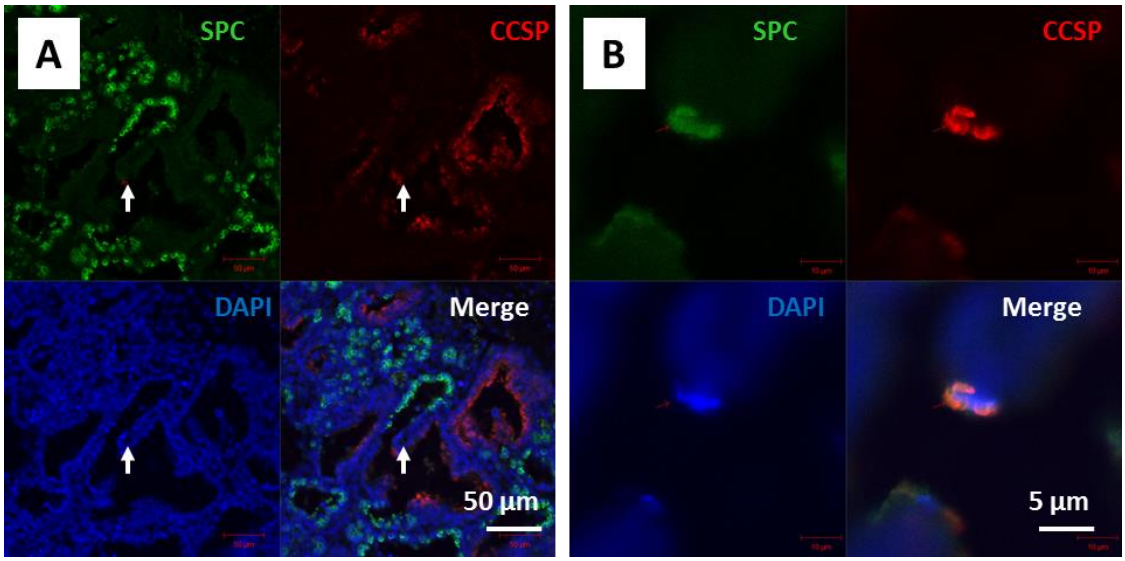

Fig. 9 Identification of BASCs in organoid sections.
(A) Paraffin embedded-sections of day 14 organoids and immunofluorescence staining for CCSP (red), SPC (green) and DAPI (blue). CCSP staining is localized in structures resembling to bronchi, SPC staining

is localized in alveolar sac-like structures. (B) CCSP/SPC dual positive cells were localized near a junction between bronchi and alveolar sacs (white arrows). (B) Higher magnification, co-localization of CCSP and SPC in the cytoplasmic compartment.

3.2. Effect of naphthalene-induced injury in adult mouse lung

Mice were treated with naphthalene, which induced bronchiolar Clara cells damage. The organs were collected at different time points. They were harvested at day 3, 6, 10 and 14 post-injury. The tissues were analyzed by light microscopy using resorcin-fuchsin staining. The tissues treated with corn oil did not present any damage of the epithelium (Fig. 10A). In contrast, tissues treated with naphthalene showed the depletion of Clara cells at day 3 post-injury (Fig. 10B). At day 6 post-injury, the bronchiolar epithelium was repopulated (Fig. 10C); the cells looked flattened compared to the corn oil where the cells showed a cuboidal shape (Fig. 10A). The same observation was made at day 10 and day 14 post-injury (Fig. 10D; 10E); the bronchiolar epithelium was regenerated and the cells displayed a flat shape. No alveolar damage was observed on the tissues treated with naphthalene in comparison to the corn oil control tissues. To support the histological analyses, real-time PCR reaction was run with day 3, 7, 14 and 21 post-injury samples (these samples were kindly provided by Prof. Dr. Saverio Bellusci from the Excellence Cluster Cardio-Pulmonary-System, Justus-Liebig-University, Giessen) and the data obtained confirmed that the levels of CCSP expression were significantly decreased at days 3 post-injury and re-increased gradually from day 7 till day 21 post-injury; and 80 % of Clara cells recovery was thus obtained at day 21 post-injury (Fig. 11).

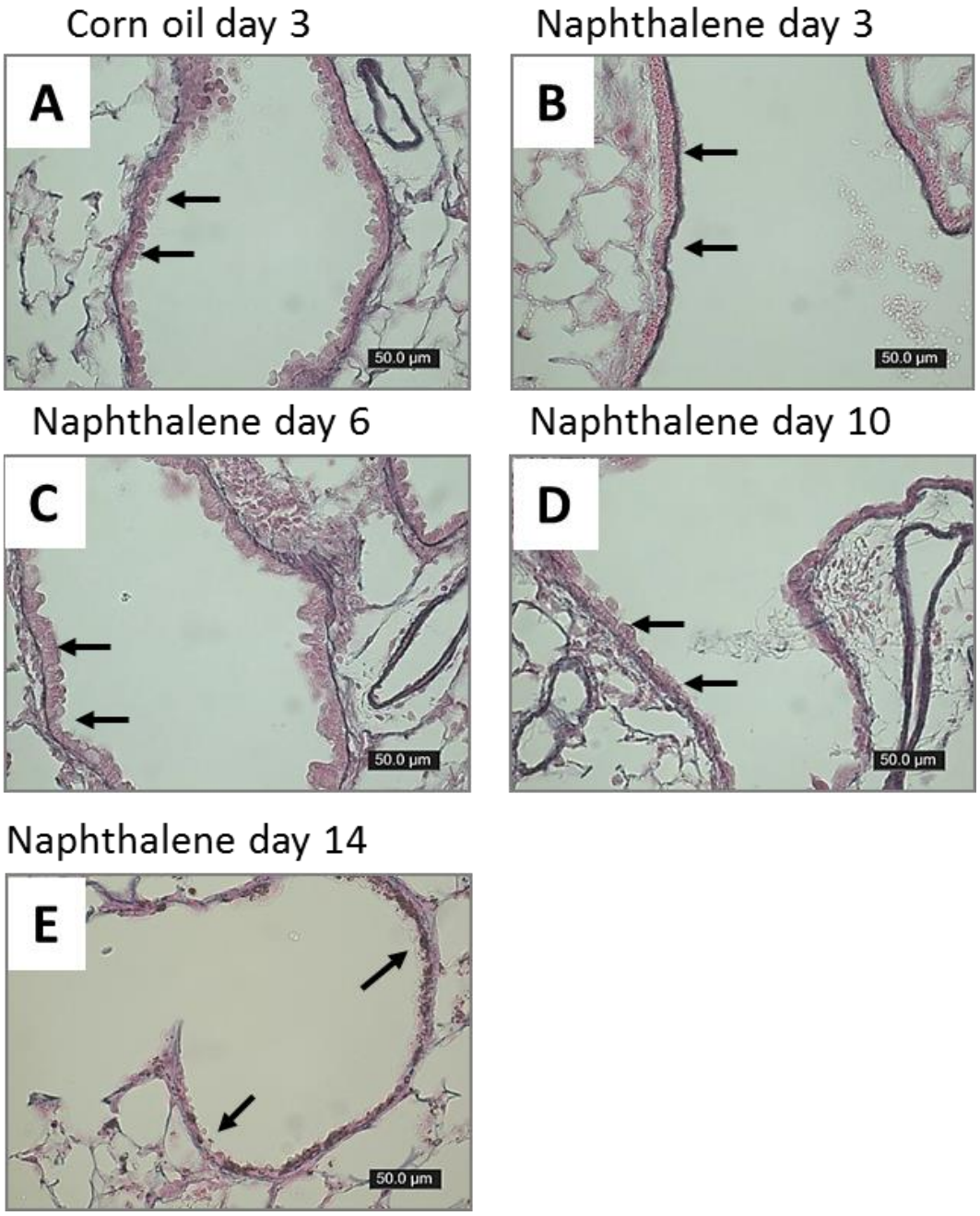

Fig. 10 Resorcin-fuchsin staining of mouse lung tissues after naphthalene injury.

Lung from adult wild type mice after corn oil treatment and naphthalene treatment. (A) Corn oil after 3 days shows a normal epithelium (arrows). (B) Naphthalene treatment after day 3 shows epithelial damages (arrows). (C) Day 6 post-injury shows a repopulated epithelium (arrows). Note that the cells have a flat shape compared to the corn oil. (D) Day 10 post-injury, the epithelium is repopulated (arrows). (E) Day 14 post-injury, the epithelium is repopulated (arrows).

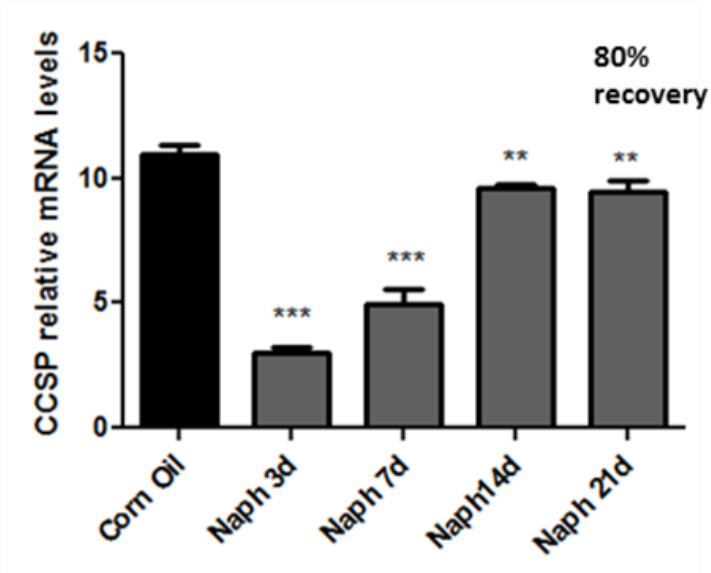

Fig. 11 mRNA levels of CCSP at different time points after naphthalene injury. Level of CCSP expression after corn oil treatment and naphthalene treatment in adult wild type mouse lung. CCSP expression decreased significantly after 3 days post-injury and increase till 21 days post- injury. Note that at day 21, 80 % of CCSP expression was recovered. Data are expressed in mean ± SEM and $n \geq 3$. **$p < 0.01$; *** $p < 0.001$.

3.3. BASCs and Clara cells are damage resistant and proliferate upon naphthalene injury

Immunofluorescence analyses were carried out on tissues embedded with paraffin after naphthalene injury and demonstrated that BASCs and Clara cells were damage-resistant (Fig. 12). As we did not see a clear difference between day 10 and day 14 post-injury in histological analyses with resorcin-fuchsin staining described in the previous paragraph, the data were collected only at day 3, 6, and 10 post-injury. Staining based on BASCs markers and PCNA, a marker for the detection of proliferating cells was performed. As seen in the Fig. 12A, at day 3 post-injury, the tissues treated with corn oil were intact. The tissues treated with naphthalene showed a depletion of Clara cells everywhere except at the BADJ where BASCs reside, and also at the neuroendocrine cell-associated Clara cells area; the damage resistant Clara and BASCs proliferated as they expressed PCNA in the nuclear compartment (Fig. 12B). At day 6 post-injury, Clara cells continued to express PCNA but BASCs did not express the marker anymore (Fig. 12C, 12D). A close look in the alveolar region at day 6 post-injury revealed the presence of clusters of Clara cells and BASCs. As observed in the bronchiolar epithelium, Clara cells expressed PCNA and BASCs did not (Fig.12E; 12F). At day 10 post- injury, the staining demonstrated one more time that BACS stopped to express PCNA and Clara cells were still expressing PCNA (Fig.13). Others analyses including flow cytometry and real-time PCR were performed. Flow cytometric analyses showed that the number of Clara cells (Fig. 14A) and BASCs (Fig. 14B) in lung homogenates were significantly increased at day 6 post-injury and then decreased at day 10 and 14 post injury.

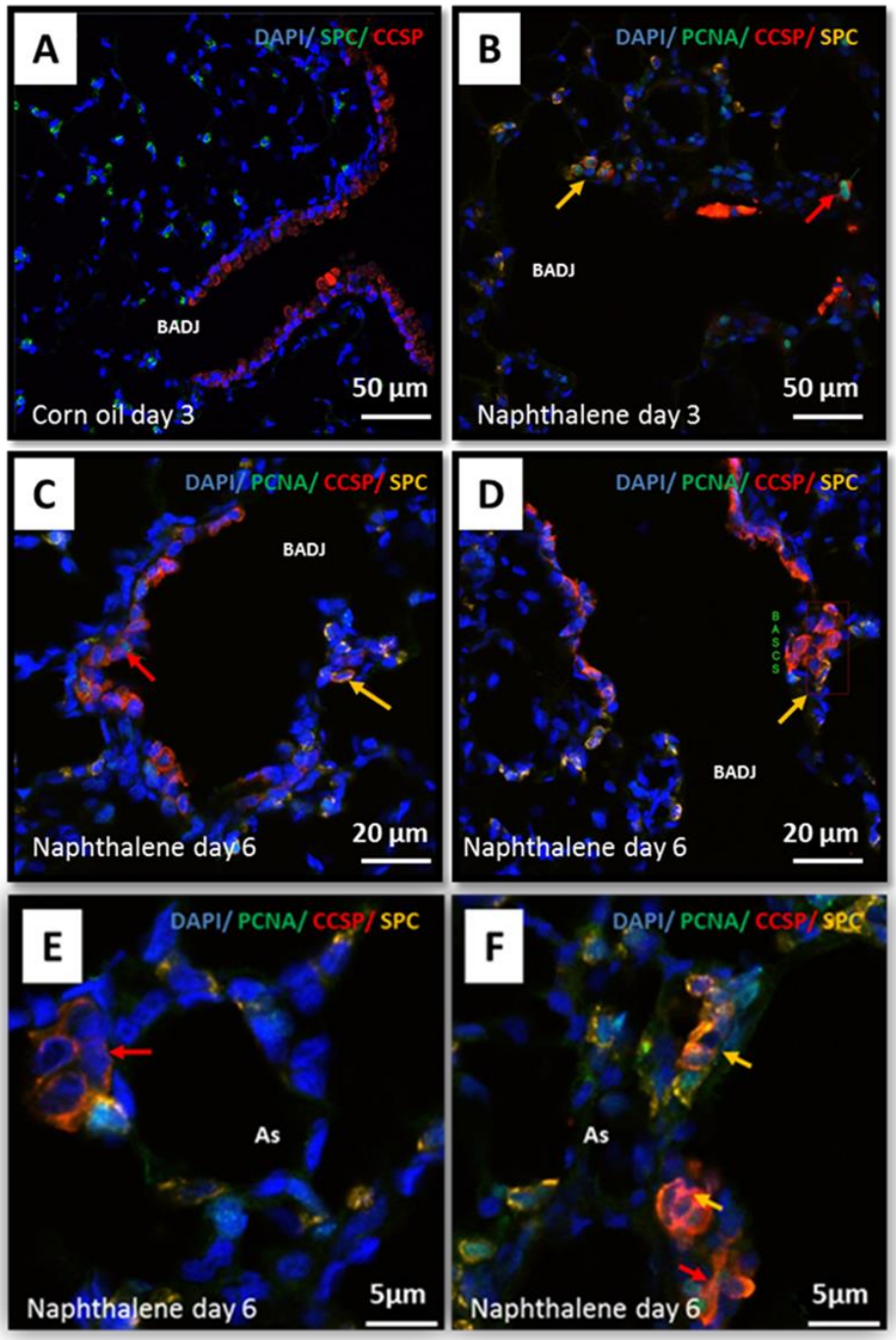

Fig. 12 Immunofluorescence of mouse lung tissues after naphthalene injury.

Immunofluorescence of adult lungs harvested after 3 and 6 days post-injury, processed with paraffin and stained with CCSP (red), SPC (yellow), PCNA (green), and DAPI (blue). (A) Corn oil at day 3 post-injury, no damage seen on tissue. (B) Day 3 post-injury, depletion of Clara cells. Clara cells (red arrow) and BASCs (yellow) are resistant to injury and express PCNA (green). (C) Day 6 post injury, the bronchiolar epithelium is regenerated. PCNA is expressed in Clara cells. (D) Day 6 post injury, PCNA is not expressed in BASCs (yellow arrow). (E) Day 6 post injury, Clara cell organized in cluster (red arrow) in the alveoli do no express PCNA. (F) Day 6 post- injury, Clara cells and BASCs organized in clusters in the alveoli. PCNA is expressed in Clara cells (red arrow) but not in BASCs (yellow arrow).

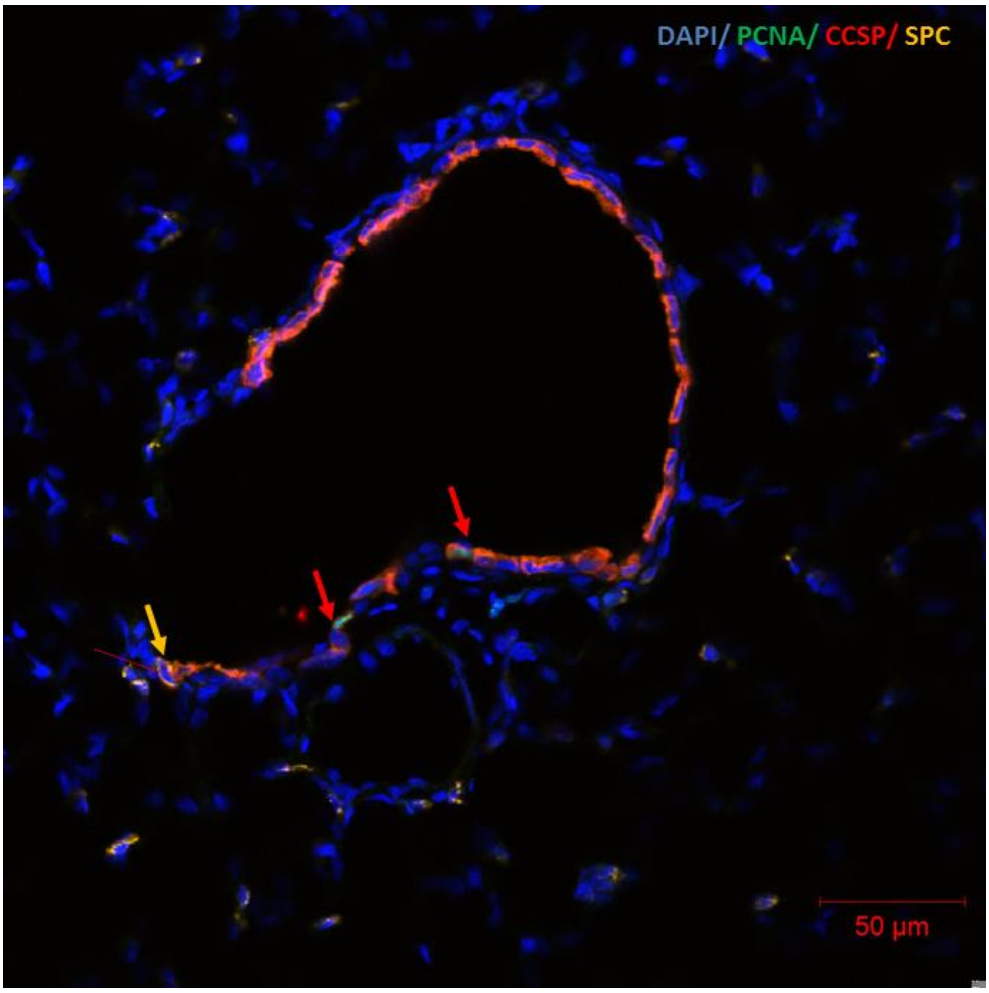

Fig. 13 Immunofluorescence of adult mouse lung tissues 10 days post-injury.
Immunofluorescence of adult lungs harvested after 10 days post-injury, processed with paraffin and stained with CCSP (red), SPC (yellow), PCNA (green), and DAPI (blue). The bronchiolar epithelium is regenerated; PCNA is expressed in Clara cells (red arrows) but not in BASCs (yellow arrow).

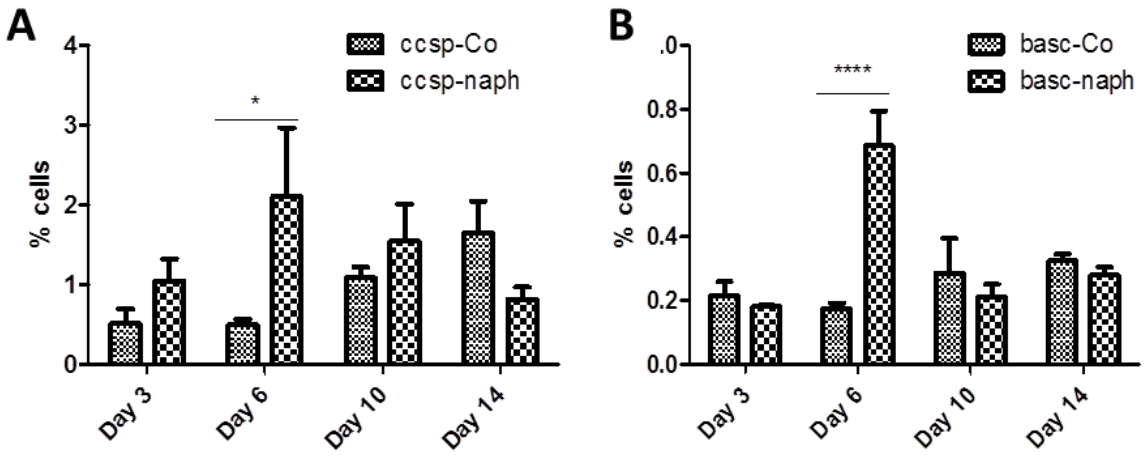

Fig. 14 Flow cytometric analyses and quantification of Clara cells and BASCs after naphthalene. Adult mouse lungs were isolated 3, 6, 10 and 14 days after treatment with corn oil (Co) or naphthalene (naph). Cell suspensions were incubated with CCSP, SPC and appropriates secondary antibodies. (A) Relative number of Clara cells. (B) Relative number of BASCs. Data are expressed in mean ± SEM and $n \geq 3$. *$p < 0.05$; **** $p < 0.0001$. ccsp-Co: cells from corn oil-treated mice and stained with CCSP; ccsp-naph: cells from naphthalene-treated mice and stained with CCSP; basc-Co: cells from corn oil-treated mice and co-stained with CCSP and SPC; basc-naph: cells from naphthalene-treated mice and co stained with CCSP and SPC.

3.4. BASCS and Clara cells proliferate after pneumonectomy

Pneumonectomy (PNX) was carried out on adult mice. The left lung was resected. The organs were harvested at day 3 and day 7 post-operation and histological analyses were performed on paraffin-embedded sections. The tissues were stained with BASCs markers and PCNA. The results showed that at day 3 post-operation, there was no proliferation observed neither in Clara cells, alveolar type 2 cells nor in BASCs since they were not expressing PCNA (Fig. 15A). On the contrary, at day 7 post-operation, all cell types did express PCNA in the nuclear compartment (Fig.15B).

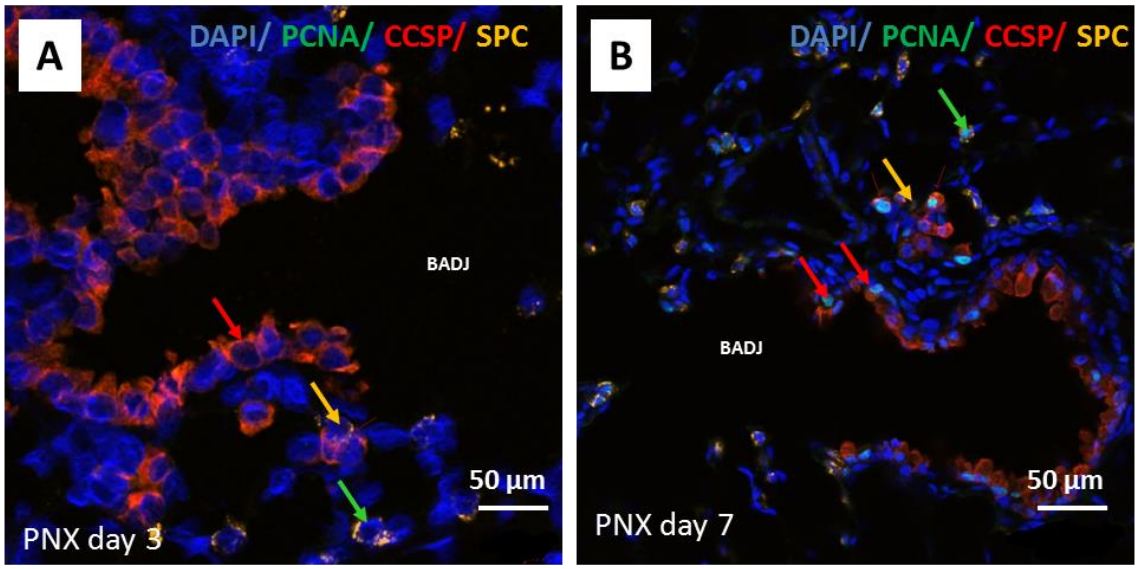

Fig. 15 Immunofluorescence of adult mouse lung tissues after pneumonectomy.

After pneumonectomy (PNX), lungs were isolated at day 3 and 7 post- surgery. The lung were embedded in paraffin and co-stained with CCSP (red), SPC (yellow), PCNA (green) and DAPI (blue). (A) Day 3 post- surgery neither Clara cells (red arrow), alveolar type 2 cells (green arrows) nor BASCs (yellow arrow) were positive for PCNA. (B) Day 7 post injury, Clara cells, alveolar type 2 cells and BASCs were positive for PCNA.

3.5. Evidence of BASCs as stem/progenitor cells of adult mouse lung

3.5.1. Relation of BASCs to EpCAM^{high}CD24^{low} epithelial stem/progenitor cells in adult wild type mice

FACS analyses, cytospin and clonogenic assays of epithelial stem/progenitors cells (ESPCs) (1.8) were carried out to determine the relation of BASCs to ESPCs. The cells isolated from adult mouse lungs were stained for CD45 and CD31 to exclude the hematopoietic cells and the endothelial cells. EpCAM (epithelial cell adhesion marker), a marker of epithelial cells and CD24 mostly found at the surface of B lymphocytes and granulocytes, were used to discriminate ESPCs from others mouse lung cell types. The EpCAM^{high}CD24^{low} cell fraction was isolated via FACS. Cells were cytospun or cultured in 3D matrigel cultures. Using FACS analysis, the EpCAM^{high}CD24^{low} cell fraction was gated (Fig. 16) .DAPI was used to exclude dead cells (Fig. 16A). CD45 and CD31 FITC-labeled cells were as well excluded (Fig. 16B) and EpCAM Cy7-labeled positive cell positive fraction was set for EpCAM^{high}CD24^{low}. CD24 cells were labeled with PercP (Fig. 16C). Immunofluorescence after cytospin showed that the EpCAM^{high}CD24^{low} cell fraction contained BASCs based on their co-expression for CCSP and SPC (Fig. 16D: merge image). The sorted cells were also used for clonogenic assay on matrigel cultures. After 7 days in hypoxic culture conditions, the matrigel cultures were stained. The assays showed different type of colonies (Fig. 17). Some colonies were expressing neither CCSP nor SPC (Fig. 17A); some were expressing only SPC (Fig.17B) or CCSP (Fig.17C) and others were co-expressing both CCSP and SPC identified as BASCs colonies (Fig. 17D).

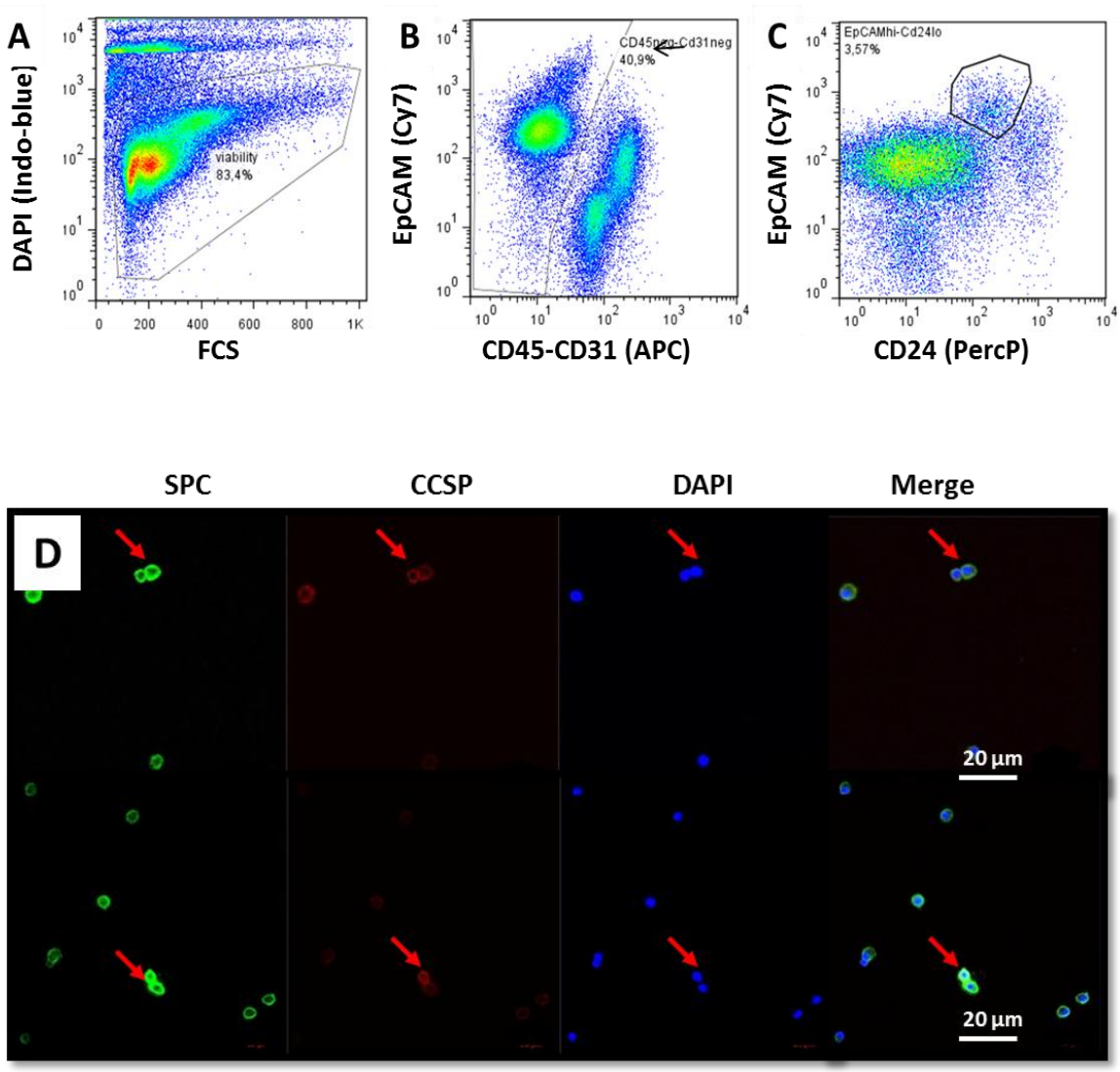

Fig. 16 FACS analyses and immunofluorescence of sorted ESPCs from adult wild type mice.

For flow cyometric analyses, whole lungs cell of adult mouse lung were isolated. The cell suspension was incubated with APC labeled CD45 and CD31, PE-Cy7 labeled EpCAM and PercP labeled CD24. (A) Dot plot representation of dead cells exclusion (DAPI positive cells). (B) Dot plot representation of CD45 and C31 positive cells exclusion (EpCAM negative cells); EpCAM positive cells represent a percentage of 40.9 % of the total epithelial cell population (EpCAM positive cells). (C) Dot plot representation of $EpCAM^{high}CD24^{low}$ epithelial stem/progenitor cell population (ESPCs) which represent 3.57% of the total epithelial cell fraction (EpCAM positive cells). (D) The $EpCAM^{high}CD24^{low}$ EPSC cell population was sorted and cytospun. The immunofluorescence of $EpCAM^{high}CD24^{low}$ EPSC cell population reveals the presence of dual CCSP/SPC positive cells which represent BASCs (red arrows and merge).

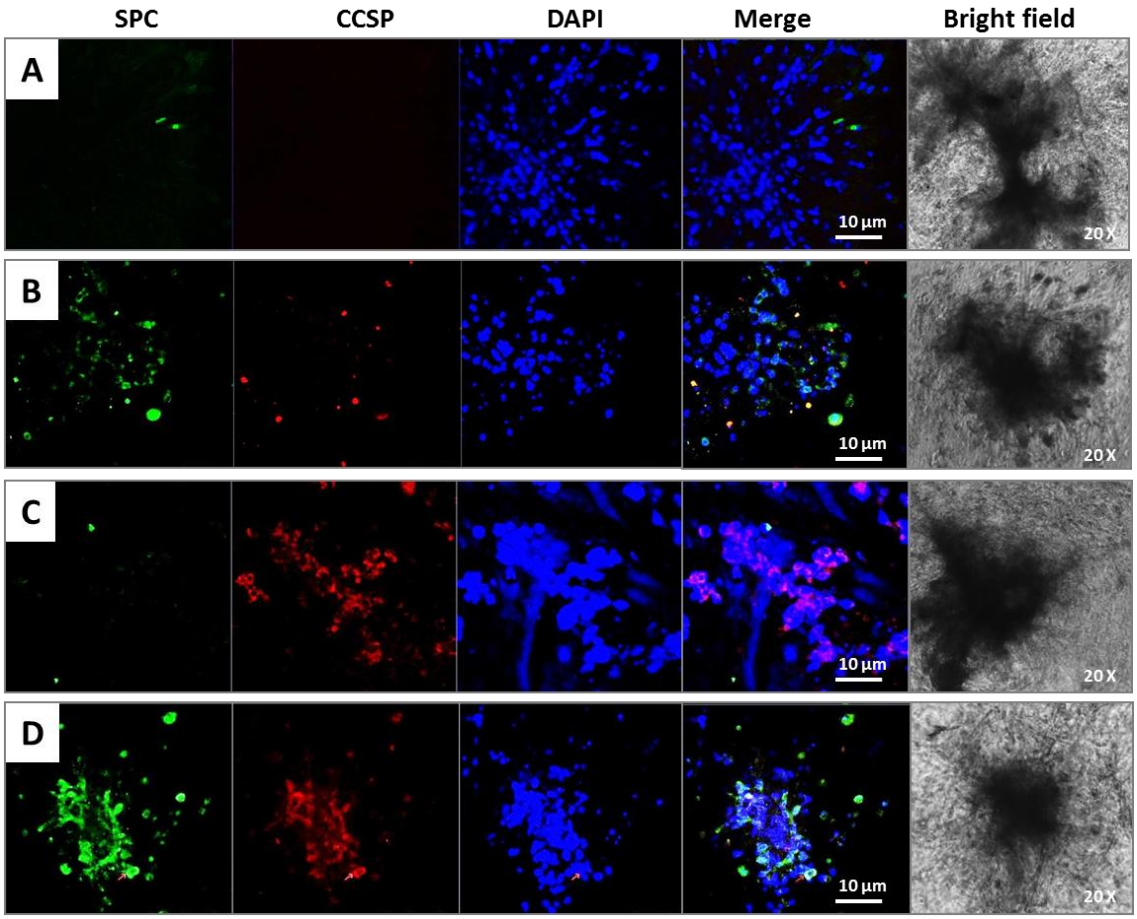

Fig. 17 Clonogenic assays of sorted ESPCs based on EpCAM^{high}CD24^{low} in the presence of matrigel. After EpCAM^{high}CD24^{low} EPSC cell population was sorted and cultured in presence of matrigel under hypoxic conditions (1% O2), ESPCs generate different size of colonies after 7 days in culture (see A, B, C and D bright field image). (A) The immunofluorescence analyses reveal that the bigger colonies are negative for SPC and CCSP. (B) The intermediate sized colonies include SPC expressing alveolar type 2 cells or (C) CCSP expressing Clara cells). (D) The smaller colonies include double positive CCSP/SPC expressing BASCs.

3.5.2. Relation of BASCs to EpCAM^{high}CD24^{low} ESPCs in transgenic mice

Single and double transgenic knock in mice expressing YFP and mCherry fluorescent proteins under the control of SPC and CCSP promoters respectively were used. Lines were created and kindly provided by Dr. Marten Szibor, MPI Bad Nauheim. CCSP-mCherry mouse line was used to detect Clara cells based on mCherry endogenous fluorescence. SPC-YFP mouse line was used for the detection of alveolar type 2 cells based on YFP endogenous fluorescence, and the double transgenic CCSP-mCherry/SPC-YFP for BASCs detection. ESPCs fraction was gated based on EpCAM^{high}CD24^{low} (Fig. 18) expression. Dead cells were excluded with DAPI (Fig. 18A); hematopoietic and endothelial cells were excluded with CD45-CD31 labeled with APC. EpCAM positive cell fraction represented 20.6 % (Fig. 18B) of the whole lung cell population. EpCAM^{high}CD24^{low} labeled with Cy7 and PercP represented 1.23 % of the total EpCAM positive cell fraction (Fig. 18C). Within the EpCAM positive cell fraction (Fig. 18B), CCSP-mCherry expressing Clara cells represented 3. 03 % of the total EpCAM positive cell population (Fig. 19B) and 29.7 % of the 3.03 % were EpCAM^{high}CD24^{low} positive ESPCs (Fig. 19C). The same analysis was achieved for SPC-YFP expressing alveolar type 2 cells which represented 21.3 % of the total EpCAM positive cell population (Fig. 20A); the relation of SPC-YFP to EpCAM^{high}CD24^{low} showed that only 1.32 % of the 21.3 % SPC cells were EpCAM^{high}CD24^{low} positive ESPCs (Fig. 20B). CCSP-mCherry/SPC-YFP double positive BASCs represented a small fraction of 0.142 % cells of the total EpCAM positive cell population (Fig. 21B). The analysis of EpCAM^{high}CD24^{low} (Fig. 22A) using these double transgenic mice revealed that this population was highly enriched in CCSP expressing Clara cells (66.7 %), but SPC expressing alveolar type 2 cells (14 %) and BASC cells (8.77 %) were less abundant (Fig. 22B).

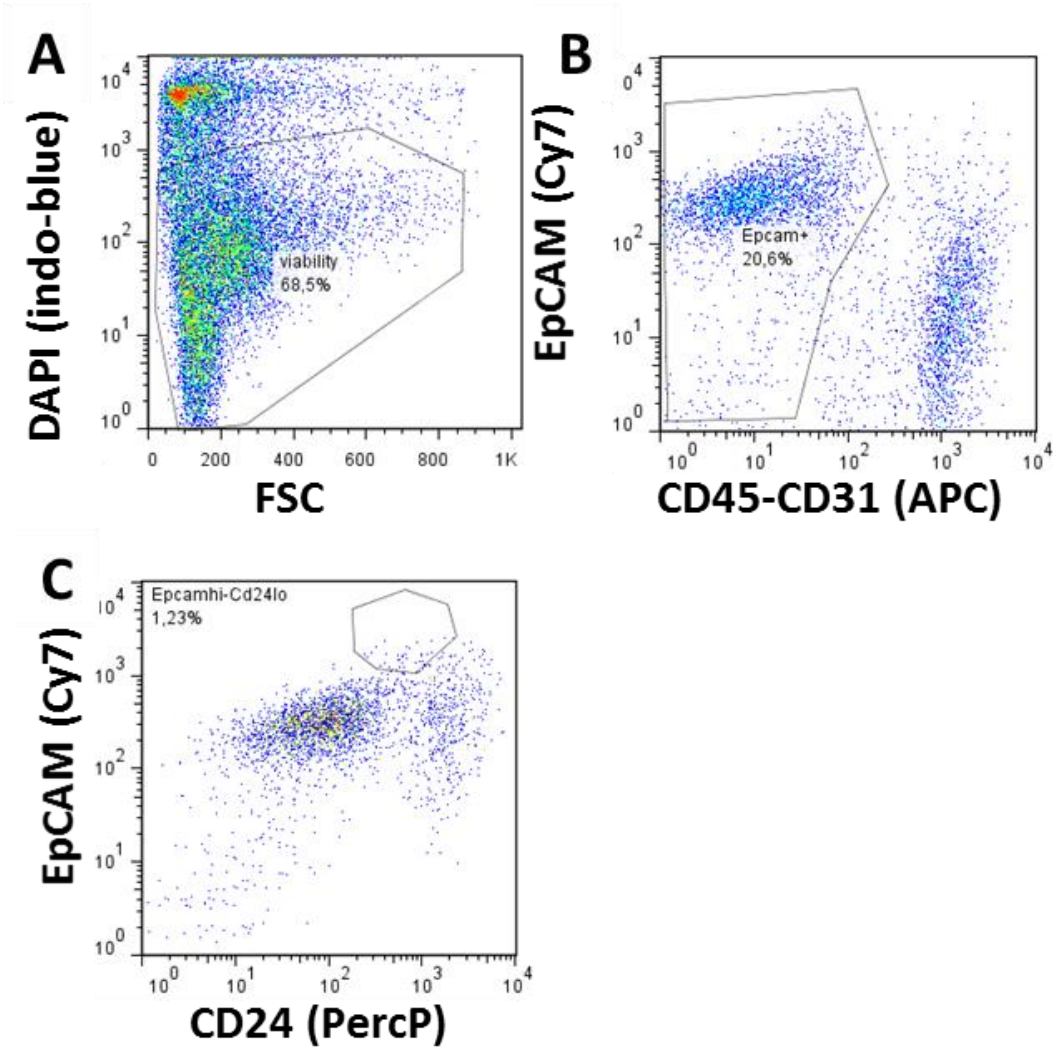

Fig. 18 Identification of EpCAM^{high}CD24^{low} cell population in CCSP-mCherry/SPC-YFP transgenic knock in mice.

Cells from double transgenic mice expressing mCherry and YFP fluorescent proteins under the control of CCSP and SPC promoter were isolated and analyzed by flow cytometry. (A) Exclusion of dead cells positive for DAPI. (B) Exclusion of CD45 and CD31 positive cells labeled with APC. EpCAM positive cells labeled with PE-Cy7 represent a percentage of 20.9 %. (C) Dot plot representation of EpCAM^{high}CD24^{low} EPSC cell population which represent 1.23 % of the total epithelial cell fraction (EpCAM positive cells).

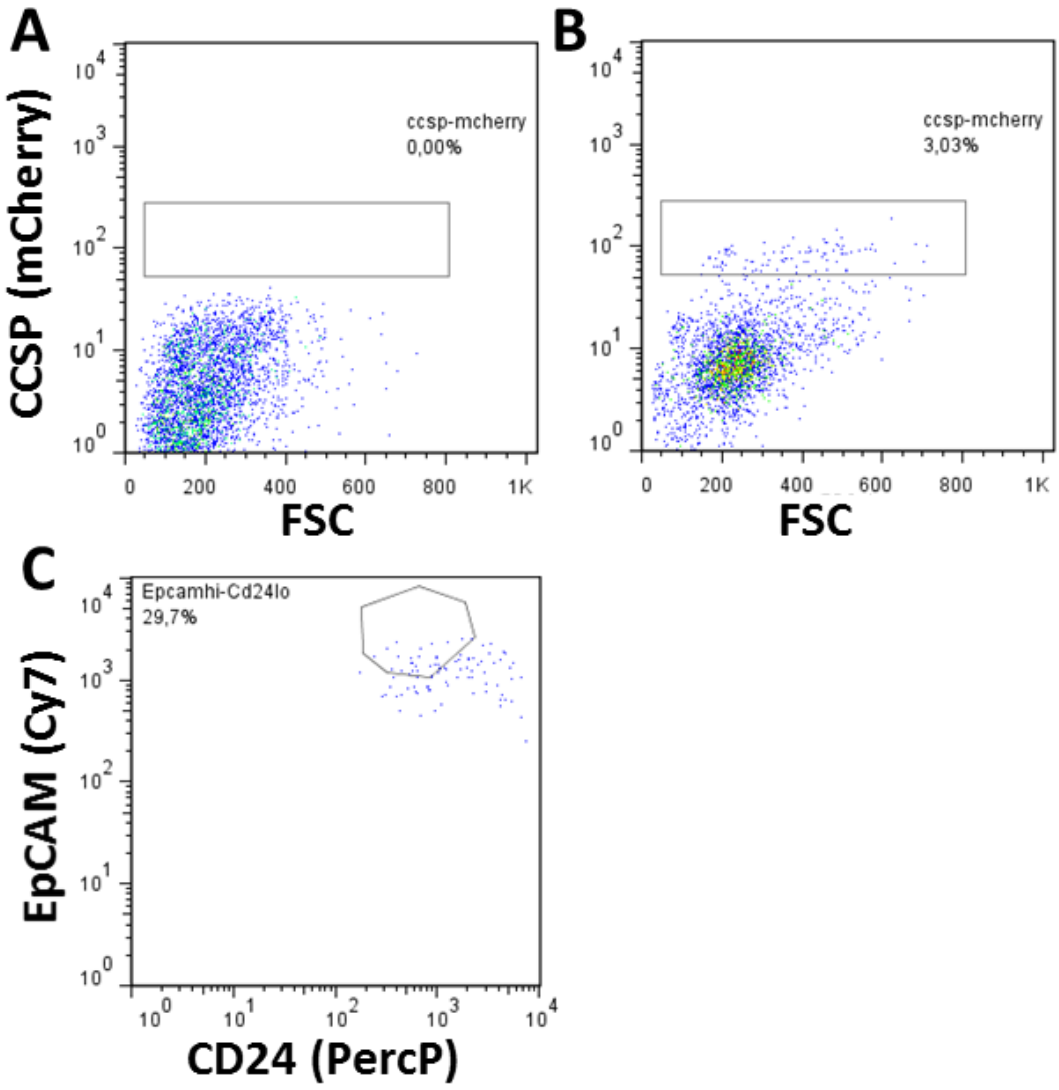

Fig. 19 A cell fraction of CCSP-mCherry positive cells is EpCAM^{high}CD24^{low}.

Cells from transgenic mice expressing mCherry fluorescent protein under the control of the CCSP promoter were isolated and analyzed by flow cytometry. (A) Negative control with unstained cells. (B) CCSP-mCherry expressing Clara cells represent 3.03 % of EpCAM positive cells (not shown but the same gating as in Fig.18B was used). (C) In the fraction of 3.03 %, 29.7 % of CCSP-mCherry positive cells are EpCAM^{high}CD24^{low} epithelial stem/progenitors cells (ESPCs).

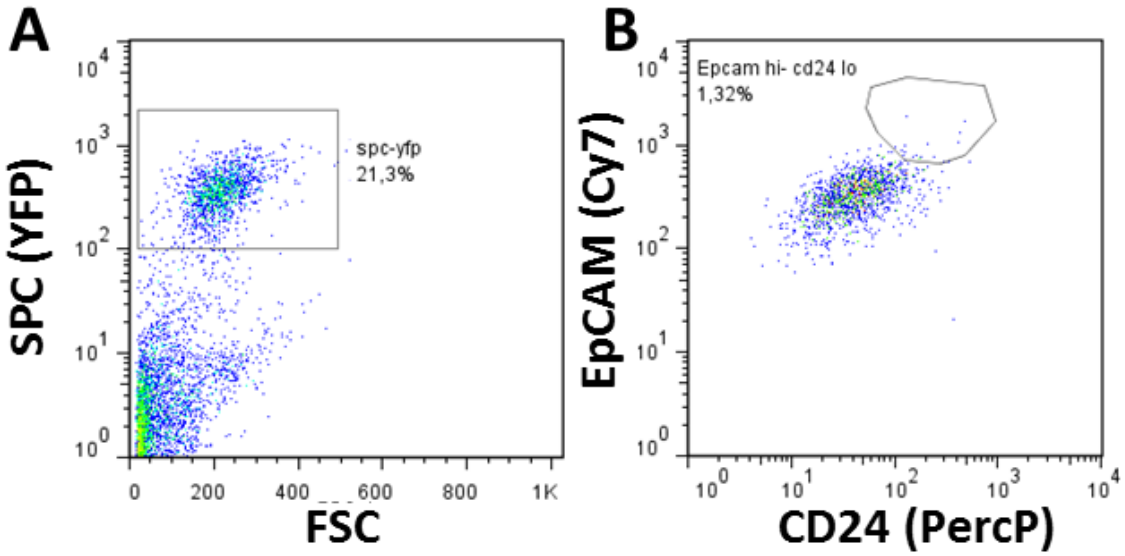

Fig. 20 A cell fraction of SPC-YFP positive cells is EpCAM^{high}CD24^{low}.

Cells from transgenic mice expressing YFP fluorescent protein under the control of the SPC promoter were isolated and analyzed by flow cytometry. (A) SPC-YFP expressing alveolar type 2 cells represent 21.3 % of EpCAM positive cells (not shown but the same gating as in Fig.18B was used). (B) In the fraction of 21.3 %, 1.32 % of SPC-YFP positive cells are EpCAM^{high}CD24^{low} epithelial stem/progenitors cells (ESPCs).

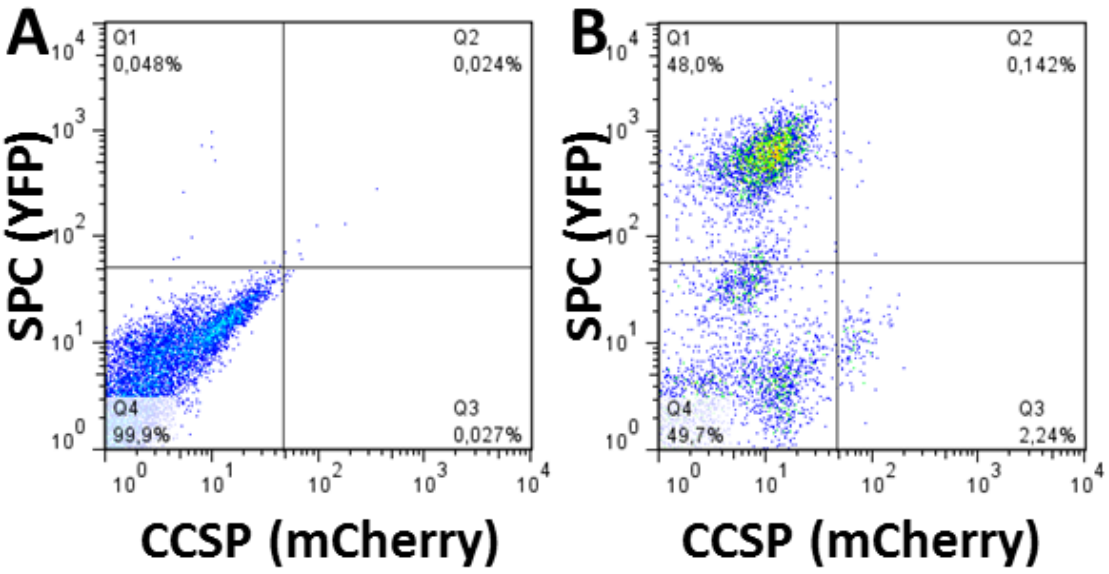

Fig. 21 Identification of BASCs in CCSP-mChrerry/ SPC-YFP double transgenic knock in mice.

Cells from double transgenic mice expressing mCherry and YFP fluorescent proteins under the control of CCSP and SPC promoter were isolated and analyzed by flow cytometry. (A) Negative control with unstained cells. (B) CCSP-mCherry/SPC-YFP expressing BASCs represent 0.142 % of EpCAM positive cells (not shown but the same gating as in Fig.17B was used)

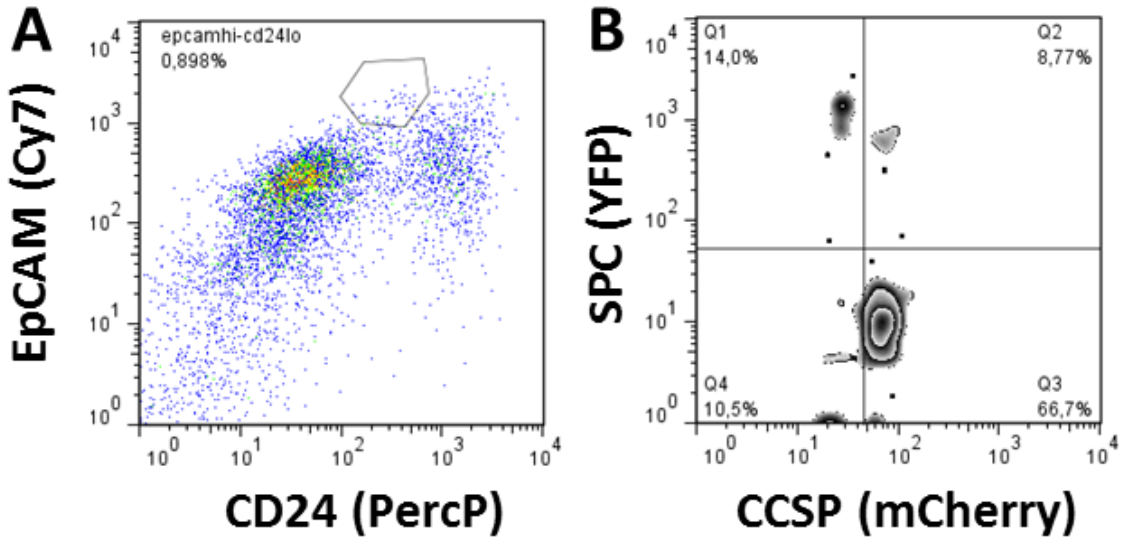

Fig. 22 BASCs are included in EpCAM^{high}CD24^{low} cell population.

Cells from double transgenic mice expressing mCherry and YFP fluorescent proteins under the control of CCSP and SPC promoter were isolated and EpCAM^{high}CD24^{low} ESPC cell population was analyzed. (A) Representative dot plot of EpCAM^{high}CD24^{low} ESPC cell population gating. (B) The analysis of the EpCAM^{high}CD24^{low} ESPC cell population in the four-quadrant contour plot displays 14 % of SPC-YFP expressing alveolar type 2 cells (Q1), 66.7% of CCSP-mCherry expressing clara cells cells (Q3) and 8.77 % of double SPC-YFP/CCSP- mCherry positive cells which are BASCs (Q2).

3.6. BASCs do not express Oct4

Paraffin-embedded tissues sections from Oct4^{GFP} transgenic mouse lungs were stained. CCSP, SPC were used to identify BASCs. GFP was used to identify Oct4 in order to determine the stemness of BASCs. The data showed the presence of BASCs at the BADJ co-expressing CCSP and SPC, but Oct4 was not expressed in these cells (Fig. 23).

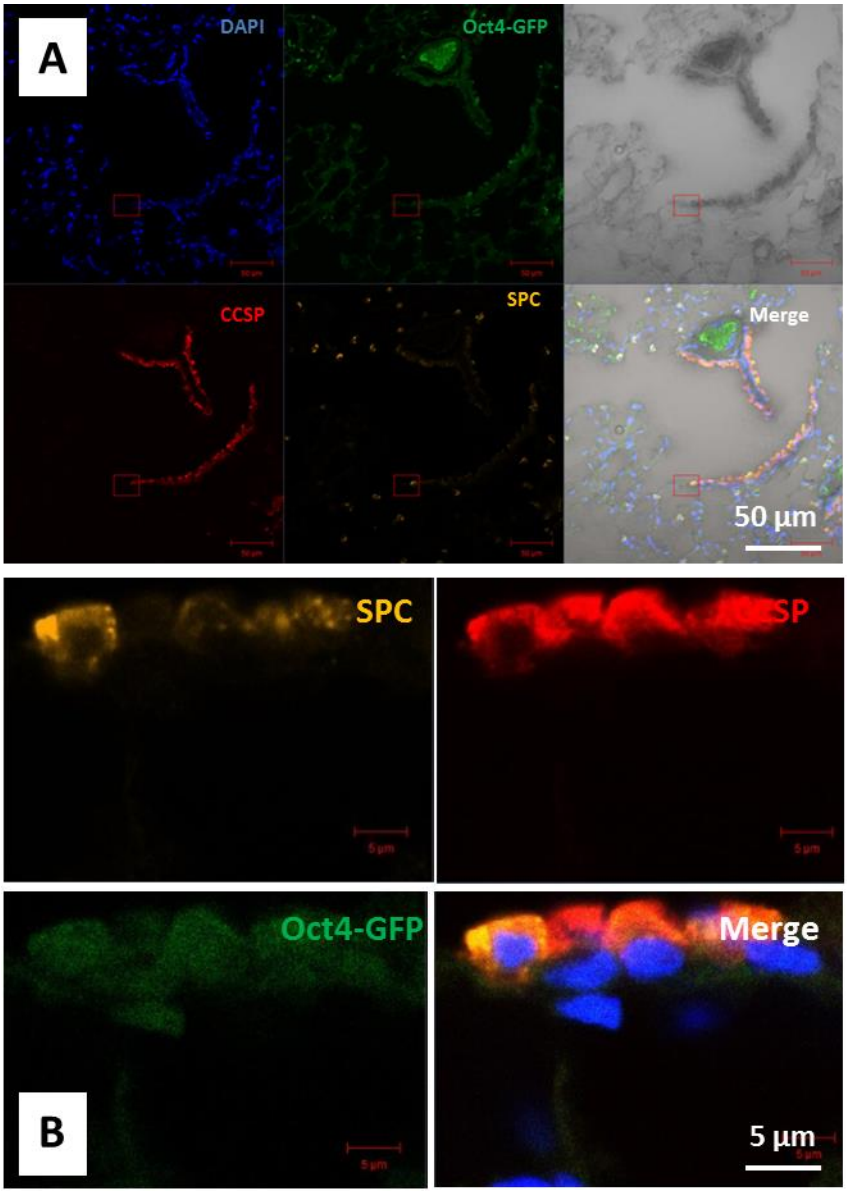

Fig. 23 Immunofluorescence analysis of Oct4 expression in BASCs. Oct4^{GFP} adult mouse lung were isolated; the tissues were embedded in paraffin and stained with CCSP (red), SPC (yellow), GFP (green) and DAPI (blue. (A) BASCs were identified at the BADJ (red square). (B Higher magnification of BASCs, Oct4 is not expressed in BASCs.

3.7. Identification of Oct4 in adult mouse lung tissues

3.7.1. Oct4 is expressed in adult mouse lung tissues

Western blot analyses were performed to detect the expression of Oct4 in whole lung cell lysate. Samples from adult wild type and Oct4^{GFP} transgenic mice were used. A band of 50 kDA was detected using Oct4 antibody in wild type cell lysate (Fig. 24A) and a band of 27 kDa was detected with the GFP antibody in transgenic cell lysate (Fig. 24B).

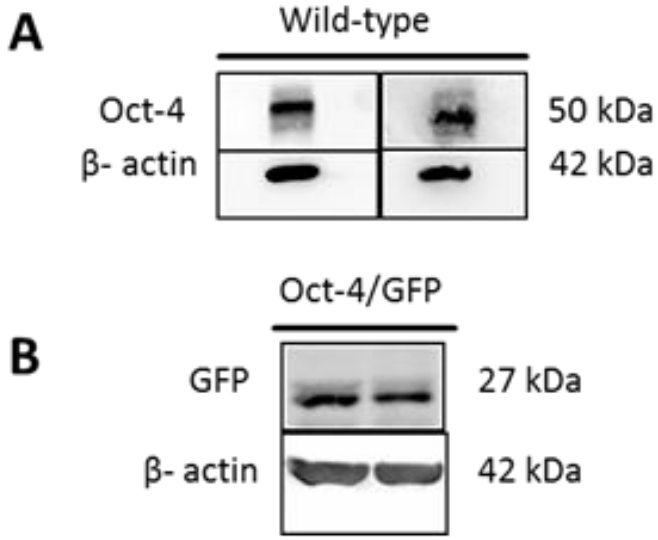

Fig. 24 Western blot of Oct4 in adult wild type mice and Oct4^{GFP} in adult transgenic mice from lung.

Protein was isolated from whole lung homogenate of adult wild type mice and adult Oct4^{GFP} transgenic mice respectively. (A) Oct4 detection shows a band size of 50 kDa (predicted molecular weight: 39-45 kDa). (B) Oct4-GFP shows a band size of 27 kDa (predicted molecular weight: 27 kDa).

3.7.2. Oct4 is expressed in perivascular and peribronchial spaces of adult mouse lung tissues and displays expression patterns like telocyte localization

The 3'3-diaminobenzinine (DAB) staining and immunofluorescence on paraffin embedded tissues sections were carried out to determine the location of Oct4. The two methods revealed the presence of Oct4 at the telocyte location in perivascular and peribronchial spaces (Fig. 25; Fig. 26). DAB staining gave a dark brown color. Oct4 was identified around the bronchus (Fig. 25A) and around the blood vessels (Fig. 25B). The immunofluorescence analysis using Oct4^{GFP} transgenic mouse line showed that the cells expressing Oct4 displayed telocyte features. The showed long extensions called telopodes which seem to create contacts between two cells (Fig. 26).

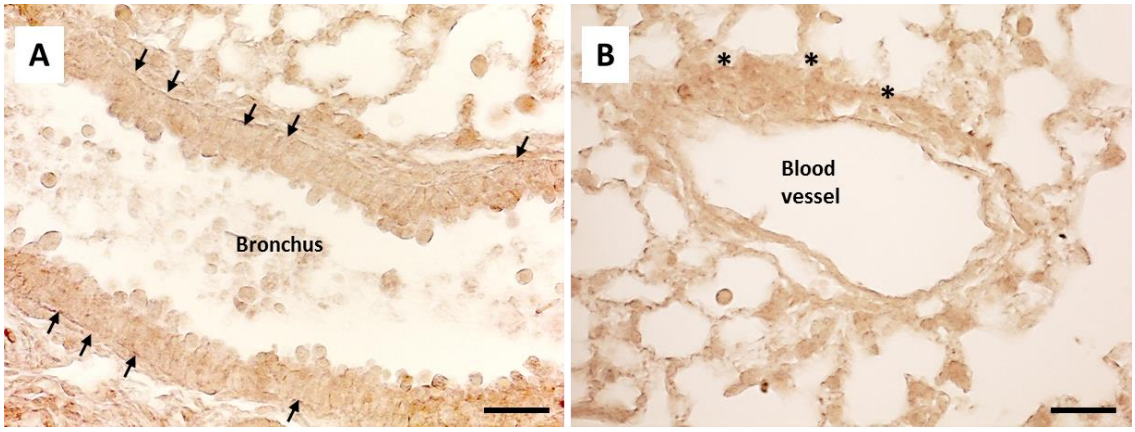

Fig. 25 Immunohistochemical staining of Oct4 in adult wild type mouse lung.

Lung from adult wild type mice embedded in paraffin and stained with anti-Oct4. (A, B) the dark brown coloration marked with arrows and asterix represents Oct4 expression on DAB-labeled tissues. (A) The staining reveals the expression of Oct4 around the bronchiolar epithelium (black arrows). (B) Expression of Oct4 around the blood vessels (black asterix). Bar = 50 µm.

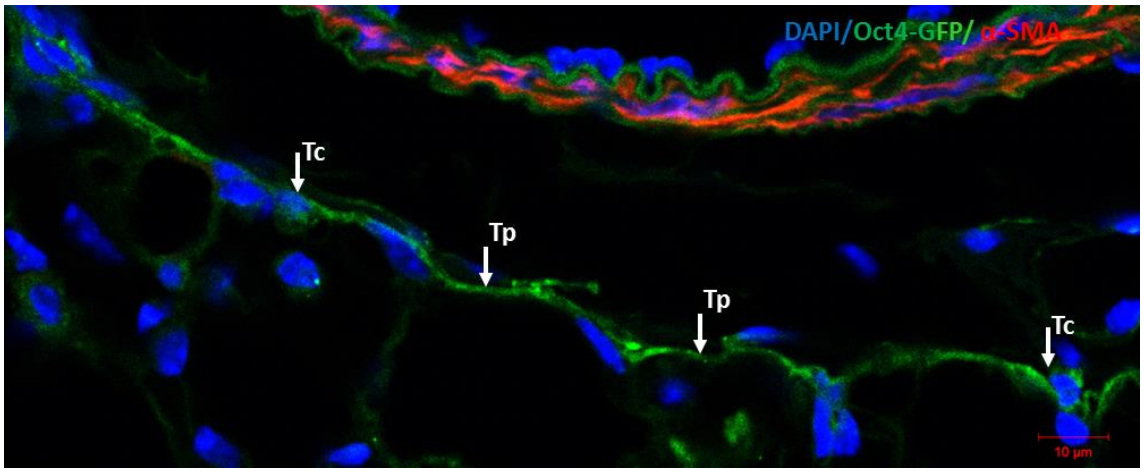

Fig. 26 Immunofluorescence staining of Oct4^{GFP} transgenic mouse lung tissues.

Oct4-GFP (green) is localized in the adventia of a blood vessel where the telocytes (Tc) are located. The cells present long extensions known as telopodes (Tp) which seem to create contacts between two cells. α-SMA (red) labels the vascular smooth muscles located in the media. Nuclear stain DAPI (blue) Bar = 10 µm.

3.8. Oct4 positive cells display telocyte features in culture

Oct4 positive cells were isolated based on GFP fluorescence. A small population which was EpCAM^{neg}CD45^{neg}Oct4-GFP^{pos} was identified (Fig. 27). Dead cells were excluded with DAPI (Fig. 27A, panel 1), CD45-APC positive cells were excluded (Fig. 27B, panel 1); EpCAM positive and EpCAM negative cells were analyzed (Fig. 27C). A small population of Oct4-GFP positive cells (EpCAM^{neg}CD45^{neg}Oct4-GFP^{pos}) which represented 1.3 % was identified in the EpCAM negative cell fraction (Fig. 27D-F, panel 2) and no Oct4-GFP positive population was detected in the EpCAM positive cell fraction (Fig. 27G-I, panel 3). Oct4-GFP positive cells were further sorted and kept in culture in normoxic conditions. After 5 days, the cells showed a fusiform shape resembling telocytes with one (Fig. 28A), two (Fig. 28B) or three (Fig. 28C) extensions. In addition, a cell with a monoliform extension was observed (Fig. 28C). The immunofluorescence staining of Oct4 positive cells showed that they were positive for vimentin (Fig. 28D), and negative for PDGFR-a (Fig. 28E).

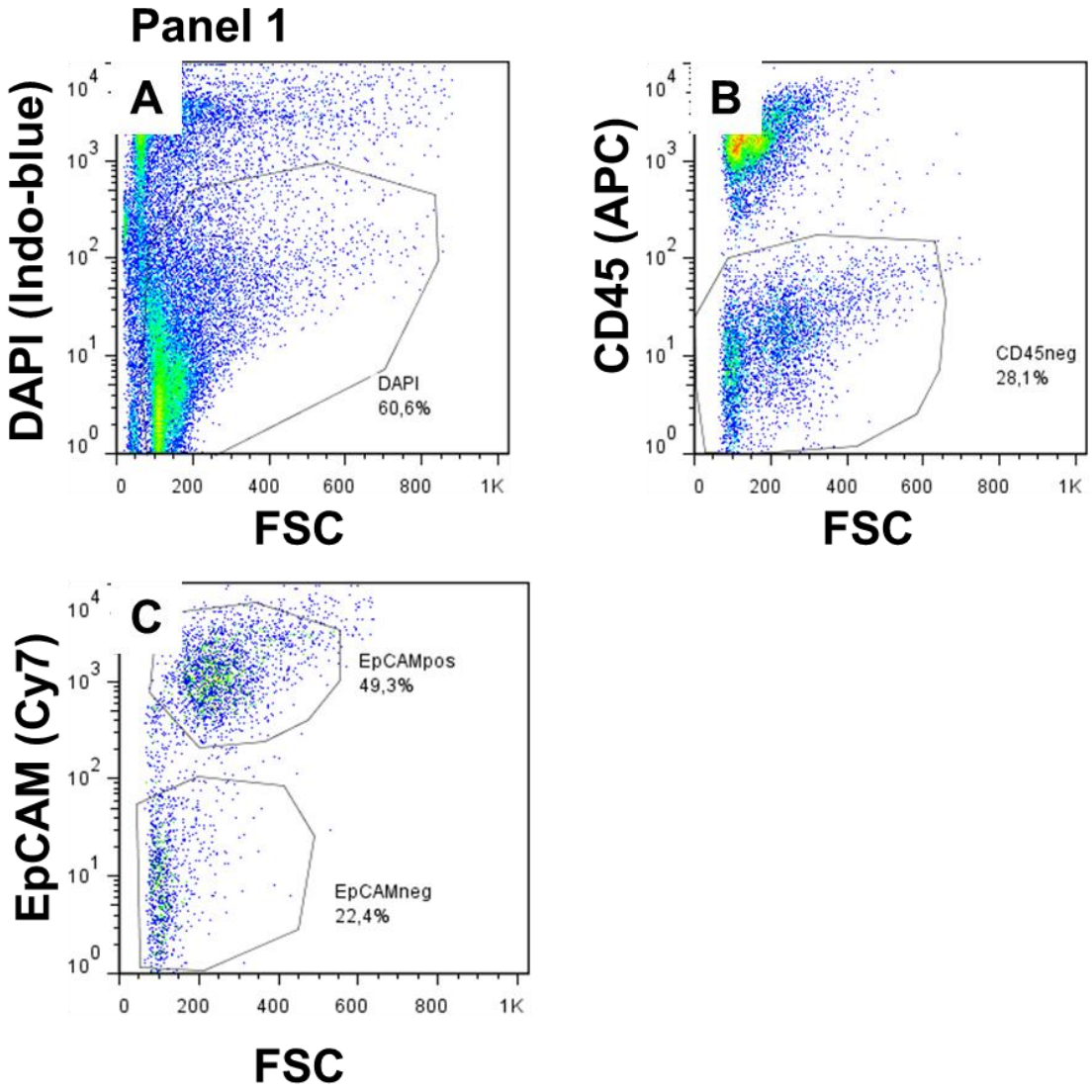

Fig. 27 (Panel 1) Flow cytometric analyses of adult Oct4^{GFP} transgenic mouse whole lung cell.
Cells from adult Oct4-GFP transgenic mice were isolated and analyzed by flow cytometry. (A) Exclusion of dead cells. (B) Exclusion of CD45 expressing hematopoietic cells and gating of CD45 negative cells. (C) Setting of CD45 negative cells in two populations; EpCAM positive and EpCAM negative cells.

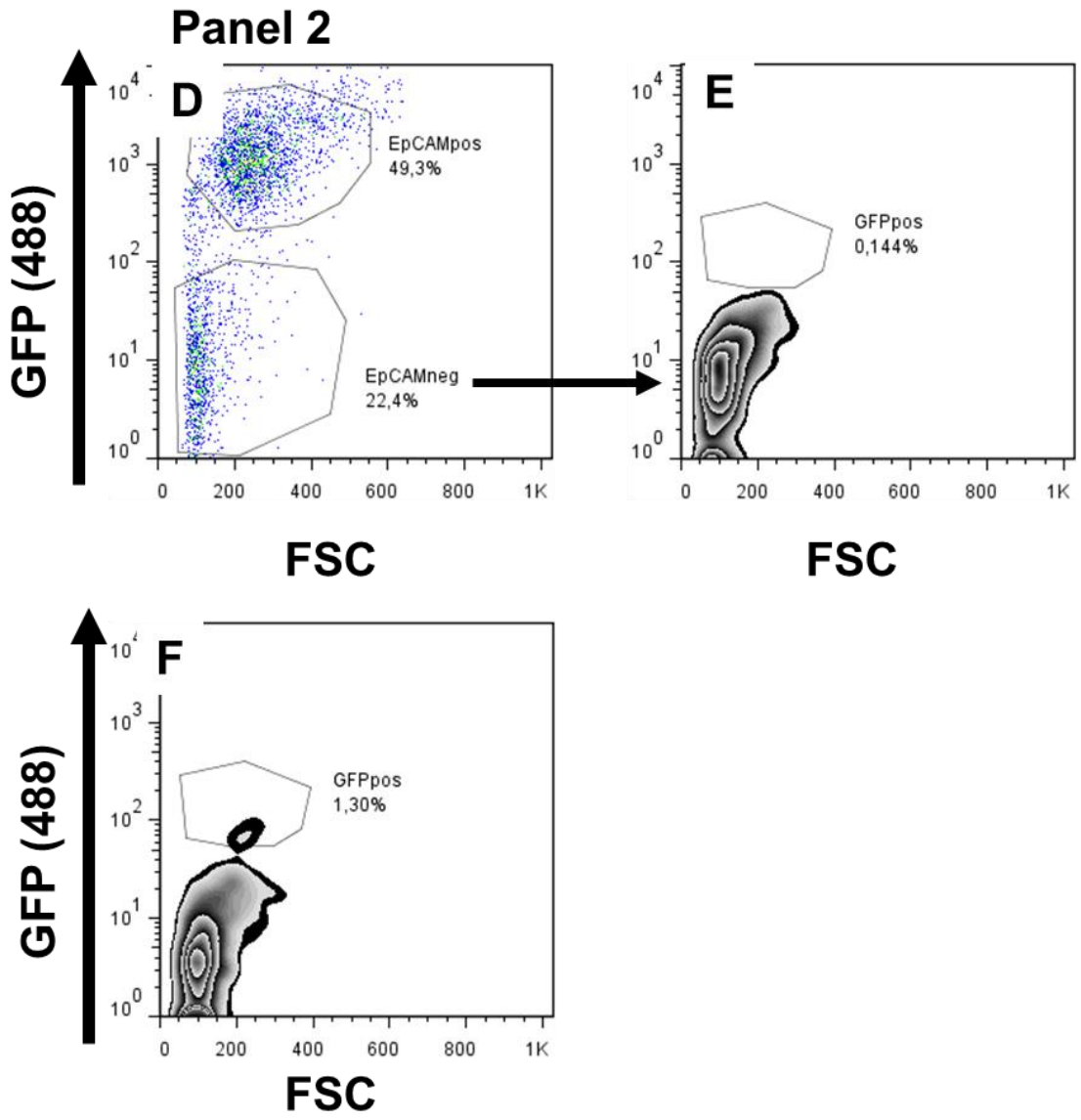

Fig. 27 (Panel 2) Flow cytometric analyses of adult Oct4^{GFP} transgenic mouse whole lung cell.
Cells from adult Oct4-GFP transgenic mice were isolated and analyzed by flow cytometry. (D) Getting of EpCAM negative cells. (E) Unstained cell as negative control. (F) GFP positive cells selected based on CD45^{neg}EpCAM^{neg}GFP^{pos}, represent 1.30 % of EpCAM negative cells.

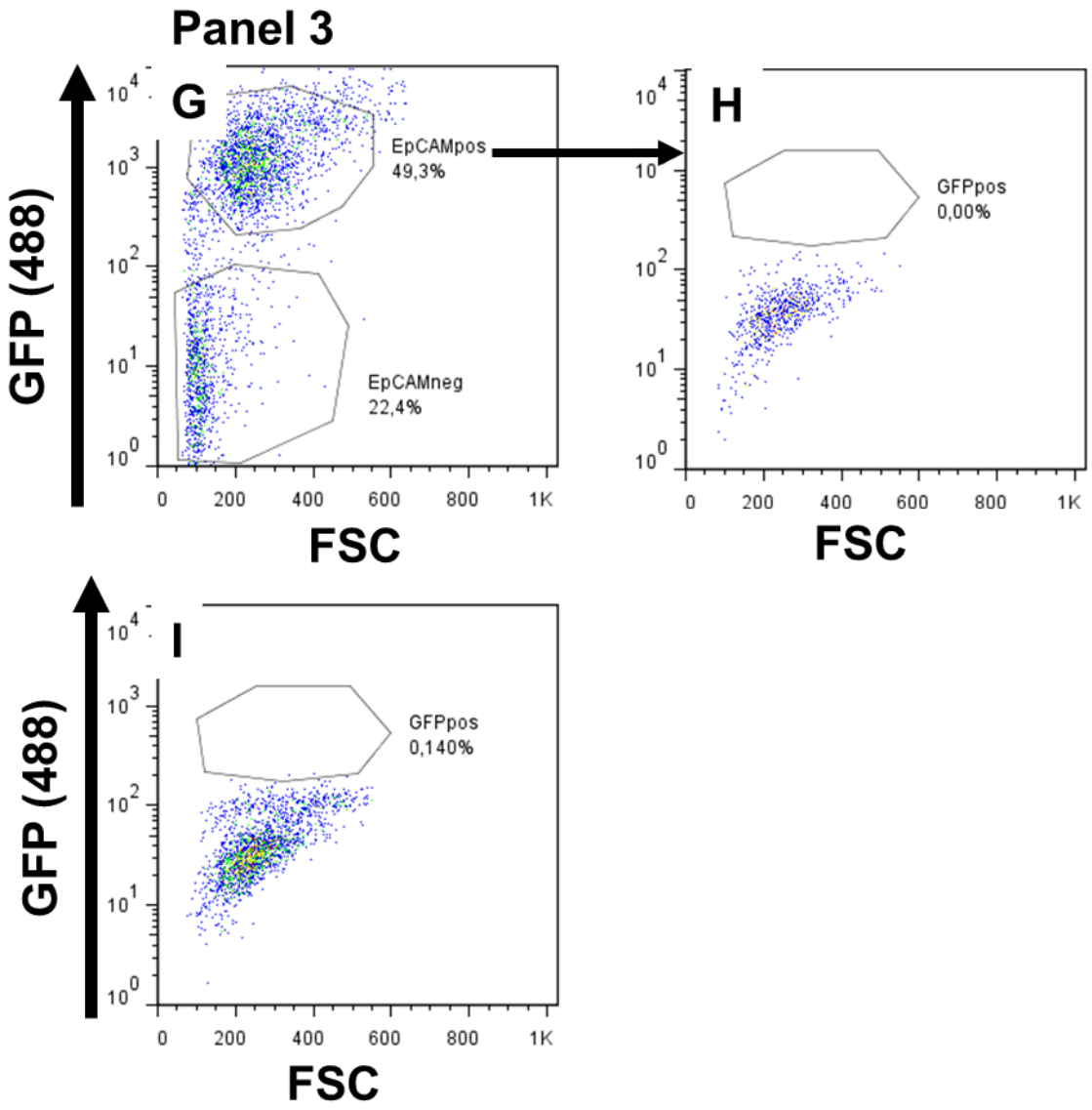

Fig. 27 (Panel 3) Flow cytometric analyses of adult Oct4^{GFP} transgenic mouse whole lung cell.
Cells from adult Oct4-GFP transgenic mice were isolated and analyzed by flow cytometry. (G) Gating of EpCAM positive cells. (H) Unstained cell as negative control. (I) EpCAM positive cells selected based on CD45^{neg}EpCAM^{pos}GFP^{pos} do not contain GFP positive cells.

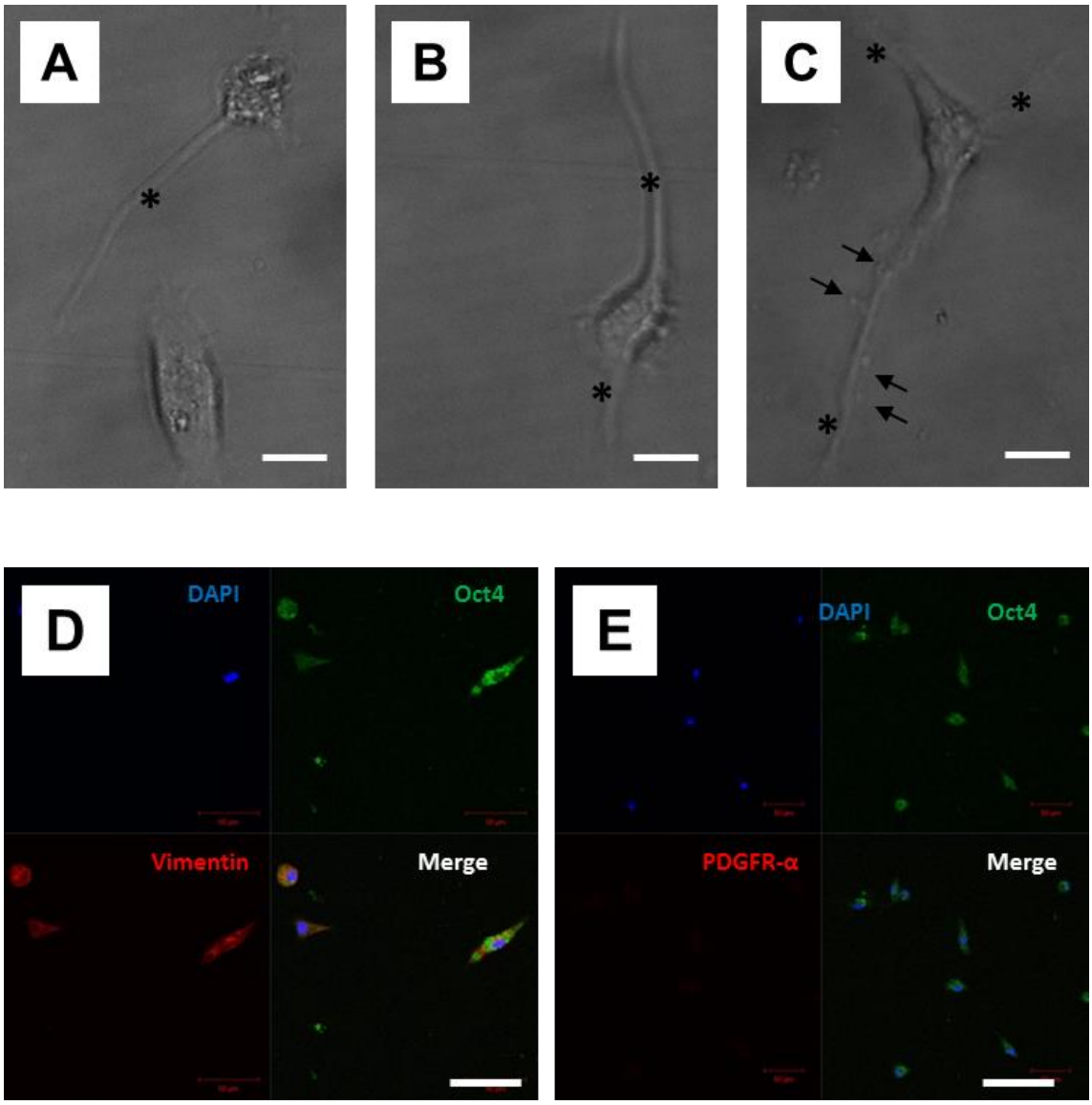

Fig. 28 Bright field visualization and immunofluorescence of 5 days cell culture of Oct4-GFP positive cells from transgenic mice sorted by FACS.

GFP positive cells of Oct4-GFP transgenic adult mice were sorted and cultured for 5 days. Immunofluorescence was performed using Oct4 (green), vimentin (red), PDGFR-a (red) and DAPI (blue) antibodies. (A-C) Bright field images show cells with a fusiform telocyte- like shape with thin prolongations (telopodes: asterix). (A) Cell with one telopode. (B) Cell with two telopodes. (C) Cell with three telopodes. Note that the telopode has a particular shape resembling to a string of beads (arrows). (D) Co-expression of Oct4 and vimentin in telocytes. (E) Co-staining of Oct4 and PDGFR-a. PDGFR-a is not expressed in the cells. Bar = 50 µm.

3.9. Oct4 positive cells express several telocyte markers in the perivascular compartment but not in the peribronchial compartment

Immunofluorescence analyses carried out on paraffin-embedded tissues of adult wild type mice showed that Oct4 positive cells expressed several markers of telocytes including vimentin, C-kit, PDGFR-b, Sca-1 and VEGF. Oct4 co-localized with vimentin in both, the peribronchial space (Fig. 29) and in the adventitia of blood vessels (Fig. 30). While no co-expression of Oct4 with C-kit (Fig. 31), PDGFR-b (Fig. 32), Sca-1 (Fig. 33) and VEGF (Fig. 34) was observed in the peribronchial space, the co-localization with the same markers was observed in the adventitia of blood vessels (Fig. 35; 36; 37; 38).

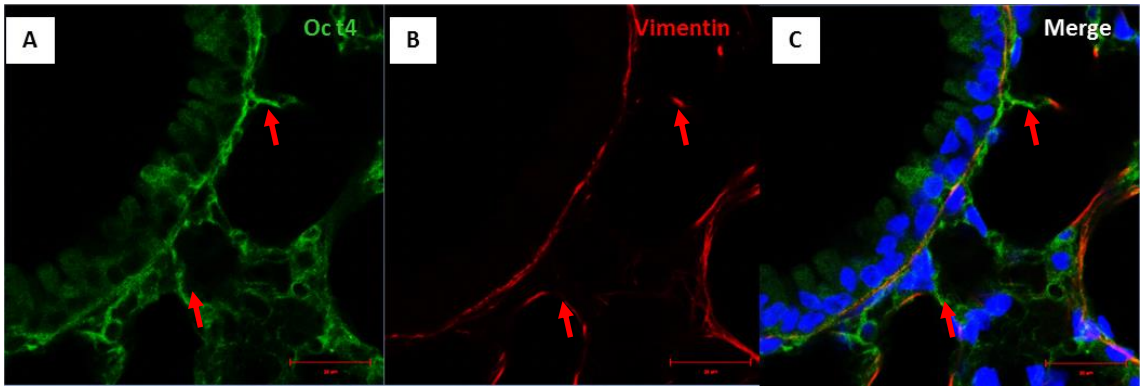

Fig. 29 Immunofluorescence of adult mouse lung bronchus against Oct4 and vimentin.
Adult wild type lung tissues embedded in paraffin, and co-stained with Oct4 (green) and vimentin (red). DAPI (blue) was used as nuclear stain. (A) Oct4 positive cells within the bronchus. (B) Vimentin is expressed in the bronchus. (C) Co-localization of Oct4 and vimentin. Note that telopodes extend to the alveolar space (red arrows). . Bar = 10 µm.

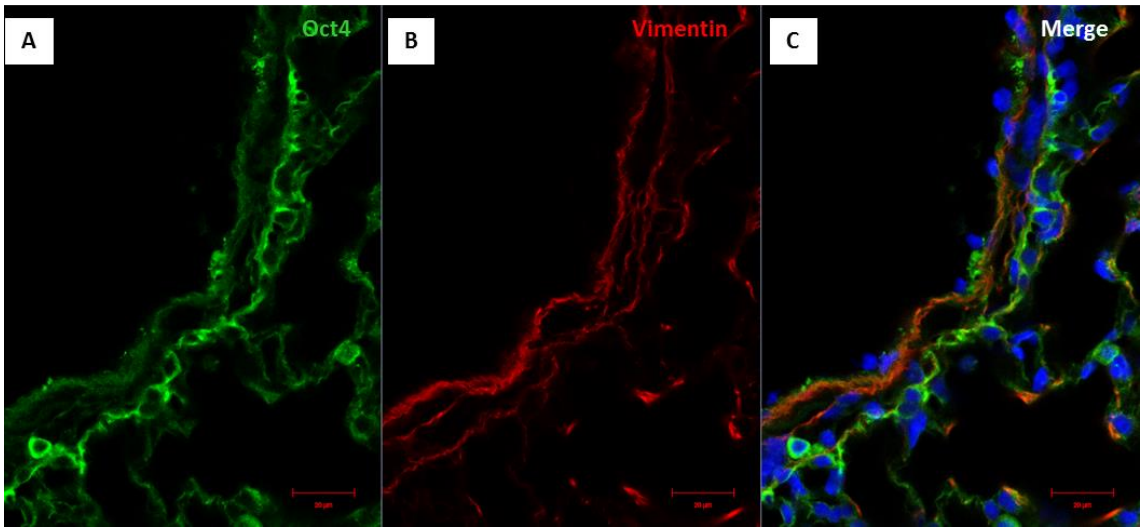

Fig. 30 Immunofluorescence of adult mouse lung blood vessels against Oct4 and vimentin.

Adult wild type lung tissues embedded in paraffin and co-stained with Oct4 (green) and vimentin (red). DAPI (blue) was used as nuclear stain. (A) Oct4 positive cells within the blood vessels. (B), vimentin is expressed in the blood vessels. (C) Co-localization of Oct4 and vimentin (C). Bar = 10 µm.

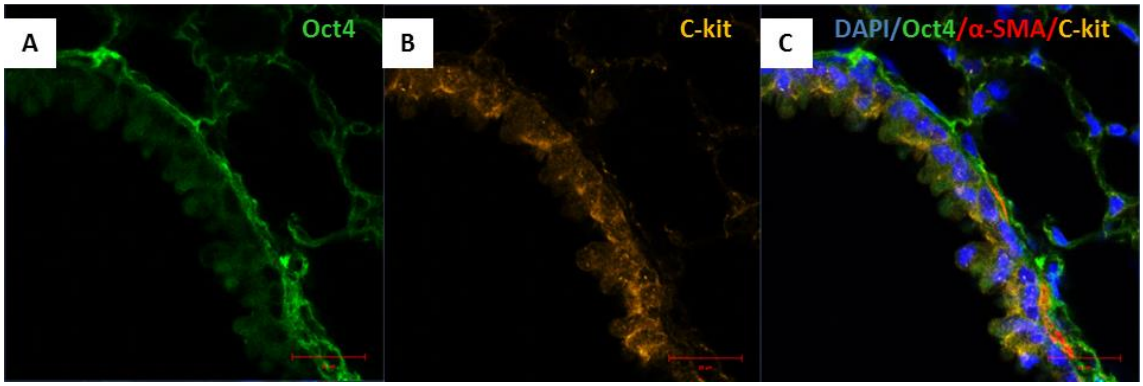

Fig. 31 Immunofluorescence of adult mouse lung bronchus against Oct4 and C-kit.

Adult wild type lung tissues embedded in paraffin and co-stained with Oct4 (green) and C-kit (yellow). DAPI (blue) was used as nuclear stain. (A) Oct4 positive within the bronchus. (B) C-kit is expressed in bronchus. (C) There is no co-localization of Oct4 and C-kit. α-SMA stains the smooth muscles lining the bronchiolar epithelium. Bar = 10 µm.

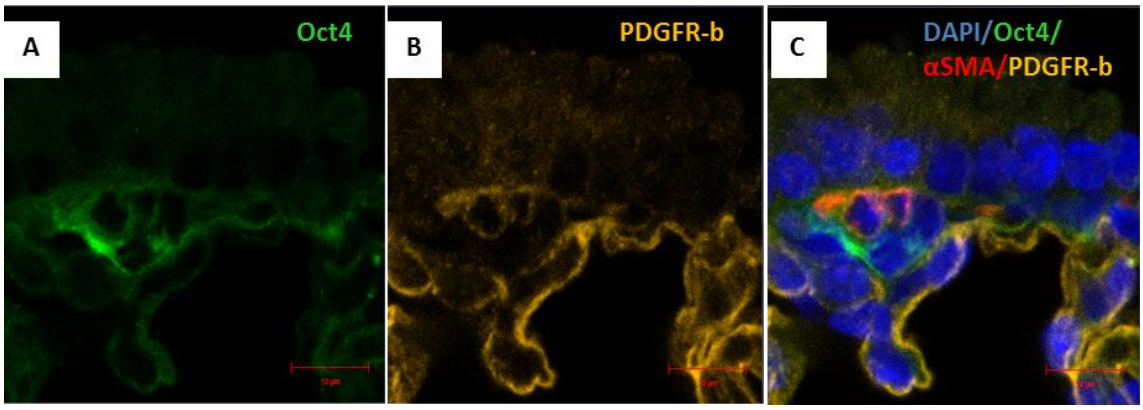

Fig. 32 Immunofluorescence of adult mouse lung bronchus against Oct4 and PDGFR-b.

Adult wild type lung tissues embedded in paraffin and co-stained with Oct4 (green) and PDGFR-b (yellow). DAPI (blue) was used as a nuclear stain. (A) Oct4 positive cells within the bronchus. (B) PDGFR-b is expressed in bronchus. (C) There is no co-localization of Oct4 and PDGR-b. α-SMA stains the smooth muscles lining the bronchiolar epithelium . Bar = 10 µm.

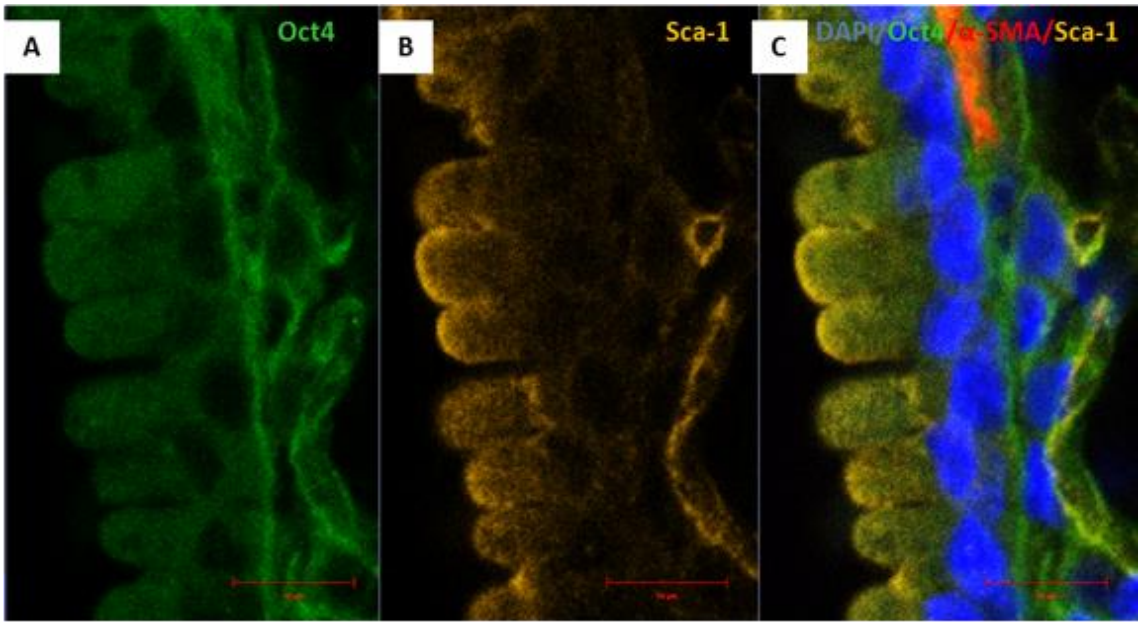

Fig. 33 Immunofluorescence of adult mouse lung bronchus against Oct4 and Sca-1.
Adult wild type lung tissues embedded in paraffin and co-stained with Oct4 (green) and Sca-1 (yellow). DAPI (blue) was used as a nuclear stain. (A) Oct4 positive cells within the bronchus. (B) Sca-1 is expressed around the bronchus. (C) There is no co-localization of Oct4 and Sca-1. α-SMA stains the smooth muscles lining the bronchiolar epithelium . Bar = 10 µm.

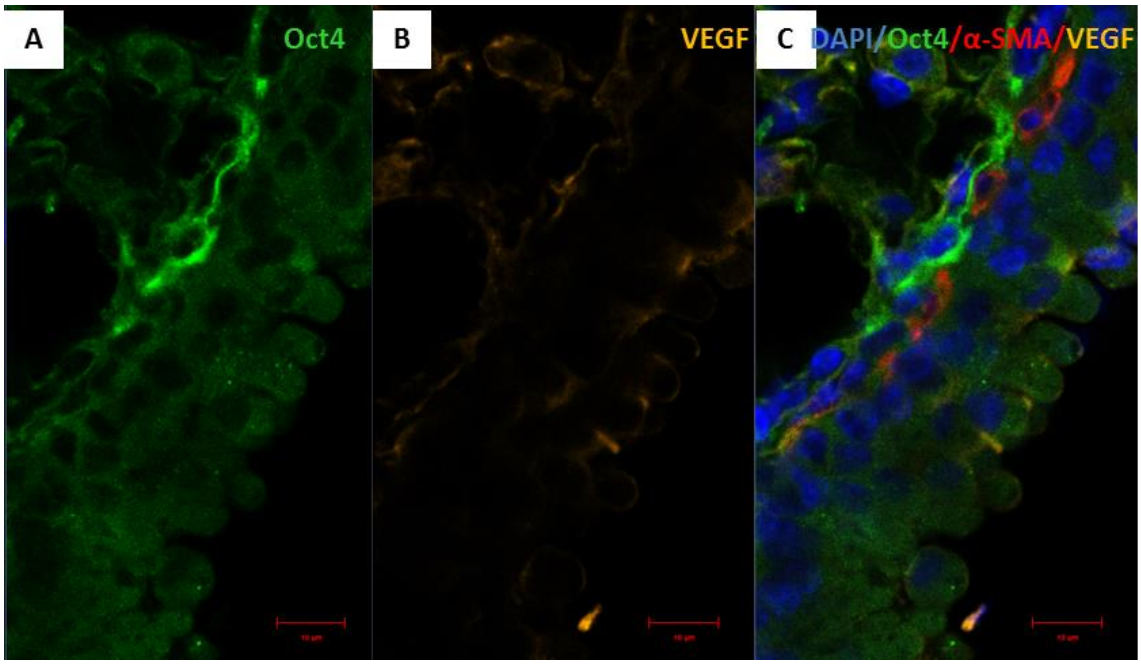

Fig. 34 Immunofluorescence of adult mouse lung bronchus against Oct4 and VEGF.
Adult wild type lung tissues embedded in paraffin and co-stained with Oct4 (green) and VEGF (yellow). DAPI (blue) was used as a nuclear stain. (A) Oct4 positive cells within the bronchus. (B) VEGF is expressed in the bronchus. (C) There is no co-localization of Oct4 and VEGF. α-SMA stains the smooth muscles lining the bronchiolar epithelium . Bar = 10 µm.

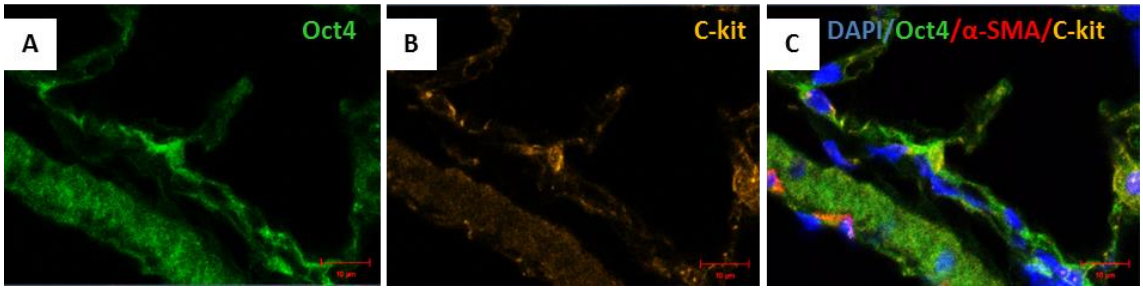

Fig. 35 Immunofluorescence of adult mouse lung blood vessels against Oct4 and C-kit.

Adult wild type lung tissues embedded in paraffin and co-stained with Oct4 (green) and C-kit (yellow). DAPI (blue) was used as nuclear stain. (A) Oct4 positive cells within the blood vessels. (B), C-kit is expressed in the blood vessels. (C) Co-localization of Oct4 and C-kit. α-SMA stains the smooth muscles expressed in the media . Bar = 10 µm.

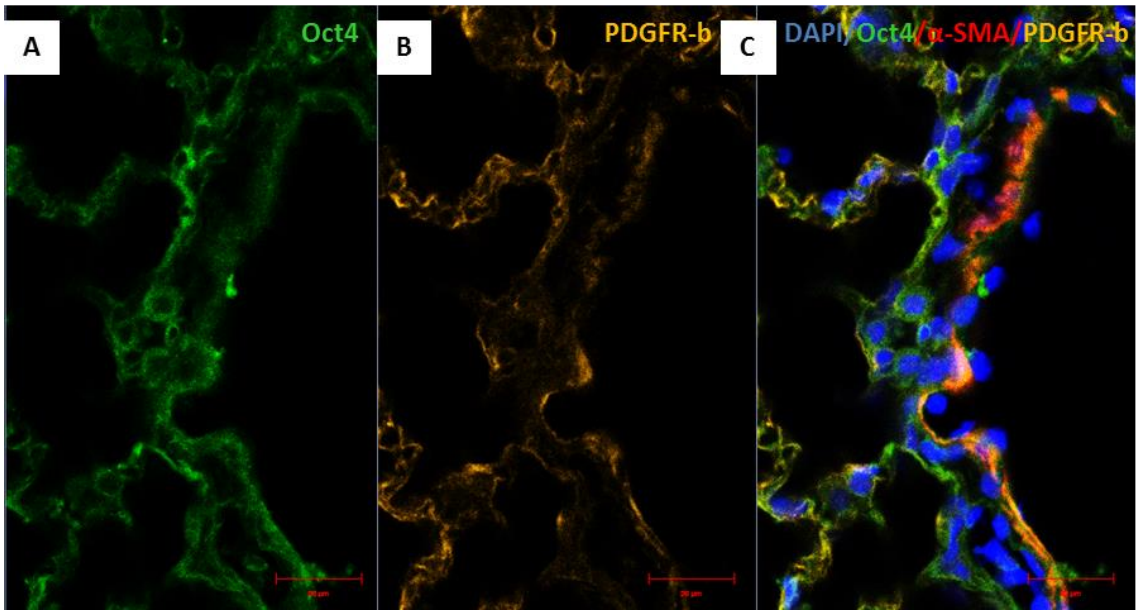

Fig. 36 Immunofluorescence of adult mouse lung blood vessels against Oct4 and PDGFR-b.

Adult wild type lung tissues embedded in paraffin and co-stained with Oct4 (green) and PDGFR-b (yellow). DAPI (blue) was used as nuclear stain. (A) Oct4 positive cells within the blood vessels. (B) PDGFR-b is expressed in the blood vessels. (C) Co-localization of Oct4 and PDGFR-b. α-SMA stains the smooth muscles expressed in the media. Bar = 10 µm.

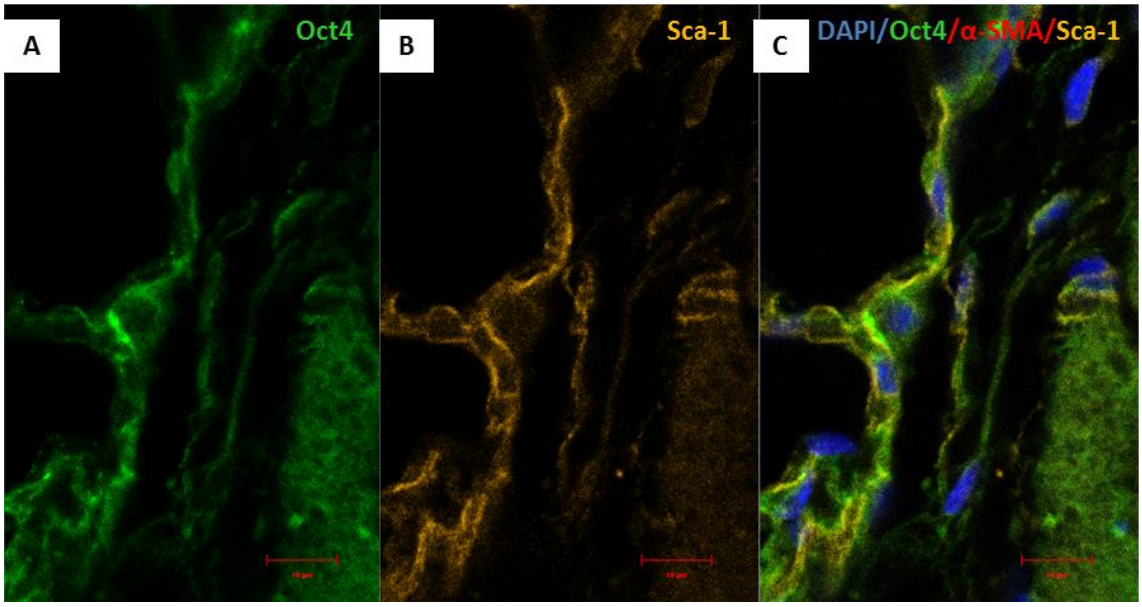

Fig. 37 Immunofluorescence of adult mouse lung blood vessels against Oct4 and Sca-1.

Adult wild type lung tissues embedded in paraffin and co-stained with Oct4 (green) and Sca-1 (yellow). DAPI (blue) was used as nuclear stain. (A) Oct4 positive cells within the blood vessels. (B) Sca-1 is expressed in the blood vessels. (C) Co-localization of Oct4 and Sca-1. α-SMA stains the smooth muscles expressed in the media. Bar = 10 µm.

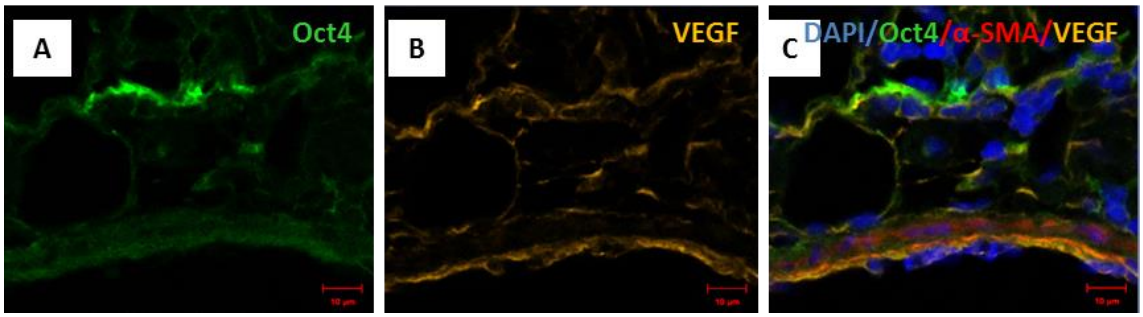

Fig. 38 Immunofluorescence of adult mouse lung blood vessels against Oct4 and VEGF.

Adult wild type lung tissues embedded in paraffin and co-stained with Oct4 (green) and VEGF (yellow). DAPI (blue) was used as nuclear stain. (A) Oct4 positive cells within the blood vessels. (B) VEGF is expressed in the blood vessels. (C) Co-localization of Oct4 and VEGF. α-SMA stains the smooth muscles expressed in the media. Bar = 10 µm.

3.10. Gene expression levels of telocyte markers in adult mouse lung tissues

Single cell picking was done via laser capture microdissection (LCM) technique at the telocyte locations .After the dissection (Fig. 39A-39C), the cells were collected (Fig. 39D) and the RNA was isolated. Gene expression levels of telocyte markers were determined by real-time quantitative PCR. Levels of Oct4 expression were low in comparison with other tested markers and similar in vessels, bronchi, and septa. Vimentin, C-kit and Sca-1 showed higher expression in vessels and septa compared to the bronchi. VEGF displayed highest expression in septa and levels of PDGFR-b expression were similar in the three compartments (Fig. 40).

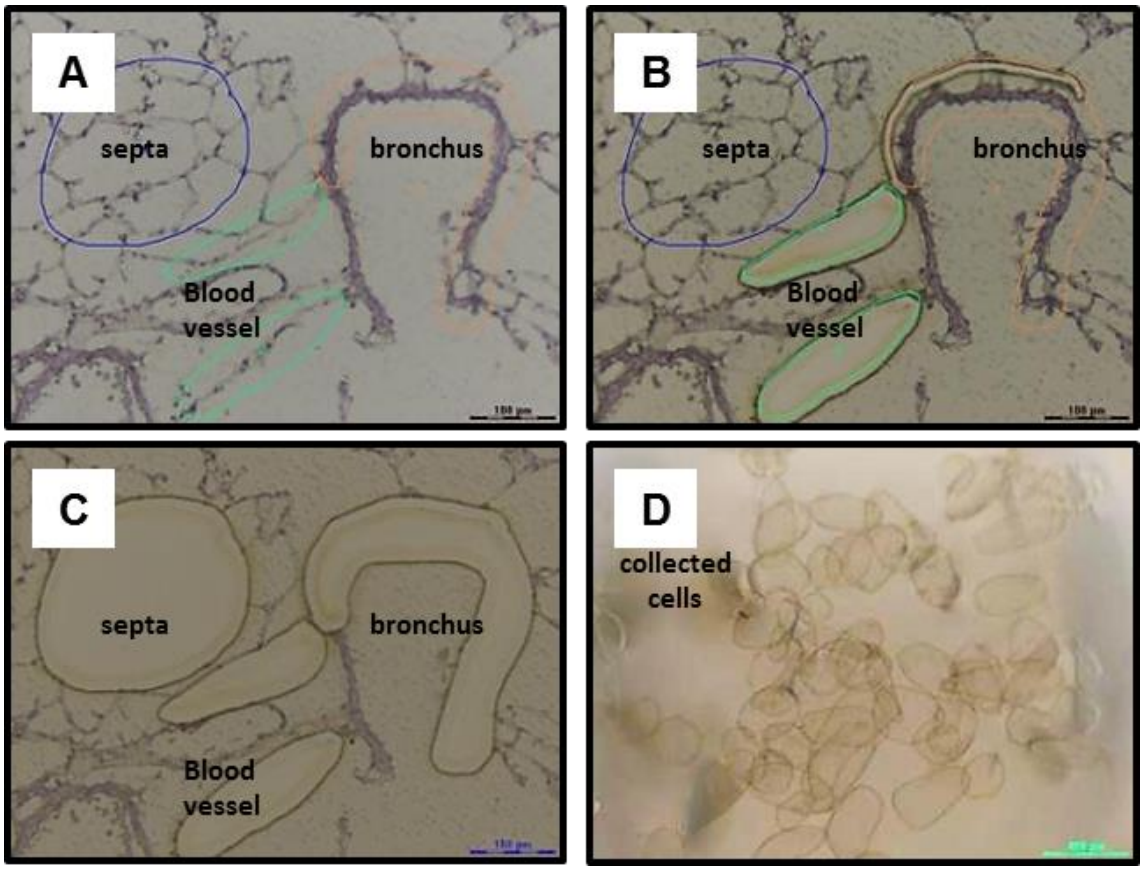

Fig. 39 Laser capture microdissection of adult wild type mouse lung cryosections.

500 vessels, bronchi and septa of cryosection tissues of adult mouse lungs were microdissected and collected into different tubes. (A) Before the capture, the regions of interest (ROI) are circled. (B) During the capture, the laser cuts the ROI. (C) After capture, the ROI fall down into the cap of collecting tubes. (D) Dissected cells in the cap of the collection tubes.

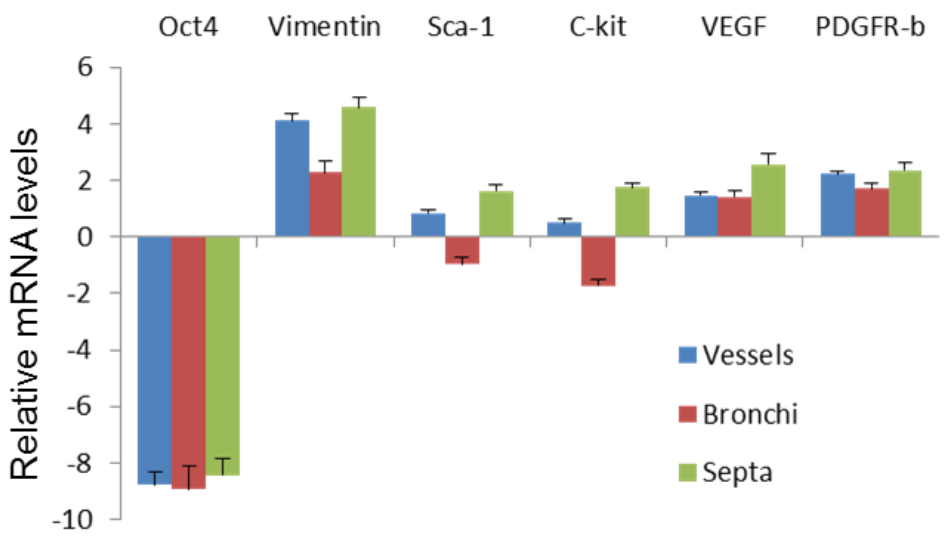

Fig. 40 Gene expression levels of telocyte markers after cell picking by LCM.

Gene expression levels of Oct4, vimentin, Sca-1, C-kit, VEGF and PDGR-b were determined by real time PCR. Cells in telocytes location including the bronchi, blood vessels and septa were selected by laser capture microdissection (LCM) and RNA was isolated. Data are expressed in mean ± SEM and n = 5 and the mRNA expression levels are shown as ΔCt values compared to GAPDH housekeeping gene control.

3.11. Oct4 expression is deregulated upon naphthalene-induced lung injury in mice

To determine whether Oct4 was regulated upon naphthalene treatment, its expression after injury was tested. The samples were collected at day 3, 7, 14 and 21 (these samples were kindly provided by Prof. Dr. Saverio Bellusci from the Excellence Cluster Cardio-Pulmonary-System, Justus-Liebig-University, Giessen) and western blot analysis was performed (Fig. 41A). The expression Oct4 was significantly decreased from day 3 post-injury until day 21 post-injury with 50 to 80 % of loss of expression (Fig. 41B).

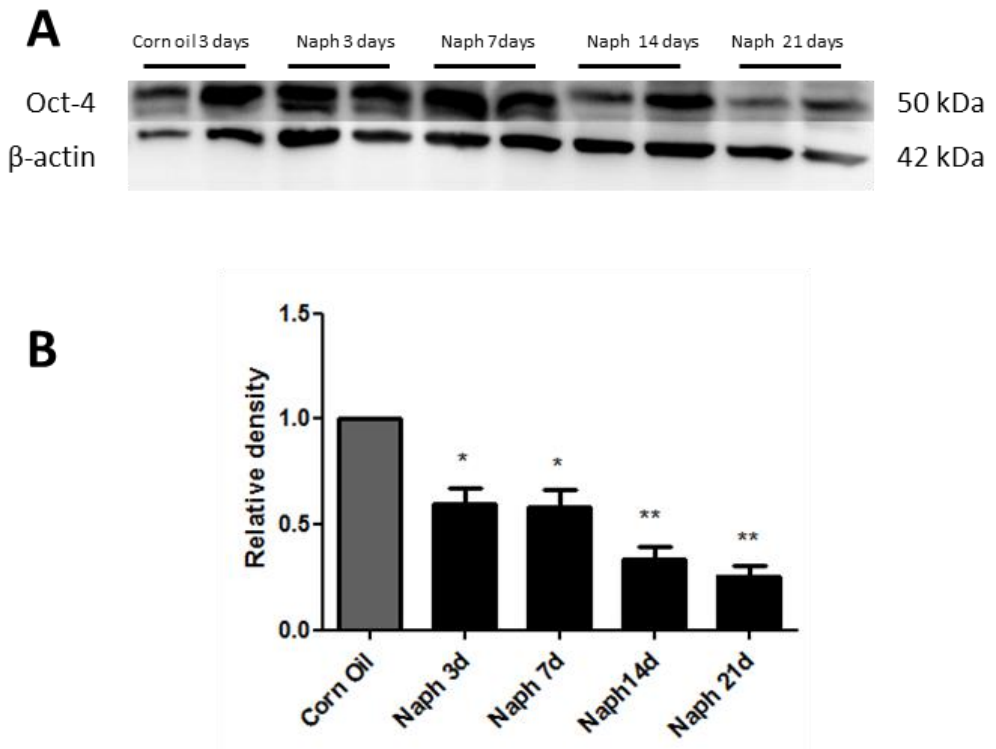

Fig. 41 Levels of Oct4 protein expression in adult wild type mice after naphthalene injury. (A) Expression of Oct4 protein detected by western blot at different time points after naphthalene treatment of adult wild type mice compared to corn oil treatment. (B) Histogram representation of relative density of Oct4 protein levels normalized to β-actin. Naph 3d, 7d, 14d and 21d: naphthalene at day 3, 7, 14 and day 21. n = 2 animals per group. Data are expressed in mean ± SEM. *$p < 0.05$; **$p < 0.01$.

SECTION 4: DISCUSSION

4.1. BASCs play a role in lung regeneration but they are not necessarily the cells involved in the bronchiolar epithelium repair after naphthalene injury

The primary purpose of this work was to characterize BASCs in adult mouse lung. BASCs were described first time in 2005 by Kim et al [12]. They reported that BASCs were cells showing stem cell characteristics and they were capable of regenerating the bronchiolar epithelium and the distal alveolar cells after naphthalene injury. Moreover, a role of BASCs in compensatory lung regrowth after PNX was as well described [101]. These findings on BASCs were highly argued among the scientific community. (i) The method used to isolate BASCs based on $Sca1^{pos}CD34^{pos}$ cell fraction was controversial as Sca1 is more representative of mesenchymal cell linages than epithelial cells [102]. (ii) The lineage tracing of BASCs did not show any evidence of BASCs of their role in lung repair [11]. In our study, first, we confirmed that BASCs were present at the BADJ based on their co-expression for CCSP and SPC; their contribution in lung repair and regeneration after naphthalene and PNX was determined based on their proliferation activity. In fact, in the naphthalene model, we only observed the proliferation of BASCs at day 3 post-injury. Clara cells were still proliferating at day 6 until day 10 post-injury. In the study conducted by Kim et al [12], they reported that after naphthalene injury, the BASCs started to proliferate at day 2 post-injury and the proliferation was not observed yet in Clara cells; the Clara cells started to proliferate at day 3 post- injury. These data conformed to our observations and this suggests that BASCs may have a limited capacity of dividing compared to Clara cells. However, it is well known that in the process of repair in wounded skin for instance, the cells at the edge of the injury are stimulated and divide rapidly to generate new cells which are able to replace the damaged cells or tissues. When the repair is done, the cells will stop to divide [103]. It is therefore possible that the BADJ where BASCS reside and the region of neuroendocrine-associated Clara cells constitute two independent sites of injury. BASCs would then contribute to the repair at the BADJ part and Clara cells would repair the bronchiolar epithelium. Moreover, the BADJ and the neuroendocrine-associated Clara cells regions have already been described as reservoirs of stem cell niches. This further supports that the BADJ might be the region where the injury occurred first and then spread to the entire bronchiolar epithelium. Since the BADJ may heal first, the BASCs will then stop dividing first and the Clara cells will continue to divide

till the complete recovery of the bronchiolar epithelium. In fact, the theory of a pluripotent stem cell for all the areas of the adult lung has not been fully accepted. Based on a concept claiming that regional niches are present at different locations, they can therefore, control the phenotype and the expansion of the stem cells through the distinct anatomical regions of the airways [3]. In the alveoli, some clusters of BASCs and Clara cells were also identified and the same observation was made. At day 6 post-injury, only Clara cells were still proliferating whereas BASCs had stopped to divide. The question remains if there is any significance of the presence of BASCs and Clara cells in alveolar space? If yes, is this aspect due to naphthalene treatment? Rawlins [11], identified in *Scgb1a1-CreER*^{TM}; *Rosa26R-eYFP* adult mouse lung sections, many of the lineage-labeled type 2 cells at the vicinity of the BADJ expressing low levels of CCSP. However, it is interesting to see that in the naphthalene model, many BASCs and Clara cells organized in clusters were identified not only at the BADJ but also in alveolar space. Thus, it is possible that this appearance was correlated to the injury. Flow cytometric analyses strengthened this observation; a significant increase of BASCs and Clara cell populations at day 6 post-injury was detected. This may lead to the conclusion that; (i) naphthalene might not have only a toxic effect on bronchiolar Clara cells but also on alveolar cells and this can be the reason why some alveolar type 2 cells proliferated upon injury. (ii) It may be possible that BASCs present in alveolar tissues constitute a complete different cell population to the one present at the BADJ. Thus, BASCs would be like Clara cells, a heterogeneous population [104]; but their niche in the alveoli remain unknown. (iii) The BASCs in the alveolar space can also be derived from Clara cells since BASCs are also called variant Clara cells. However, although BASCs do express the CCSP Clara cell marker, there is no current evidence showing a correlation between Clara cells and BASCs cell types? From these observations, a lot of questions remain open about the cells or tissues which are impaired by naphthalene and which ones exactly contribute effectively to the repair in this model. Nevertheless, Clara cells seem to be the cells which actually contribute to the replacement of the depleted Clara cells. Besides, the question about the role of BASCs in adult mouse lung has not been yet elucidated. Moreover, our data don´t show a clear evidence of BASCs being the cells responsible for the bronchiolar epithelium repair. The effectiveness of BASCs as cells capable of repair and regeneration has been already proved in response to PNX in previous studies. It was shown in telomerase null mice , that the number of BASCs was reduced in the tissues compared to the wild type mouse tissue suggesting that BASCs play a role in lung regeneration [105]. We demonstrated in adult wild type mice that, at day 7 post-

surgery, BASCs responded to PNX by proliferating, indicating BASCs as a functional stem cell pool required for the regeneration of adult lung tissues. In this study, our data demonstrated that although BASCs proliferated following PNX and naphthalene, these cells are not necessarily the cells responsible for the replacement of damaged Clara cells in the bronchiolar epithelium upon naphthalene injury in adult mouse lung.

4.2. BASCs are a potential stem/progenitor cell type in adult mouse lung

We provided the first evidence that BASCs are related to the $EpCAM^{high}CD24^{low}$ stem/progenitor cell fraction described by McQualter et al [70]. McQualter showed by real-time PCR that the $EpCAM^{high}CD24^{low}$ cell fraction was enriched in CCSP-expressing Clara cells. Moreover, the $EpCAM^{high}CD24^{low}$ cell fraction had a self-renewal capacity and also the ability to grow and generate different types of colonies including CCSP and SPC positive colonies. Our results confirmed these data but addition demonstrated for the first time that BASCs were also included in the $EpCAM^{high}CD24^{low}$ cell fraction. By immunocytochemistry of sorted ESPCs, we demonstrated for the first time that BASCs are $EpCAM^{high}CD24^{low}$. By flow cytometry using the double fluorescent Cre reporter line CCSP-mCherry/SPC-YFP, we confirmed indeed, that CCSP positive cells alone represented 66 % of the $EpCAM^{high}CD24^{low}$ cell fraction. Moreover, BASCs which were less abundant were also included in $EpCAM^{high}CD24^{low}$ cell fraction. These data suggest that BASCs are potential stem/progenitor cells in adult mouse lung. Nevertheless, the question whether BASCs contribute to lung turnover, repair and regeneration in adult mouse lung remains still to be defined in various lung diseases models. These open question give rise to current debate if BASCs exist or not. Our data clearly demonstrated the evidence of cells expressing CCSP and SPC in the same cell at the BADJ and alveolar space. In addition, these cells also show the capacity to proliferate upon injury. Thus, our data might serve as a solid basis for further analysis elucidating the role of BASCS in pulmonary diseases and remodeling.

4.3. Oct4 as a novel marker for the characterization of lung telocytes

The aim of the present study was to characterize and analyze BASCs function and their stemness activity. Therefore we traced Oct4 positive cells in adult mouse lung in order to elucidate if BASCs do express this marker of stemness. But the expression of Oct4 was not detected in BASCs. Surprisingly, Oct4 expression was restricted to a distinct cell type, the telocytes. Moreover, based on flow cytometric analyses using Oct4-GFP transgenic mouse

line, Oct4 positive cells were not detected in the epithelial ($EpCAM^{pos}$) cell fraction. The expression of Oct4 in adult tissues is a controversial topic in the field of adult stem cells research. The presence of Oct4 in adult tissue has been related to either PCR product artifacts, Oct4 pseudogenes or to other members of Oct family [77, 106, 107]. In the present study, we have demonstrated that Oct-4 was expressed in adult mouse lung tissues. But our data demonstrated Oct4 expression using transgenic mice and thus showed a reliable expression. In the present study, Oct4 positive cells were located in the peribronchial and perivascular spaces. Our data agree with recent the findings, that in the mouse pulmonary tissues telocytes are lining the blood vessels and the bronchi [108-110]. In the present study, we were able to isolate Oct4 positive cells and maintain them in culture. Oct4 positive cells displayed *in vitro* similar structural features of telocytes which were already described in several studies of isolated telocytes from different organs [84, 111, 112]. In particular, we found similar numbers and the shape of telopodes furrowing and extending from Oct4 positive cells in accordance with those from Sca-1 telocytes [79]. Furthermore, we observed within the Oct4 positive cells, monoliform prolongations with thin cell body shape as also described for telocytes. Actually, telocytes are identified based on the number of their telopodes; with up to five telopodes with monoliform shape within, a succession of enlarged segments called podoms and thin segments called podomers [95, 113]. We identified also Oct4 in peripheral mononuclear blood cells but we did not focus on this cell type. They were discriminated during the isolation with anti-CD45 antibody and therefore, only the $CD45^{neg}EpCAM^{neg}Oct4\text{-}GFP^{pos}$ cell fraction was characterized. Moreover, the staining of Oct4-GFP positive after culture showed that they were all positive for vimentin and negative for PDGFR-a, a marker which is more representative of fibroblast cell lineages. Indeed, studies conducted on the gene expression profile of telocytes compared to fibroblasts in murine lung demonstrated that telocytes are not fibroblasts [114]. Numerous studies have demonstrated that telocytes have different ultrastructure and phenotype than fibroblasts [95, 115]. By immunofluorescence, we confirmed that Oct4 positive cells share several markers with telocytes. They co-localized with several telocyte markers including C-kit, PDGFR-b, Sca-1 and VEGF [109, 116] in blood vessel compartment, whereas no co-localization was observed in the peribronchial space. These observations suggest that telocytes represent, at least immunophenotypically, a heterogenous cell type. The expression of the different above mentioned markers were confirmed on mRNA level by real-time PCR of the telocytes captured with laser microdissection from different locations including blood vessels, bronchi and the septa. It

is obvious that the mRNA levels of some markers including C-kit, Sca-1, PDGFR-b and VEGF do not fully concur with the immunohistochemical analyses. This especially applies to the peribronchial telocytes. However, it is possible that such a difference in the expression profile might be due to contamination with the adjacent cells which express different markers. In summary, we were able to show that Oct4 is expressed in adult mouse lung. We have demonstrated for the first time that Oct4 positive cells closely resemble the morphology of telocytes seen by electron microscopy. Thus Oct4 positive telocytes might represent a new candidate for stem cell function in the lung and might contribute to lung regeneration. In fact, Oct4 is well-known as a transcription factor and a stem cell marker and it is localized in the nucleus of ESCs. In our studies, western blot analysis revealed a band of 50 kDa which is 5 kDa bigger than the expected band size of Oct4 which expressed in the nuclear compartment of cells. This suggests that it might be a different isoform of Oct4 which is expressed in adult tissues. It is reported in the literature that human OCT4 gene for example, can produce at least three transcripts by alternative splicing (Oct4A, Oct4B, and Oct4B1) and four protein isoforms (Oct4A, Oct4B-190, Oct4B-265, and Oct4B-164). Oct4A is expressed in nucleus and Oct4B is expressed in the cytoplasm. While it is well established that Oct4A is responsible for the pluripotency and the self-renewal of ESCs, the function of Oct4B remains unclear. Studies suggested that Oct4B is involved in cell stress response [117-120]. Two different isoforms of Oct4 exist in mouse (Oct4A and Oct4B). Oct4A is the long isoform with an expected size of 39-45 kDa and the short isoform Oct4B, which may exist in the somatic tissues, has an expected size of 37 kDa. In the present work, it seems that a completely different isoform may exist in adult mouse lung tissues and there are no current studies which report its expression in peribronchial and perivascular spaces. Therefore, the necessity for further studies of which Oct4 isoforms exactly are expressed in somatic tissues are required, and this may hence, challenge the role of Oct4 as a marker of pluripotency. As a matter of fact, in our study we were not able to show that Oct4 plays a role in lung repair. Its expression was downregulated after naphthalene injury suggesting that Oct4 is not also required for lung repair and regeneration of adult mouse lung tissues in response to naphthalene. But it might be different upper other disease models which has not been tested yet. However, these observations might also support the hypothesis that Oct4 might have other functions than to be a marker of pluripotency and its presence is not necessarily a hallmark of pluripotency [121]. Nevertheless, the function of Oct4 positive telocytes in different diseases contexts needs to be elucidated in the future. Since telocyte's function might be very complex due

to their inter cell connecting properties. They might be a useful target for regenerative medicine.

SECTION 5: CONCLUSIONS-PERSPECTIVES

5.1. Conclusions

In conclusion, we showed for the first time that BASCs are related to the $EpCAM^{high}CD24^{low}$ ESPC cell fraction suggesting that they are a progenitor or a stem cell population in adult mouse lung. Even though we were able to demonstrate that BASCS may have a role in lung repair and regeneration after Clara cells damage because of their ability to proliferate, we were not able to provide the evidence that they are necessarily the cells which replenish the bronchiolar epithelium. But, we clearly demonstrated the presence of CCSP/SPC positive cells at the BADJ and in the alveolar compartment. Thus our study represents a solid basis for the existence of BASCs. Based on this, further studies are needed to analyze BASCs in different pulmonary disease and regeneration models. Following this line, we identified Oct4 positive telocytes as new possible candidates for lung regeneration and repair.

5.2. Perspectives

Further studies are clearly needed to elucidate BASCs in different disease and regenerative models. Distinct transgenic lineage tracing approaches have to be generated to trace BASCs in this context and to elucidate their differentiation capacity. Thus, their contribution to the regeneration of specific cell types might be clarified. The double fluorescent CCSP-mCherry/SPC-YFP transgenic mouse line which was used in the present study represents a useful tool for these analyses. Long term *in vitro* cell culture of BASCs is needed to test their ability to self-renew and differentiation. *In vivo* lung organoid assays may also be useful to test to test the contribution of BASCs to lung development. The generation of new transgenic approaches to trace and manipulate telocytes is necessary to give insights into telocyte function in disease and regeneration.

SUMMARY

Bronchioalveolar stem cells (BASCs) have been shown to be a regional stem cell population in the distal lung. They are CCSP (Clara cell secretory protein) and SPC (surfactant protein C) positive. They respond to bronchiolar and alveolar injuries. BASCs are thought to maintain the bronchiolar Clara cells and the alveolar type 2 cells. Previous studies showed that Clara cells contribute to the renewal of the bronchiolar epithelium after oxidant mediated damages. Importantly, after the depletion of Clara cells through administration of naphthalene, residual cells of terminal bronchioles were fully capable of epithelial renewal and restoration. These naphthalene-resistant Clara cells were present at the bronchioalveolar duct junction (BADJ). BASCs were isolated based on positive staining for CD34, a marker for skin epithelial cells and hematopoietic stem cells, and for Sca-1, a marker for stem cells. Others studies performed in adult mouse lung indicate that Sca-1^{pos} cell fractions are predominantly representative of mesenchymal cell lineages. This highlights that Sca-1 is not a selectable marker for epithelial stem cells in the adult murine lung, and therefore the need of alternative functional assays for the identification and characterization of BASCs. In the present study, we characterized BACS by alternative methods. We identified by immunofluorescence the proposed BASC cell population co-expressing SPC, a marker for alveolar type 2 cells, and CCSP, a marker for bronchial epithelial Clara cells, that resides at the BADJ. BASCs were then identified by flow cytometry using double-fluorescent Cre reporter mice that express YFP and mCherry under the control of SPC and CCSP promoters; also based on an adjusted McQualter protocol for their expression of $EpCAM^{high}$ and $CD24^{low}$. Clonogenic assays of $EpCAM^{high}$ and $CD24^{low}$ sorted cells cultured on feeders and matrigel showed BASCs as small colony-forming-units. The proliferative activity of BASCs after naphthalene injury and pneumonectomy was also determined. Based on their expression of $EpCAM^{high}$-$CD24^{low}$, we showed the evidence of BASCs as a potential progenitor/stem cells for distal murine lung**.** We further aim to establish *in vivo* differentiation assays for BASCs to address changes in stemness and proliferative activity during experimental lung disease and lung regeneration.

Oct4, specifically expressed in embryonic stem cells, can also be detected in adult stem cells such as bone marrow-derived mesenchymal stem cells. A role for maintaining pluripotency and self-renewal of embryonic stem cells is ascribed to Oct4 as a

pluripotency marker. Several studies suggest a role for Oct-4 in sustaining self-renewal capacity of adult somatic stem cells. Other scientists have produced the evidence that Oct-4 gene ablation in the somatic stem cells revealed no abnormalities in homeostasis or regenerative capacity. Data strongly argue that Oct-4, even if expressed at low levels in somatic cells, is dispensable for the self-renewal of somatic stem cells, for tissue homeostasis, and for the regeneration of tissue in the adult. The aim of this project was to trace Oct4 positive cells in adult mouse lung. We identified a distinct pulmonary Oct4 expressing cell compartment that belongs based on its localization to telocytes. The hypothesis is supported from the literature reporting that telocytes are located in the perivascular wall and extended by their telopodes to the peribronchial and alveolar spaces. They express Oct-4, vimentin, Sca-1, PDGFR-b, C-kit and VEGF. We confirmed these results by immunofluorescence confoncal microscopy of adult wild type mouse lung. Flow cytometric analyses using Oct4-GFP reporter mice identified a population of Oct4-GFP positive cells. Oct4-GFP positive cells were sorted cultured and were growing with long extensions like telocytes. Laser capture microdissection and qRT-PCR were also established to support immunofluorescence data on mRNA level. Since our data confirmed the hypothesis in which Oct4 positive cells are telocytes, our next goal is first to study the role of telocytes in adult mouse lung and determine the function of Oct4 in these cells.

ZUSAMMENFASSUNG

Bronchioalveolare Stammzellen (bronchioalveolar stem cells, BASCs) wurden als eine regionale Stammzellpopulation in der distalen Lunge charakterisiert. Sie sind CCSP (Clara cell secretory protein) und SPC (surfactant protein C) positiv und reagieren bei bronchiolaren und alveolaren Verletzungen. Es wird vermutet, dass die BASCs den Bestand bronchiolarer Clara Zellen und der Alveolaren Typ II Zellen aufrechterhalten. Vorangegangene Studien haben gezeigt, dass Clara Zellen nach der Schädigung durch oxidativen Stress zur Erneuerung des bronchiolaren Epitheliums beitragen. Erwähnenswert ist, dass nach der Entfernung von Clara Zellen durch die Gabe von Naphtalen die verbliebenen Zellen im terminalen Bronchiolus in der Lage sind, das Epithel vollständig wiederherzustellen. Diese Naphtalen-resistenten Clara Zellen sind in den bronchioalveolaren Verbindungen, den sogenannten bronchioalveolar duct junctions (BADJ) lokalisiert. BASCs werden durch eine Positivfärbung für CD34, einem Marker für Hautepithelzellen und hämatopoetische Stammzellen sowie eine Positivfärbung für Sca-1, einem Marker für Stammzellen, identifiziert und isoliert. Andere in der Maus durchgeführte Studien deuten darauf hin, dass Sca-1^{pos} Zellfraktionen überwiegend mesenchymale Zelllinien repräsentieren. Das wiederum zeigt, dass Sca-1 kein selektiver Marker für epitheliale Stammzellen in der adulten Mauslunge ist. Daher ist es notwendig, alternative funktionale Assays zur Identifizierung und Charakterisierung von BASCs zu etablieren. In der hier vorliegenden Studie werden die BASCs mit Alternativmethoden charakterisiert. Die durch die Koexpression von SP-C, dem Marker für alveolare Typ II Zellen, und CCSP, dem Marker für bronchiolare epitheliale Clara Zellen, definierte BASC Zellpopulation wurde mittels Immunofluoreszenz in den BADJ lokalisiert. Weiterhin wurden die BASCs mit Hilfe der Durchflusscytometrie (flow cytometry) identifiziert. Hierbei wurde eine Cre-Reportermauslinie verwendet, die eine Doppelfluoreszenz aus YFP und mCherry unter der Kontrolle der Promotoren für SPC und CCSP ausbildete, sowie ein angepasstes McQualter Protokoll für die Expression von EpCAMhigh and CD24low in BASCs. Klonogene Assays für diese auf EpCAM^{high} and CD24l^{ow} isolierten Zellen, die auf Futter-Zellen (Feeder) und Matrigel kultiviert wurden, zeigten BASCs als kleine, koloniebildende Einheiten. Die Proliferationsaktivität der BASCs nach einer Naphtalenbehandlung und Pneumonektomie wurde ebenfalls ermittelt. Basierend auf der EpCAM^{high} and CD24^{low} Expression in den BASCs konnte bewiesen

werden, dass diese Zellen potentielle Vorläufer/Stammzellen für die distale Mauslunge darstellen. Weiterhin soll ein in vivo Differenzierungs-Assay für BASCs etabliert werden, um die Veränderungen in der Stammzell- und Proliferationsaktivität während experimentell induzierter Lungenerkrankungen und Lungenregeneration zu untersuchen. Oct4, das spezifisch in embryonalen Stammzellen exprimiert wird, kann ebenfalls in adulten Stammzellen detektiert werden, dort z. B. in mesenchymalen Stammzellen aus dem Knochenmark. Oct4 wird als Pluripotenz-Marker charakterisiert, wobei ihm eine Rolle in der Erhaltung von Pluripotenz und Selbsterneuerung embryonaler Stammzellen zugesprochen wird. Verschiedene Studien lassen vermuten, dass Oct4 zur Beibehaltung der Selbsterneuerungsfähigkeit adulter somatischer Stammzellen beiträgt. Andere Studien hingegen zeigen, dass eine Ausschaltung des Oct4 Gens in somatischen Stammzellen keine Anomalitäten in der Homöostase oder der Regenerationsfähigkeit dieser Zellen zur Folge hat. Einige Daten deuten sehr stark darauf hin, dass Oct4, auch wenn es in geringfügig in somatischen Zellen exprimiert wird, für die Selbsterneuerungsfähigkeit von somatischen Stammzellen, Gewebehomöostase und für die Regeneration von Gewebe in Adulten entbehrlich ist. Das Ziel dieses Projektes war die Detektion von Oct4 positiven Zellen in der adulten Mauslunge. Es konnte eine distinkte, Oct4 exprimierende Zellpopulation identifiziert werden, die auf Grund ihrer Lokalisation den Telozyten zugeordnet wurde. Diese Hypothese wird durch die Literatur gestützt, die Telozyten perivaskulär lokalisieren, wobei ihre Telopoden in den peribronchialen und alveolären Raum hineinreichen. Sie exprimieren Oct4, Vimentin, Sca-1, PDGFR-beta, C-kit und VEGF. Diese Resultate konnten in der Lunge adulter Wildtypmäuse mit Hilfe der konfokalen Mikroskopie durch Immunofluoreszenz bestätigt werden. Durch die Analyse mittels Durchflusszytometrie konnte auf der Basis von Oct4-GFP Reportermäusen eine Population von Oct4-GFP positiven Zellen identifiziert werden. Diese Zellen wurden isoliert und kultiviert und zeigten ein charakteristisches Wachstum mit langen Extensionen wie bei Telozyten. Laser-Mikrodissektion und qRT-PCR wurden etabliert um die Immunofluoreszenzdaten auf mRNA Ebene zu bestätigen. Da die Daten die Hypothese unterstreichen, dass es sich bei den Oct4-positiven Zellen um Telozyten handelt, ist das nächste Ziel, die Rolle der Telozyten in der adulten Mauslunge zu untersuchen und die Rolle von Oct4 in diesen Zellen zu ermitteln.

BIBLIOGRAPHY

1. van der Flier, L.G. and H. Clevers, *Stem Cells, Self-Renewal, and Differentiation in the Intestinal Epithelium.* Annual Review of Physiology, 2009. **71**: p. 241-260.
2. Blanpain, C. and E. Fuchs, *Epidermal homeostasis: a balancing act of stem cells in the skin.* Nature Reviews Molecular Cell Biology, 2009. **10**(3): p. 207-U67.
3. Klimanskaya, I. and R. Lanza, *Adult Stem Cells*. 2006: Elsevier Science.
4. Schwarz, M.I. and T.E. King, *Interstitial Lung Disease*. 2010: People's Medical Publishing House.
5. Sargurupremraj, M. and M. Wjst, *Transposable elements and their potential role in complex lung disorder.* Respiratory Research, 2013. **14**.
6. Sdrimas, K. and S. Kourembanas, *MSC microvesicles for the treatment of lung disease: A new paradigm for cell-free therapy.* Antioxid Redox Signal, 2014.
7. El Agha, E., et al., *Fgf10-positive cells represent a progenitor cell population during lung development and postnatally.* Development, 2014. **141**(2): p. 296-306.
8. Volckaert, T., et al., *Parabronchial smooth muscle constitutes an airway epithelial stem cell niche in the mouse lung after injury.* J Clin Invest, 2011. **121**(11): p. 4409-19.
9. Giangreco, A., et al., *Stem cells are dispensable for lung homeostasis but restore airways after injury.* Proceedings of the National Academy of Sciences of the United States of America, 2009. **106**(23): p. 9286-9291.
10. Giangreco, A., S.D. Reynolds, and B.R. Stripp, *Terminal bronchioles harbor a unique airway stem cell population that localizes to the bronchoalveolar duct junction.* Am J Pathol, 2002. **161**(1): p. 173-82.
11. Rawlins, E.L., et al., *The role of Scgb1a1+ Clara cells in the long-term maintenance and repair of lung airway, but not alveolar, epithelium.* Cell Stem Cell, 2009. **4**(6): p. 525-34.
12. Kim, C.F., et al., *Identification of bronchioalveolar stem cells in normal lung and lung cancer.* Cell, 2005. **121**(6): p. 823-35.
13. Gonzalez, M.A. and A. Bernad, *Characteristics of adult stem cells.* Adv Exp Med Biol, 2012. **741**: p. 103-20.
14. Noth, U., A.F. Steinert, and R.S. Tuan, *Technology Insight: adult mesenchymal stem cells for osteoarthritis therapy.* Nature Clinical Practice Rheumatology, 2008. **4**(7): p. 371-380.
15. Mountford, J.C., *Human embryonic stem cells: origins, characteristics and potential for regenerative therapy.* Transfusion Medicine, 2008. **18**(1): p. 1-12.
16. Shenghui, H., D. Nakada, and S.J. Morrison, *Mechanisms of Stem Cell Self-Renewal.* Annual Review of Cell and Developmental Biology, 2009. **25**(1): p. 377-406.
17. Shahriyari, L. and N.L. Komarova, *Symmetric vs. Asymmetric Stem Cell Divisions: An Adaptation against Cancer?* PLoS One, 2013. **8**(10): p. e76195.
18. Yamashita, Y.M., et al., *Polarity in stem cell division: asymmetric stem cell division in tissue homeostasis.* Cold Spring Harb Perspect Biol, 2010. **2**(1): p. a001313.
19. Martinez-Agosto, J.A., et al., *The hematopoietic stem cell and its niche: a comparative view.* Genes & Development, 2007. **21**(23): p. 3044-3060.

20. Leedham, S.J., et al., *Intestinal stem cells.* Journal of Cellular and Molecular Medicine, 2005. **9**(1): p. 11-24.
21. Alberts, B., *Essential Cell Biology*. 1998: Garland Pub.
22. Pauklin, S. and L. Vallier, *The Cell-Cycle State of Stem Cells Determines Cell Fate Propensity.* Cell, 2013. **155**(1): p. 135-147.
23. Hartwell, L.H. and T.A. Weinert, *Checkpoints - Controls That Ensure the Order of Cell-Cycle Events.* Science, 1989. **246**(4930): p. 629-634.
24. Calegari, F. and W.B. Huttner, *An inhibition of cyclin-dependent kinases that lengthens, but does not arrest, neuroepithelial cell cycle induces premature neurogenesis.* J Cell Sci, 2003. **116**(Pt 24): p. 4947-55.
25. White, J. and S. Dalton, *Cell cycle control of embryonic stem cells.* Stem Cell Rev, 2005. **1**(2): p. 131-8.
26. Morris, Samantha A., Y. Guo, and M. Zernicka-Goetz, *Developmental Plasticity Is Bound by Pluripotency and the Fgf and Wnt Signaling Pathways.* Cell Reports, 2012. **2**(4): p. 756-765.
27. Panno, J., *Stem Cell Research: Medical Applications and Ethical Controversy*. 2009: Facts On File, Incorporated.
28. Weissman, I.L., *Stem Cells: Units of Development, Units of Regeneration, and Units in Evolution.* Cell, 2000. **100**(1): p. 157-168.
29. Forman, L., *Stem Cell Research*. 2010: Abdo Publishing Company.
30. Luo, G., et al., *Developmental plasticity of stem cells and diseases.* Medical Hypotheses, 2010. **75**(6): p. 507-510.
31. Lakshmipathy, U. and C. Verfaillie, *Stem cell plasticity.* Blood Reviews, 2005. **19**(1): p. 29-38.
32. Research, G.B.P.H.o.L.S.C.o.S.C., *Stem cell research: report from the Select Committee*. 2002: Stationery Office.
33. Madeja, Z.E., et al., *Changes in sub-cellular localisation of trophoblast and inner cell mass specific transcription factors during bovine preimplantation development.* Bmc Developmental Biology, 2013. **13**.
34. Allman, T., *Stem Cells*. 2005: Lucent Books.
35. Keener, J. and J. Sneyd, *Mathematical Physiology: II: Systems Physiology*. 2009: Springer.
36. Singh, R., et al., *Stem cells in the skin and their role in oncogenesis.* Journal of the European Academy of Dermatology and Venereology, 2013: p. n/a-n/a.
37. C, B. and F. E, *Epidermal stem cells of the skin.* Annu. Rev. Cell Dev. Biol., 2006. **22**: p. 339.
38. Mcwhir, J. and A. Thomson, *Gene Targeting and Embryonic Stem Cells*. 2004: Taylor & Francis.
39. Alison, M., A.M. Wobus, and K.R. Boheler, *Stem Cells*. 2006: Springer.
40. Pain, B., et al., *Long-term in vitro culture and characterisation of avian embryonic stem cells with multiple morphogenetic potentialities.* Development, 1996. **122**(8): p. 2339-2348.
41. Hoffman, L.M. and M.K. Carpenter, *Characterization and culture of human embryonic stem cells.* Nat Biotech, 2005. **23**(6): p. 699-708.
42. Rastogi, V.B., *Modern Biology*. 1997: Pitambar Publishing.
43. Alcamo, I.E. and B. Krumhardt, *Anatomy and Physiology the Easy Way*. 2004: Barron's.
44. Dudek, R.W., *High-yield Lung*. 2006: Lippincott Williams & Wilkins.

45. Okano, H., *Adult Neural Stem Cells and Central Nervous System Repair*, in *Stem Cells in Reproduction and in the Brain*, J. Morser, S.I. Nishikawa, and H.R. Schöler, Editors. 2006, Springer Berlin Heidelberg. p. 215-228.
46. Chunmeng, S. and C. Tianmin, *Skin: a promising reservoir for adult stem cell populations.* Medical Hypotheses, 2004. **62**(5): p. 683-688.
47. Ramiya, V.K., et al., *Reversal of insulin-dependent diabetes using islets generated in vitro from pancreatic stem cells.* Nature medicine, 2000. **6**(3): p. 278-82.
48. Catacchio, I., et al., *Evidence for Bone Marrow Adult Stem Cell Plasticity: Properties, Molecular Mechanisms, Negative Aspects, and Clinical Applications of Hematopoietic and Mesenchymal Stem Cells Transdifferentiation.* Stem Cells International, 2013.
49. Theise, N.D., et al., *The canals of hering and hepatic stem cells in humans.* Hepatology, 1999. **30**(6): p. 1425-1433.
50. Seale, P., A. Asakura, and M.A. Rudnicki, *The Potential of Muscle Stem Cells.* Developmental Cell, 2001. **1**(3): p. 333-342.
51. McCulley, C., *Stem Cell Information.* College & Research Libraries News, 2008. **69**(7): p. 419-419.
52. Hu, W., et al., *Concurrent deletion of cyclin E1 and cyclin-dependent kinase 2 in hepatocytes inhibits DNA replication and liver regeneration in mice.* Hepatology, 2013.
53. Oswald, J., et al., *Mesenchymal stem cells can be differentiated into endothelial cells in vitro.* Stem Cells, 2004. **22**(3): p. 377-384.
54. Sinclair, K., S.T. Yerkovich, and D.C. Chambers, *Mesenchymal stem cells and the lung.* Respirology, 2013. **18**(3): p. 397-411.
55. Crisan, M., et al., *A perivascular origin for mesenchymal stem cells in multiple human organs.* Cell Stem Cell, 2008. **3**(3): p. 301-313.
56. Sabatini, F., et al., *Human bronchial fibroblasts exhibit a mesenchymal stem cell phenotype and multilineage differentiating potentialities.* Laboratory Investigation, 2005. **85**(8): p. 962-971.
57. Friedenstein, A.J., R.K. Chailakhjan, and K.S. Lalykina, *The development of fibroblast colonies in monolayer cultures of guinea-pig bone marrow and spleen cells.* Cell Tissue Kinet, 1970. **3**(4): p. 393-403.
58. Rehan, V.K., et al., *Evidence for the presence of lipofibroblasts in human lung.* Experimental Lung Research, 2006. **32**(8): p. 379-393.
59. Mendez-Ferrer, S., et al., *Mesenchymal and haematopoietic stem cells form a unique bone marrow niche.* Nature, 2010. **466**(7308): p. 829-U59.
60. Tropea, K.A., et al., *Bronchioalveolar stem cells increase after mesenchymal stromal cell treatment in a mouse model of bronchopulmonary dysplasia.* American Journal of Physiology-Lung Cellular and Molecular Physiology, 2012. **302**(9): p. L829-L837.
61. Aslam, M., et al., *Bone Marrow Stromal Cells Attenuate Lung Injury in a Murine Model of Neonatal Chronic Lung Disease.* American Journal of Respiratory and Critical Care Medicine, 2009. **180**(11): p. 1122-1130.
62. Akram, K.M., et al., *Mesenchymal stem cells promote alveolar epithelial cell wound repair in vitro through distinct migratory and paracrine mechanisms.* Respiratory Research, 2013. **14**.
63. Zepeda, M.L., M.R. Chinoy, and J.M. Wilson, *Characterization of Stem-Cells in Human Airway Capable of Reconstituting a Fully Differentiated Bronchial Epithelium.* Somatic Cell and Molecular Genetics, 1995. **21**(1): p. 61-73.

64. Boers, J.E., A.W. Ambergen, and F.B.J.M. Thunnissen, *Number and proliferation of basal and parabasal cells in normal human airway epithelium.* American Journal of Respiratory and Critical Care Medicine, 1998. **157**(6): p. 2000-2006.
65. Hong, K.U., et al., *Basal cells are a multipotent progenitor capable of renewing the bronchial epithelium.* American Journal of Pathology, 2004. **164**(2): p. 577-588.
66. Kotton, D.N. and A. Fine, *Lung stem cells.* Cell Tissue Res, 2008. **331**(1): p. 145-56.
67. Rawlins, E.L. and B.L. Hogan, *Epithelial stem cells of the lung: privileged few or opportunities for many?* Development, 2006. **133**(13): p. 2455-65.
68. Piro, D., J. Rejman, and M. Conese, *Stem cell therapy for cystic fibrosis: current status and future prospects.* Expert Rev Respir Med, 2008. **2**(3): p. 365-80.
69. Barkauskas, C.E., et al., *Type 2 alveolar cells are stem cells in adult lung.* Journal of Clinical Investigation, 2013. **123**(7): p. 3025-3036.
70. McQualter, J.L., et al., *Evidence of an epithelial stem/progenitor cell hierarchy in the adult mouse lung.* Proc Natl Acad Sci U S A, 2010. **107**(4): p. 1414-9.
71. Nolen-Walston, R.D., et al., *Cellular kinetics and modeling of bronchioalveolar stem cell response during lung regeneration.* Am J Physiol Lung Cell Mol Physiol, 2008. **294**(6): p. L1158-65.
72. Xian, W. and F. McKeon, *Adult stem cells underlying lung regeneration.* Cell Cycle, 2012. **11**(5).
73. Chapman, H.A., et al., *Integrin α6β4 identifies an adult distal lung epithelial population with regenerative potential in mice.* The Journal of Clinical Investigation, 2011. **121**(7): p. 2855-2862.
74. Ling, T.Y., et al., *Identification of pulmonary Oct-4(+) stem/progenitor cells and demonstration of their susceptibility to SARS coronavirus (SARS-CoV) infection in vitro.* Proceedings of the National Academy of Sciences of the United States of America, 2006. **103**(25): p. 9530-9535.
75. Liedtke, S., M. Stephan, and G. Kogler, *Oct4 expression revisited: potential pitfalls for data misinterpretation in stem cell research.* Biol Chem, 2008. **389**(7): p. 845-50.
76. Tai, M.H., et al., *Oct4 expression in adult human stem cells: evidence in support of the stem cell theory of carcinogenesis.* Carcinogenesis, 2005. **26**(2): p. 495-502.
77. Lengner, C.J., et al., *Oct4 expression is not required for mouse somatic stem cell self-renewal.* Cell Stem Cell, 2007. **1**(4): p. 403-15.
78. Bojin, F.M., et al., *Telocytes within human skeletal muscle stem cell niche.* Journal of Cellular and Molecular Medicine, 2011. **15**(10): p. 2269-2272.
79. Popescu, L.M., et al., *Telocytes and putative stem cells in the lungs: electron microscopy, electron tomography and laser scanning microscopy.* Cell Tissue Res, 2011. **345**(3): p. 391-403.
80. Cretoiu, S.M., et al., *Telocytes: ultrastructural, immunohistochemical and electrophysiological characteristics in human myometrium.* Reproduction, 2013. **145**(4): p. 357-70.
81. Hinescu, M., et al., *Telocytes in pleura: two- and three-dimensional imaging by transmission electron microscopy.* Cell and Tissue Research, 2011. **343**(2): p. 389-397.
82. Popescu, L.M., et al., *Telocytes in human epicardium.* Journal of Cellular and Molecular Medicine, 2010. **14**(8): p. 2085-2093.

83. Gherghiceanu, M., C.G. Manole, and L.M. Popescu, *TELOCYTES IN ENDOCARDIUM: Electron Microscope Evidence.* Journal of Cellular and Molecular Medicine, 2010. **14**(9): p. 2330-2334.
84. Zheng, Y., et al., *Telocytes in the urinary system.* Journal of Translational Medicine, 2012. **10**(1): p. 188.
85. Mou, Y., et al., *Immunohistochemical characterization and functional identification of mammary gland telocytes in the self-assembly of reconstituted breast cancer tissue in vitro.* Journal of Cellular and Molecular Medicine, 2013. **17**(1): p. 65-75.
86. Bosco, C., et al., *Ganglionar nervous cells and telocytes in the pancreas of Octodon degus: Extra and intrapancreatic ganglionar cells and telocytes in the degus.* Autonomic Neuroscience, 2013. **177**(2): p. 224-230.
87. Gherghiceanu, M. and L.M. Popescu, *Interstitial Cajal-like cells (ICLC) in human resting mammary gland stroma. Transmission electron microscope (TEM) identification.* Journal of Cellular and Molecular Medicine, 2005. **9**(4): p. 893-910.
88. Cretoiu, S., et al., *Interstitial Cajal-like cells of human Fallopian tube express estrogen and progesterone receptors.* J Mol Histol, 2009. **40**: p. 387 - 394.
89. Hinescu, M.E. and L.M. Popescu, *Interstitial Cajal-like cells (ICLC) in human atrial myocardium.* Journal of Cellular and Molecular Medicine, 2005. **9**(4): p. 972-5.
90. Hinescu, M.E., et al., *Interstitial Cajal-like cells (ICLC) in atrial myocardium: ultrastructural and immunohistochemical characterization.* Journal of Cellular and Molecular Medicine, 2006. **10**(1): p. 243-57.
91. Popescu, L., S. Ciontea, and D. Cretoiu, *Interstitial Cajal-like cells in human uterus and fallopian tube.* Ann N Y Acad Sci, 2007. **1101**: p. 139 - 165.
92. Ramón y Cajal, S., *Histologie du système nerveux de l'homme & des vertébrés*. Vol. v. 1. 1909, Paris :: Maloine.
93. Faussone Pellegrini, M.S., C. Cortesini, and P. Romagnoli, *[Ultrastructure of the tunica muscularis of the cardial portion of the human esophagus and stomach, with special reference to the so-called Cajal's interstitial cells]*. Arch Ital Anat Embriol, 1977. **82**(2): p. 157-77.
94. Thuneberg, L., *Interstitial cells of Cajal: intestinal pacemaker cells?* Adv Anat Embryol Cell Biol, 1982. **71**: p. 1-130.
95. Popescu, L. and M. Faussone-Pellegrini, *TELOCYES-a case of serendipity: the winding way from Interstitial Cells of Cajal (ICC), via Interstitial Cajal-Like Cells (ICLC) to Telocytes.* Journal of Cellular and Molecular Medicine, 2010. **4**: p. 729 - 740.
96. Lecoin, L., G. Gabella, and N. LeDouarin, *Origin of the c-kit-positive interstitial cells in the avian bowel.* Development, 1996. **122**(3): p. 725-733.
97. Ardeleanu, C. and G. Bussolati, *Telocytes are the common cell of origin of both PEComas and GISTs: an evidence-supported hypothesis.* Journal of Cellular and Molecular Medicine, 2011. **15**(12): p. 2569-2574.
98. Ceafalan, L., et al., *Telocytes in human skin; are they involved in skin regeneration.* Journal of Cellular and Molecular Medicine, 2012. **16**(7): p. 1405 - 20.
99. Yoshimizu, T., et al., *Germline-specific expression of the Oct-4/green fluorescent protein (GFP) transgene in mice.* Dev Growth Differ, 1999. **41**(6): p. 675-84.
100. Schatten, H., *Germ Cell Protocols: Molecular embryo analysis, live imaging, transgenesis, and cloning*. 2004: Humana Press.

101. Dovey, J.S., et al., *Bmi1 is critical for lung tumorigenesis and bronchioalveolar stem cell expansion.* Proceedings of the National Academy of Sciences of the United States of America, 2008. **105**(33): p. 11857-11862.
102. McQualter, J.L., et al., *Endogenous fibroblastic progenitor cells in the adult mouse lung are highly enriched in the sca-1 positive cell fraction.* Stem Cells, 2009. **27**(3): p. 623-33.
103. Stocum, D.L., *Regenerative Biology and Medicine*. 2012: Academic Press.
104. West, J.A.A., et al., *Heterogeneity of Clara cell glutathione - A possible basis for differences in cellular responses to pulmonary cytotoxicants.* American Journal of Respiratory Cell and Molecular Biology, 2000. **23**(1): p. 27-36.
105. Jackson, S., et al., *Response of Bronchoalveolar Stem Cells to Partial Pneumonectomy in Telomerase Null Mice.* American Journal of Respiratory and Critical Care Medicine, 2009. **179**.
106. Liedtke, S., et al., *Oct4 and its pseudogenes confuse stem cell research.* Cell Stem Cell, 2007. **1**(4): p. 364-6.
107. Takeda, J., S. Seino, and G.I. Bell, *Human Oct3 Gene Family - Cdna Sequences, Alternative Splicing, Gene Organization, Chromosomal Location, and Expression at Low-Levels in Adult Tissues.* Nucleic Acids Research, 1992. **20**(17): p. 4613-4620.
108. Popescu, L., et al., *Telocytes and putative stem cells in the lungs: electron microscopy, electron tomography and laser scanning microscopy.* Cell Tissue Res, 2011. **345**: p. 391 - 403.
109. Suciu, L.C., et al., *Platelet-derived growth factor receptor-β-positive telocytes in skeletal muscle interstitium.* Journal of Cellular and Molecular Medicine, 2012. **16**(4): p. 701-707.
110. Vannucchi, M.-G., et al., *Telocytes express PDGFRα in the human gastrointestinal tract.* Journal of Cellular and Molecular Medicine, 2013. **17**(9): p. 1099-1108.
111. Hatta, K., et al., *Culture of rat endometrial telocytes.* Journal of Cellular and Molecular Medicine, 2012. **16**: p. 1392 - 6.
112. Zhou, J., et al., *Telocytes accompanying cardiomyocyte in primary culture: two- and three-dimensional culture environment.* Journal of Cellular and Molecular Medicine, 2010. **14**: p. 641 - 2645.
113. Cretoiu, S.M., D. Cretoiu, and L.M. Popescu, *Human myometrium - the ultrastructural 3D network of telocytes.* Journal of Cellular and Molecular Medicine, 2012. **16**(11): p. 2844-2849.
114. Zheng, Y., et al., *Genetic comparison of mouse lung telocytes with mesenchymal stem cells and fibroblasts.* Journal of Cellular and Molecular Medicine, 2013. **17**(4): p. 567-577.
115. Suciu, L., et al., *Telocytes in human term placenta: morphology and phenotype.* Cells Tissues Organs, 2010. **192**: p. 325 - 339.
116. Popescu, L., et al., *Identification of telocytes in skeletal muscle interstitium: implication for muscle regeneration.* Journal of Cellular and Molecular Medicine, 2011. **15**: p. 1379 - 1392.
117. Wang, X., et al., *Alternative translation of OCT4 by an internal ribosome entry site and its novel function in stress response.* Stem Cells, 2009. **27**(6): p. 1265-75.
118. Wang, X. and J. Dai, *Concise Review: Isoforms of OCT4 Contribute to the Confusing Diversity in Stem Cell Biology.* Stem Cells, 2010. **28**(5): p. 885-893.

119. Di, J., et al., *The stem cell markers Oct4A, Nanog and c-Myc are expressed in ascites cells and tumor tissue of ovarian cancer patients.* Cellular Oncology, 2013. **36**(5): p. 363-374.
120. Atlasi, Y., et al., *OCT4 Spliced Variants Are Differentially Expressed in Human Pluripotent and Nonpluripotent Cells.* Stem Cells, 2008. **26**(12): p. 3068-3074.
121. Zangrossi, S., et al., *Oct-4 expression in adult human differentiated cells challenges its role as a pure stem cell marker.* Stem Cells, 2007. **25**(7): p. 1675-1680.

APPENDICES

Appendix 1: Oct4^{GFP} transgenic mice genotyping

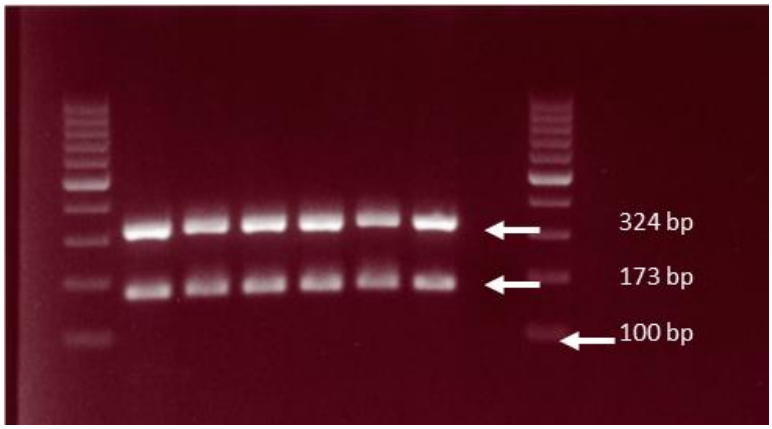

Fig. 42 Genotyping of Oct4^{GFP} transgenic mice.

Transgene GFP, gene of interest = 173 bp and internal positive control = 324 bp. The internal control primers typically amplify a genomic DNA region that is unrelated to your gene of interest. Successful amplification of the internal control indicates your DNA is suitable for PCR.

Parameters	Step 1	Step 2	Step 3	Step 4	Step 5	Step 6
Temperature (°C)	94	94	60	72	72	10
Minutes	1.5	0.5	1	1	1	∞
Note	—	35 cycles	35 cycles	35 cycles	—	

Table 11: Thermal cycling program of the PCR for the genotyping of Oct4^{GFP} transgenic mice.

Primers	Forward	Reverse
GFP	5´-aagttcatctgcaccaccg-3´	5´-tccttgaagaagatggtgcg-3´
Internal positive control	5´-ctaggccacagaattgaaagatct-3´	5´-gtaggtggaaattctagcatcatcc-3´

Table 12: Primers used for the genotyping of Oct4^{GFP} transgenic mice.

Components	Volume per reaction (µl)
ddH_2O	3.39
10 X PCR buffer II (ABI)	1.20
25 mM $MgCl_2$	0.96
2.5 mM dNTP	0.96
GFP forward primer	0.6
GFP reverse primer	0.6
Internal positive control forward primer	0.3
Internal positive control reverse primer	0.3
5 mMDNA loading dye	1.66
5 U/µl Taq polymerase	0.03
DNA template	2

Table 13: Master mix per reaction of the PCR for the genotyping of Oct4^{GFP} transgenic mice.

Appendix 2: Oct4 staining vs. negative control in Oct4^{GFP} transgenic mice

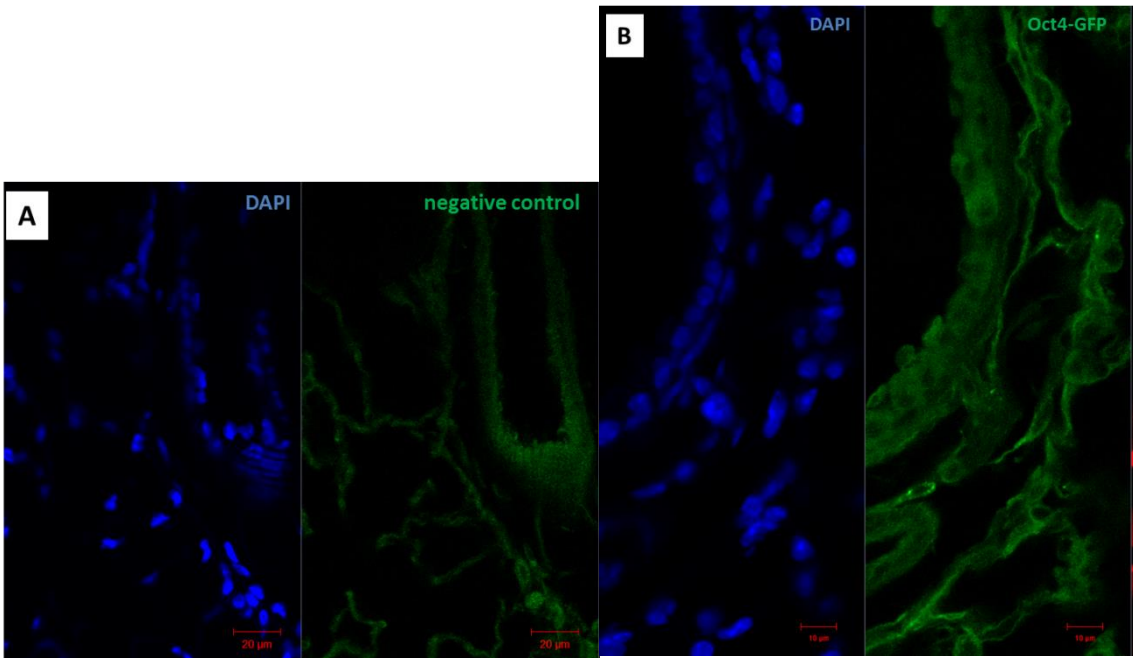

Fig. 43 Expression of Oct4 in adult lung tissues compared to the negative control in transgenic mice.

Alexa 488 was used for the negative control staining (A), and GFP-FITC was used for the positive staining (B).

Appendix 3: Oct4 staining vs. negative control in wild type mice

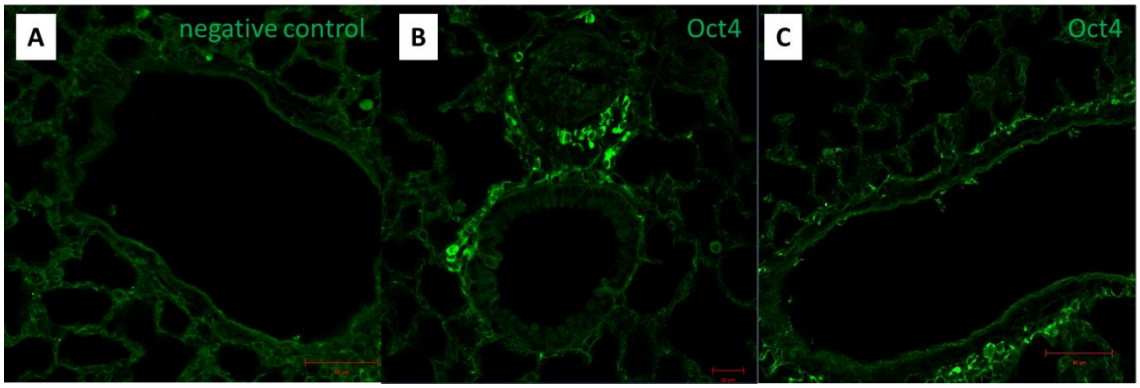

Fig. 44 Expression of Oct4 in adult lung tissues compared to the negative control in wild type mice. (A), alexa488 was used for the negative control staining. (B), expression of Oct4 around a bronchus and (C), around a blood vessel using Oct4 antibody.

Appendix 4: supplemental data of the laser capture microdissection

The samples from vessels, bronchi and septa of Oct4 real-time PCR reaction after LCM were run on 1.5 % agarose gel. This was helpful for the analysis of the real-time PCR; the gel revealed single bands corresponding to the predicted amplicon length of 230-250 bp.

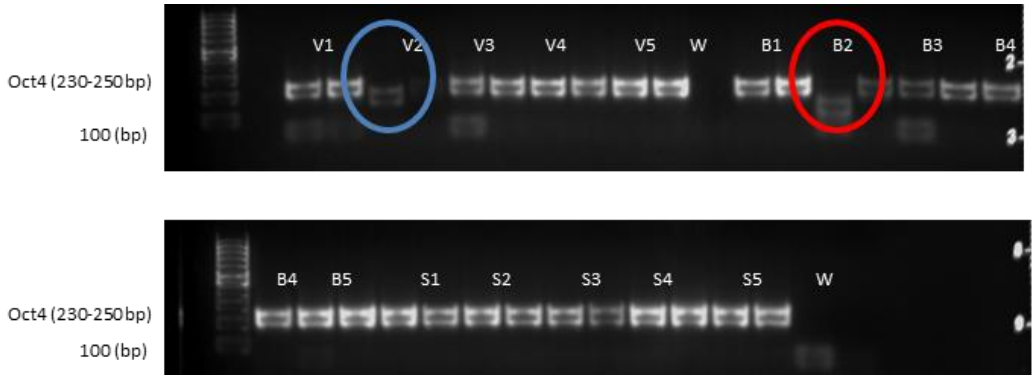

Fig. 45 Agarose gel of Oct4 real-time PCR reaction.

(V1-V5) represents the 5 different samples of the vessel compartment used for the PCR; same was done for the bronchi (B1-B5) and for the septa (S1-S2). W (water) is the master mix reaction without the cDNA template. The circles show bands with non-expected amplicon length probably due the quality of the RNA.

FIGURES

TABLES

Eidesstattliche Erklärung

Ich erkläre: Ich habe die vorgelegte Dissertation selbständig, ohne unerlaubte fremde Hilfe und nur mit den Hilfen angefertigt, die ich in der Dissertation angegeben habe. Alle Textstellen, die wörtlich oder sinngemäß aus veröffentlichten oder nicht veröffentlichten Schriften entnommen sind, und alle Angaben, die auf mündlichen Auskünften beruhen, sind als solche kenntlich gemacht. Bei den von mir durchgeführten und in der Dissertation erwähnten Untersuchungen habe ich die Grundsätze guter wissenschaftlicher Praxis, wie sie in der „Satzung der Justus-Liebig-Universität Gießen zur Sicherung guter wissenschaftlicher Praxis“ niedergelegt sind, eingehalten.

_____ _____

Ort, Datum Unterschrift

ACKNOWLEDGEMENTS

I would like to thank Prof. Dr. Werner Seeger for giving me the opportunity to do my PhD at Max-Planck-Institute for Heart and Lung Research in the Department IV-Lung Development and Remodeling, and for all the support he gave me in one way or in another in making this PhD thesis a success.

Foremost, I would like to express my sincere gratitude to my advisor PD. Dr. med Robert Voswinckel for the continuous support of my Ph.D study and research, for his patience, motivation, enthusiasm, and immense knowledge. His guidance helped me throughout the time of research and writing of this thesis.

Besides my advisor, I would like to thank Prof. Dr. Adriaan Dorresteijn for the honor he granted me for being the Director of my thesis, for his encouragements and insightful comments on my thesis.

My sincere thanks also go to Dr. Rory Morty for giving me the opportunity to join the MBML program which led me to do my PhD at Max-Planck institute; for his encouragements and discussions which enlightened me in research.

My sincere thanks also go to Dr. med. Katrin Ahlbrecht for giving me the opportunity to join their group at Max-Planck-Institute and her leading whilst working in the Department of Lung Development and Remodeling. I would like to express my sincere gratitude for her guidance and knowledge in research and in the writing of this thesis.

Many thanks go to Diana Fuchs for her technical assistance, for her kindness and endless generosity.

Many thanks to Uta Eule for her technical assistance and generosity.

I thank my fellow labmates: Dr. Sven Becker, Dr.med. Maria Raissi, Dr. Vandana Nikam, Sandeep Nikam, Minmin Yin, Anita Golec, Peter Rauschkolb, Manish Kumar, Friederike Klein, Daria Dontireddy, Nicola Kuse and Nilüfer Bouhya Erdogan, for the stimulating discussions, for the tiring days we were working together , and for all the fun we have had in the last three years.

Many thanks to Monika Haselbauer for her support in all the administrative matters, for her generosity and kindness.

I would like to thank the entire Department of Lung Development and Remodeling for the support and exciting discussions which enlightened me in research.

I would like to thank my churchmates for their support in prayer and for taking me as part of family and friends.

Last but not the least; I would like to thank my family:

My lovely husband Stefan Galiger, I often heard him telling me: YOU ARE THE BEST

My parents, Angelique and Jean-Bernard Mouele for giving me birth specially and for being there for me throughout life, for encouraging me all the time and for their support in prayer.

My parents "second degree", Ambroisine and Jean-Claude Obame who raised me up and taught me the values of hardworking and made me become what I am today.

To my lovely sister Lydie Nkouelet and her husband Franck Nkouelet, many thanks for their support, encouragements and prayers.

To my Uncle Jonas Moussavou who encouraged me to come to study in Germany, for his encouragements and for his support in prayer.

To all other members of my family: sisters, brothers, uncles, aunts, nephews, nieces and friends who participated in one way or in another in making my life and study a success.

Thank you to all of you…